Aus dem Institut für Physiologie
der Medizinischen Fakultät Charité – Universitätsmedizin Berlin

DISSERTATION

Functional relevance of Na^+-coupled neutral amino acid transporter SNAT2 as master regulator of alveolar homeostasis and its critical role in ARDS

Funktion des Na^+-gekoppelten Aminosäure-Transporters SNAT2 als Masterregulator der alveolären Homöostase und seine kritische Rolle im akuten Lungenschaden

zur Erlangung des akademischen Grades

Doctor rerum medicinalium (Dr. rer. medic.)

vorgelegt der Medizinischen Fakultät
Charité – Universitätsmedizin Berlin

von

Sarah Weidenfeld

aus Viersen (Geburtsort)

Datum der Promotion: 04. März 2022

Vorwort

Teilergebnisse der vorliegenden Arbeit wurden veröffentlicht in:

American Journal of Physiology Lung Cellular and Molecular Physiology/ Januar 2021

Title: "Sodium coupled neutral amino acid transporter SNAT2 counteracts cardiogenic pulmonary edema by driving alveolar fluid clearance,"

Table of Content

List of Figures

List of Tables

List of Abbreviations

AA	amino acids
AAR	amino acid response
AFC	alveolar fluid clearance
AFS	alveolar fluid secretion
ALI	acute lung injury
AM	alveolar macrophages
ANOVA	analysis of variance
AQP	aquaporin
ARDS	acute respiratory distress syndrome
ASK1	apoptosis signal-regulating kinase 1
ATF	activating transcription factor
ATI	alveolar type I cells
ATII	alveolar type II cells
BALF	bronchoalveolar lavage fluid
BCA	bicinchoninic acid assay
BiP	immunoglobulin binding protein
BSA	bovine serum albumin
BW	body weight
cDNA	complementary DANN
CFTR	cystic fibrosis transmembrane conductance regulator
CHOP	CCAAT-enhancer-binding protein homologous protein
Da	Dalton
DIDT	double-indicator dilution technique
DNA	deoxyribonucleic acid
DP5	death protein 5
DR5	death receptor 5
eIF2α	eukaryotic translation initiation factor 2α
E4-BP1	eIF4E-binding protein 1
ELF	epithelial lining fluid
ENaC	epithelial sodium channel
ER	endoplasmic reticulum
ERAD	ER-assisted degradation
Ero1α	ER oxidoreductase 1α
FasL	Fas ligand
FasR	Fas receptor
FCS	fetal calf serum
GAPDH	Glycerinaldehyd-3-phosphat-Dehydrogenase
GCN2	general control non-derepressible 2
HBSS	Hanks' balanced salt solution
HCl	hydrochloric acid
HgCl2	mercury chloride
hPAEpCs	human primary alveolar epithelial cells
HRP	horseradish peroxidase
IFN	Interferon
IL	interleukin
IPL	isolated perfused lung
IRE1	inositol-requiring enzyme 1

JNK	c-Jun N-terminal kinase
LPS	lipopolysaccharide
MeAIB	N-methyl-aminoisobutyric acid
MOMP	mitochondrial outer membrane permeabilization
mRNA	messenger RNA
mTORC	mammalian target of rapamycin complex
Na^+-K^+-ATPase	Na^+-K^+-adenosine triphosphatase
Nedd4-2	E3 ubiquitin ligase
NHE	Na^+/H^+ antiporter
NKCC	Na^+-K^+- Cl^- co-transporter
NO	nitric oxide
PAF	platelet activating factor
PAP	pulmonary artery pressure
PBS	phosphate-buffered saline
PCR	polymerase chain reaction
PERK	protein kinase-like ER kinase
PLA	left atrial pressure
PLY	Pneumolysin
qRT-PCR	quantitative real time qPCR
Raptor	regulatory-associated protein of mTOR
Rictor	rapamycin-insensitive companion of mTOR
RIPA	radioimmunoprecipitation assay buffer
RNA	ribonucleic acid
ROS	reactive oxygen species
RPL13	ribosomal protein L13a
S1P	site 1 protease
S2P	site 2 protease
S6K	ribosomal S6 kinases
SDS	sodium dodecyl sulfate
SDS-PAGE	SDS-polyacrylamide gel electrophoresis
SGK1	glucocorticoid-inducible kinase-1
siRNA	small interfering RNA
SLC38	solute carrier 38
Slc38a2$^{+/-}$	heterozygous-deficient SNAT2 mice
SNAT	Na^+-coupled neutral amino acid transporter
TBS	tris buffered saline
TGF	transforming growth factor
TNF	tumor necrosis factor
TNFR	TNF receptor
TRAF2	TNF receptor associated factor 2
tRNA	transfer RNA
ULK1	Unc-51-like autophagy activating kinase 1
UPR	unfolded protein response
WT	Wild type

Abstract

Acute respiratory distress syndrome (ARDS), a life-threatening disease, is the most frequent cause of death in critical care medicine. Despite numerous clinical trials, effective pharmacological treatments to improve overall survival in ARDS patients are still lacking. This unmet medical need stresses the necessity for a better understanding of the underlying pathophysiology.

Dysregulation or inhibition of alveolar fluid clearance (AFC) and loss of alveolar-capillary barrier function due to increased epithelial cell apoptosis are central pathomechanisms in ARDS that promote pulmonary edema, impair gas exchange, and drive respiratory failure.

The sodium-coupled neutral amino acid transporter SNAT2 might provide a novel therapeutic target to counteract edema formation and alleviate lung injury. SNAT2, which co-transports a neutral amino acid (AA) along with Na^+, may promote AFC by mediating epithelial Na^+ uptake but may also counteract alveolar apoptosis via its role as AA transporter. In this study, the role of SNAT2 in AFC and alveolar hemostasis was analyzed in isolated perfused mouse lungs (IPL), different murine models of acute lung injury (ALI), and pulmonary epithelial cells.

In IPL, edema formation was induced by hydrostatic stress (left atrial pressure = 7 cmH_2O) or fluid instillation (100 µl) in heterozygous SNAT2-deficient (*Slc38a2*$^{+/-}$) and corresponding wild type (WT) mice in the presence or absence of SNAT substrate L-alanine, or of SNAT inhibitor α-methylaminoisobutyric acid (MeAIB). Impaired AFC was assessed as changes in lung wet-to-dry weight (wet/dry) ratios. *In vivo*, ALI was induced in *Slc38a2*$^{+/-}$ and WT mice by intratracheal instillation of hydrochloric acid (HCl) or intranasal application of lipopolysaccharide (LPS). Protein and RNA expression profiles and wet/dry ratios were analyzed after 2 h or 24 h, respectively. In the epithelial cell line NCI-H441, SNAT2 expression was determined after stimulation with cytomix (TNFα, IFN-γ, IL-1β, LPS) or pneumolysin (PLY).

In IPL, *Slc38a2*$^{+/-}$ mice had elevated wet/dry ratios as compared to WT in response to hydrostatic stress or fluid instillation. L-alanine instillation rescued AFC in WT, yet not in *Slc38a2*$^{+/-}$ mice. This rescue was sensitive to MeAIB. In response to HCl, wet/dry ratios were increased in *Slc38a2*$^{+/-}$ mice as compared to WT. In LPS-induced ALI, expressions of ER stress marker ATF4 and pro-apoptotic protein CHOP in lung lysates were elevated in *Slc38a2*$^{+/-}$ mice compared to WT. Finally, SNAT2 protein expression was decreased in response to cytomix and PLY in NCI-H441 cells.

The results of this work identify a crucial role for SNAT2 in alveolar AFC and epithelial cell homeostasis. SNAT2 counteracts lung edema formation, probably by mediating the Na^+ uptake that drives AFC. Additionally, SNAT2 maintains alveolar epithelial homeostasis presumably through its role as AA transporter. SNAT2 activation may thus provide for a novel multi-pronged strategy to counteract lung injury.

Zusammenfassung

Der akute Lungenschaden (ARDS, *acute respiratory distress syndrome*) ist die häufigste Todesursache der Intensivmedizin. Trotz zahlreicher klinischer Studien fehlen bislang Interventionen, die die Mortalität bei ARDS Patienten mindern, was die Notwendigkeit eines besseren Verständnisses der ARDS Pathophysiologie verdeutlicht. Dysregulation bzw. Hemmung des alveolären Flüssigkeitstransports und Verlust der alveolo-kapillaren Barriere aufgrund erhöhter epithelialer Apoptose sind zentrale ARDS Pathomechanismen, die das Lungenödem fördern, und zum respiratorischen Versagen führen.

Der Na^+-gekoppelten neutrale Aminosäure (AA)- Transporter SNAT2 könnte als neues therapeutisches Target der Lungenödembildung im ARDS entgegenwirken. Als Na^+ Transporter fördert SNAT2 vermutlich die alveoläre Flüssigkeitsabsorption. Zusätzlich könnte der SNAT2-vermittelte AA-Transport der alveolären Apoptose entgegenwirken. Hier wurde die funktionelle Bedeutung von SNAT2 im Lungenepithel in isoliert perfundierten Mauslungen (IPL), Mausmodellen des akuten Lungenschadens (ALI) und pulmonalen Epithelzellen analysiert.

In der IPL wurde die Ödembildung durch hydrostatischen Stress (linker Vorhofdruck = 7 cmH_2O) oder Flüssigkeitsinstillation in heterozygoten SNAT2-defizienten (*Slc38a2*$^{+/-}$) und entsprechenden Wildtyp (WT) Mäusen mit oder ohne SNAT Substrat L-Alanin bzw. SNAT-Inhibitor Methylaminoisobuttersäure (MeAIB) induziert. Gestörte Flüssigkeitsabsorption und Ödembildung wurden als Anstieg des Feucht-/Trockengewicht der Lunge (*wet/dry ratio*) erfaßt. *In vivo* wurde ein akuter Lungenschaden in Lungen von *Slc38a2*$^{+/-}$ oder WT-Mäusen durch Salzsäure (HCl) oder Lipopolysaccharid (LPS) induziert. Nach 2 h bzw. 24 h wurden Protein- und RNA-Expressionsprofile und *wet/dry ratios* der Lungen untersucht. Die SNAT2 Proteinexpression in der Epithelzelllinie NCI-H441 wurde nach Stimulation mit Cytomix (TNFα, IFN-γ, IL-1β, LPS) oder Pneumolysin (PLY) analysiert.

In der IPL zeigten *Slc38a2*$^{+/-}$ Mäuse durch hydrostatischen Stress oder Flüssigkeitsinstillation erhöhte *wet/dry ratios* im Vergleich zum WT. L-alanin verminderte die *wet/dry ratios* im WT und MeAIB antagonisierte den protektiven Effekt von L-alanin. Im HCl-ALI, wiesen *Slc38a2*$^{+/-}$ Mäuse im Vergleich zum WT erhöhte *wet/dry ratios* auf. Im Modell des LPS-ALI war die Expression des ER-Stressmarkers ATF4 und des pro-apoptotischen Proteins CHOP in Lungen von *Slc38a2*$^{+/-}$ Mäusen im Vergleich zum WT erhöht. Cytomix oder PLY verminderten in NCI-H441-Zellen die SNAT2 Proteinexpression.

Die Ergebnisse weisen eine funktionelle Rolle von SNAT2 im alveolären Flüssigkeitshaushalt nach. SNAT2 wirkt der Lungenödembildung vermutlich durch Vermittlung der epithelialen Na^+-Aufnahme, die die alveoläre Flüssigkeitsabsorption antreibt, entgegen. Darüber hinaus vermag SNAT2 durch seine Rolle als AA-Transporter die ER-stressbedingte Apoptose zu reduzieren. Die pharmakologische Aktivierung von SNAT2 könnte daher eine neue Strategie zur Bekämpfung des ARDS darstellen.

1 Introduction

1.1 Acute respiratory distress syndrome (ARDS)

Acute respiratory distress syndrome (ARDS) is defined as acute hypoxemic respiratory failure caused by a number of clinical risk factors including sepsis, pneumonia, aspiration, trauma, pancreatitis, blood transfusions, and smoke or toxic gas inhalation (138). ARDS is associated with high morbidity and a mortality rate of over 40% (148). Furthermore, those who survive ARDS additionally suffer from significant long-term limitations in cardiopulmonary function and a reduced quality of life (45). With an estimated incidence of 86.2 per 100,000 person-years (56), ARDS also poses a tremendous financial burden on global health systems. Despite decades of research in the ARDS field and numerous clinical trials, to date no effective treatment exists. Supportive measures such as mechanical ventilation with low tidal volumes or prone positioning in severe ARDS reduce mortality, yet pharmacological interventions to improve overall survival in patients are still lacking (84). This striking discrepancy between incidence and severity of the disease on the one hand, and the lack of approved therapeutic treatments on the other, poses a key unmet medical need in critical care medicine, and stresses the necessity for a better understanding of the underlying pathomechanisms.

1.1.1 Definition

In 1967, Ashbaugh and colleagues were the first to use the term ARDS to describe 12 patients with respiratory failure (5). In 1994, a first definition of ARDS and acute lung injury (ALI), a milder form of ARDS, was proposed by the American-European Consensus Conference (AECC). ARDS was defined as an acute onset of hypoxemia (partial pressure of arterial oxygen to fraction of inspired oxygen, PaO_2/FIO_2 ≤200 mmHg) with bilateral infiltrates on chest x-ray (8). ALI was described by similar criteria, though with less severe hypoxemia (PaO_2/FIO_2 ≤ 300 mmHg). To address the need for a more specific and generalizable definition of ARDS, an initiative of the European Society of Intensive Care Medicine authorized by the American Thoracic Society and the Society of Critical Care Medicine invited a panel of international experts in 2011 to develop the so-called Berlin definition of ARDS (108). According to the Berlin definition, ARDS can be classified into three stages based on the extent of hypoxemia: i) mild (PaO_2/FiO_2 of 200 – ≤ 300 mmHg), ii) moderate (PaO_2/FiO_2 of 100 – ≤ 200 mmHg), and iii) severe (PaO_2/FiO_2 ≤ 100 mmHg). Further criteria of ARDS include an acute onset, established within one week, the presence of bilateral pulmonary infiltrates on chest radiograph and the

exclusion of hydrostatic origin of edema (108). With this revised clinical definition, the panel significantly optimized the criteria for the diagnosis of ARDS. However, 40% of actual cases still remain undetected, and therefore untreated, since consistent diagnostic procedures or standardized physiological parameters for diagnosis are still lacking (21).

1.1.2 Pathophysiology

At the pathophysiological level, ARDS is characterized by a loss of alveolar-capillary barrier function with a consequent influx of protein-rich fluid into the alveolus resulting in the development of pulmonary edema (Figure 1-1). Accumulation of fluid in the alveolar space causes a severe impairment of gas exchange, with reduced oxygen uptake (hypoxemia) and carbon dioxide excretion from the blood (hypercapnia), characteristic for respiratory failure (86).

The second cardinal feature of ARDS is the excessive inflammatory response, evident as abundant migration of neutrophils and monocytes from the pulmonary capillaries into the air space. In the alveolus, activated neutrophils injure the alveolar epithelium by the release of oxidants, proteases and leukotrienes, thus causing the disruption of junctional proteins and inducing epithelial apoptosis (85). In parallel, alveolar macrophages and lung parenchymal cells release pro-inflammatory mediators, which inhibit the production and release of surfactant, thus further damaging alveolar function. Over and above that, injury to the alveolo-capillary barrier prevents the removal of fluid from the airspace and, as such, the resolution of pulmonary edema (83). As the mortality in ARDS patients has been repeatedly shown to correlate with the persistence of alveolar edema (83, 124, 125, 139), it may be concluded that therapeutic strategies should largely be focused on processes leading to the resolution of pulmonary edema.

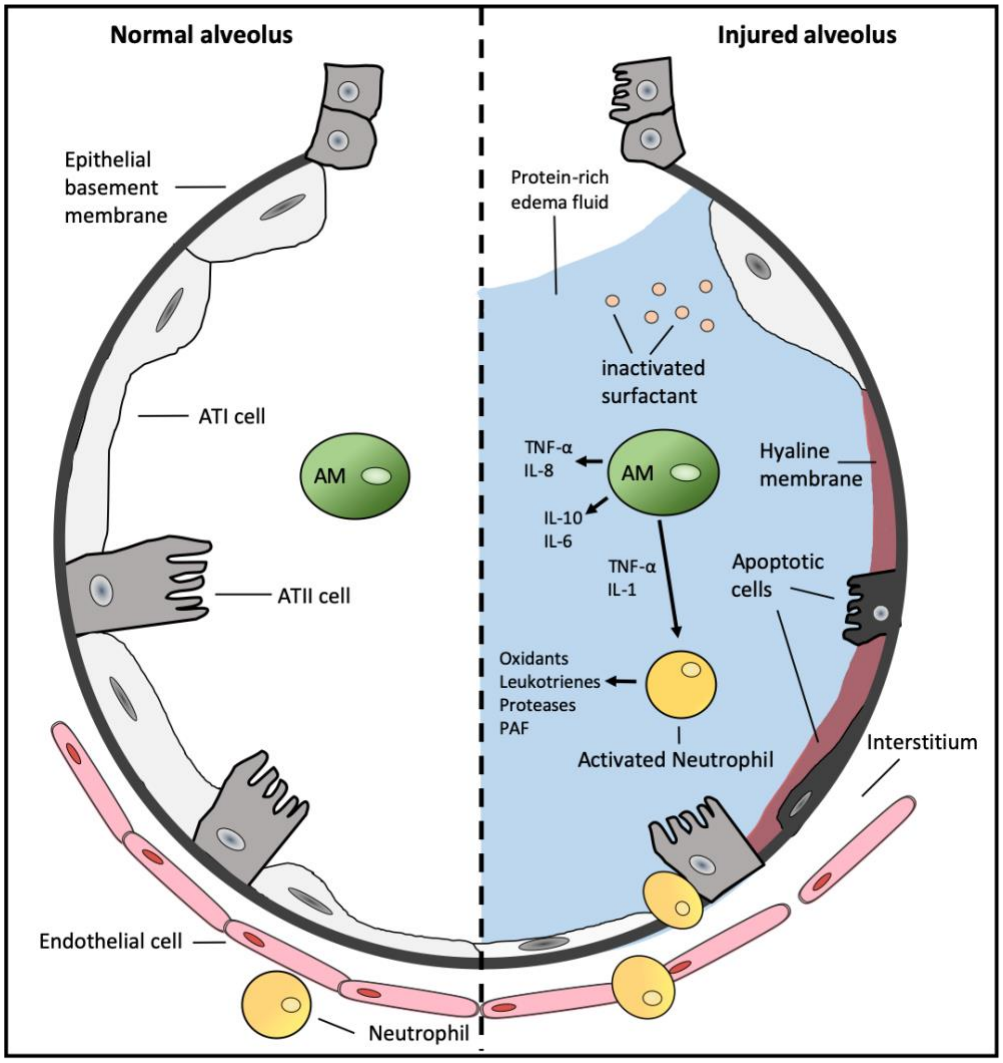

Figure 1-1: Overview of the normal (left) and the injured (right) alveolus.

In ARDS, the alveolo-capillary barrier becomes disrupted leading to the influx of protein-rich edema fluid and the migration of neutrophils from the alveolar capillaries into the alveolus. In the air space, alveolar macrophages (AM) secrete pro-inflammatory cytokines that stimulate chemotaxis and activate neutrophils which in turn produce and release further cytokines (adapted from Weidenfeld & Kuebler (141)).

1.2 The alveolar epithelial barrier

The alveolar epithelium covers more than 99% of the internal lung surface and is critical to maintain barrier function between the vascular- and the air-filled compartments. It is comprised of two distinct cell types: i) the thin and squamous-shaped type I pneumocytes, or alveolar type I (ATI) cells; and ii) the larger and cuboidal formed type II pneumocytes, or alveolar type II (ATII) cells. More than 95% of the alveolar surface is covered by ATI cells, as they form the large surface area for diffuse gas exchange. ATII cells, which are distributed between ATI cells, fulfill various functions. Besides the production and release of surfactant, a lipoprotein complex which reduces alveolar surface tension, ATII cells play a key role in the recognition of pathogens and the initiation of inflammatory responses. In parallel they serve as progenitors for ATI cells (69). Both cell types are interconnected via tight junctions, thus

forming a tight barrier to control movement of protein and fluid as well as sustaining cell polarity under physiological conditions (9).

1.2.1 Alveolar fluid transport

A strict regulation of the epithelial lining fluid (ELF), a fluid film which covers the alveolar surface, is essential for efficient gas exchange and normal lung function. In order to regulate alveolar liquid volume and to prevent or counteract fluid accumulation in the alveolar space, the tight alveolar barrier of the intact lung allows for a small constant removal of ions and fluid from the alveolar space across the alveolar epithelial layer. The primary driving force of this so-called alveolar fluid clearance (AFC) (81) is the active transport of ions, most prominently Na^+ and Cl^-, across the epithelium. The importance of this process is evident not only in ARDS, but is also highlighted by its crucial function in clearing the lungs of fluid at birth (55).

Under physiological conditions, the active absorption of Na^+ and Cl^- from the alveolar space is mediated by a series of ion channels, transporters and pumps located on the apical and basolateral side of alveolar epithelial cells, respectively (Figure 1-2). On the apical surface, Na^+ moves selectively through Na^+ channels and transporters, most notably the epithelial sodium channel (ENaC) (32), the main channel involved in amiloride-sensitive fluid clearance. Extrusion of Na^+ into the interstitial space is driven primarily by the basolateral Na^+-K^+-adenosine triphosphatase (Na^+-K^+-ATPase or Na^+-K^+-pump) (117) and partially also the Na^+/H^+ antiporter (98). To maintain electroneutrality, Cl^- moves via paracellular routes, but also transcellularly via Cl^- channels, primarily the cystic fibrosis transmembrane conductance regulator (CFTR) (54). Water follows for osmotic balance either through water channels – particularly aquaporin 5 (AQP5) (77) - or paracellularly.

Originally, it was assumed that alveolar fluid transport is primarily mediated by ATII cells, yet more recent studies have also identified functional ion channels and pumps like ENaC, CFTR, and Na^+-K^+-ATPase in ATI cells, indicating their potential role in active alveolar fluid transport (57, 110).

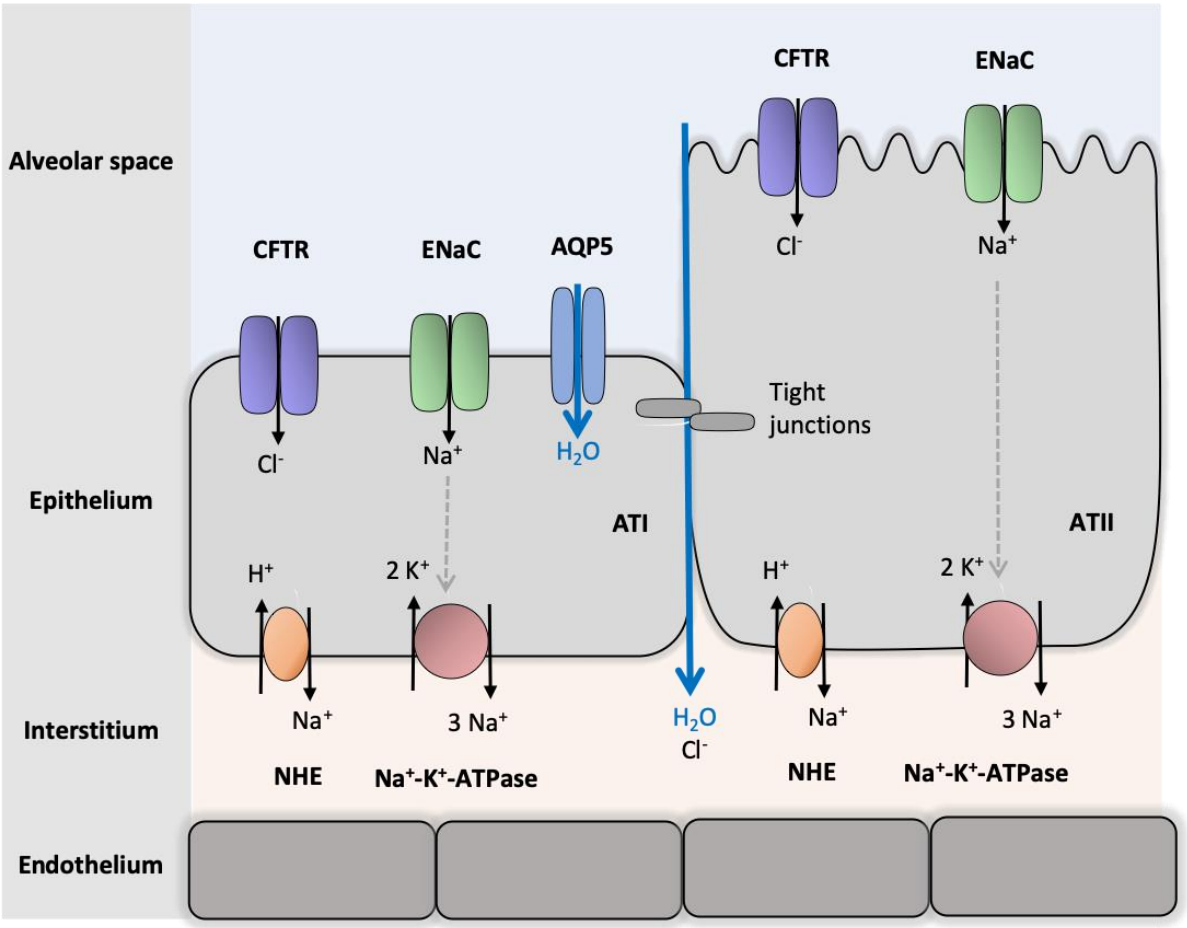

Figure 1-2: Channels, transporters and pumps involved in alveolar fluid clearance (AFC).

Fluid transport is mediated by both ATI and ATII cells, which are interconnected via tight junctions. On the apical surface, Na^+ is transported through the epithelial sodium channel (ENaC). Basolateral extrusion is mediated mainly by Na^+-K^+-ATPase but also through the Na^+/H^+ antiporter (NHE). For osmotic balance and electroneutrality, Cl^- and water follow either by paracellular routes, or through Cl^- channels (cystic fibrosis conductance regulator; CFTR) or water channels (AQP5), respectively.

1.2.2 Alveolar fluid clearance in ARDS

While active ion and fluid transport protects the lung from the development of edema under physiological conditions, this protection is lost in lung injury (133, 139). In ARDS, a combination of different pathomechanisms can cause the loss of efficient AFC, thus promoting the formation of pulmonary edema (Figure 1-3 A). Primarily, released inflammatory mediators stimulate pro-inflammatory signaling pathways that lead to reduced expression and activity of ion channels and pumps. Along these lines, Lee and colleagues showed impaired AFC in ATII cells after incubation with edema fluid from ARDS patients (70). Their data demonstrated that high levels of cytokines including interleukin (IL) -1β, IL-8, Tumor necrosis factor (TNF) -α, and transforming growth factor (TGF) -β1, which were detected in pulmonary edema fluid, cause a downregulation of both ENaC and the Na^+-K^+-ATPase. Furthermore, the pro-inflammatory response impairs AFC, and additionally the low oxygen and high carbon dioxide levels in ARDS

affect ion transporters and channels. Under hypercapnic and hypoxic conditions, transcription and trafficking of ENaC is downregulated, and the efficient function of the Na^+- K^+-ATPase is impaired (130, 135, 148). This is partly caused by emerging reactive oxygen species (ROS), which have been shown to increase internalization of ENaC via ubiquitination by Nedd4-2, an E3 ubiquitin-ligase (23).

Additionally, biomechanical stress caused by high tidal volume ventilation and elevated airway pressures can further injure the epithelium and reduce AFC (109). Notably, the latter effect may contribute to the clinical finding that low tidal volume ventilation improves overall survival and reduces mortality in ARDS patients (68).

On top of that, AFC may not only be reduced but can even reverse into active alveolar fluid secretion (AFS), thus promoting rather than resolving edema formation (Figure 1-3 A). In a model of cardiogenic-induced pulmonary edema, which is caused by elevated hydrostatic pressures in the pulmonary vasculature, our group previously showed that an acute increase in left atrial pressure decreases epithelial amiloride-sensitive Na^+ absorption. This inhibition of apical Na^+ entry generates a gradient for basolateral Na^+ and Cl^- entry via the basolateral expressed Na^+-K^+- Cl^- co-transporter 1 (NKCC1) (121). Secretion of Cl^- into the alveolar space is then mediated by a reversal of Cl^- transport across apical CFTR, which – like all ion channels - permits bidirectional ion flux (111).

Besides impaired AFC, the major pathophysiological mechanism of edema formation is the failure of the epithelial barrier due to the loss of tight junctions and increased epithelial cell apoptosis.

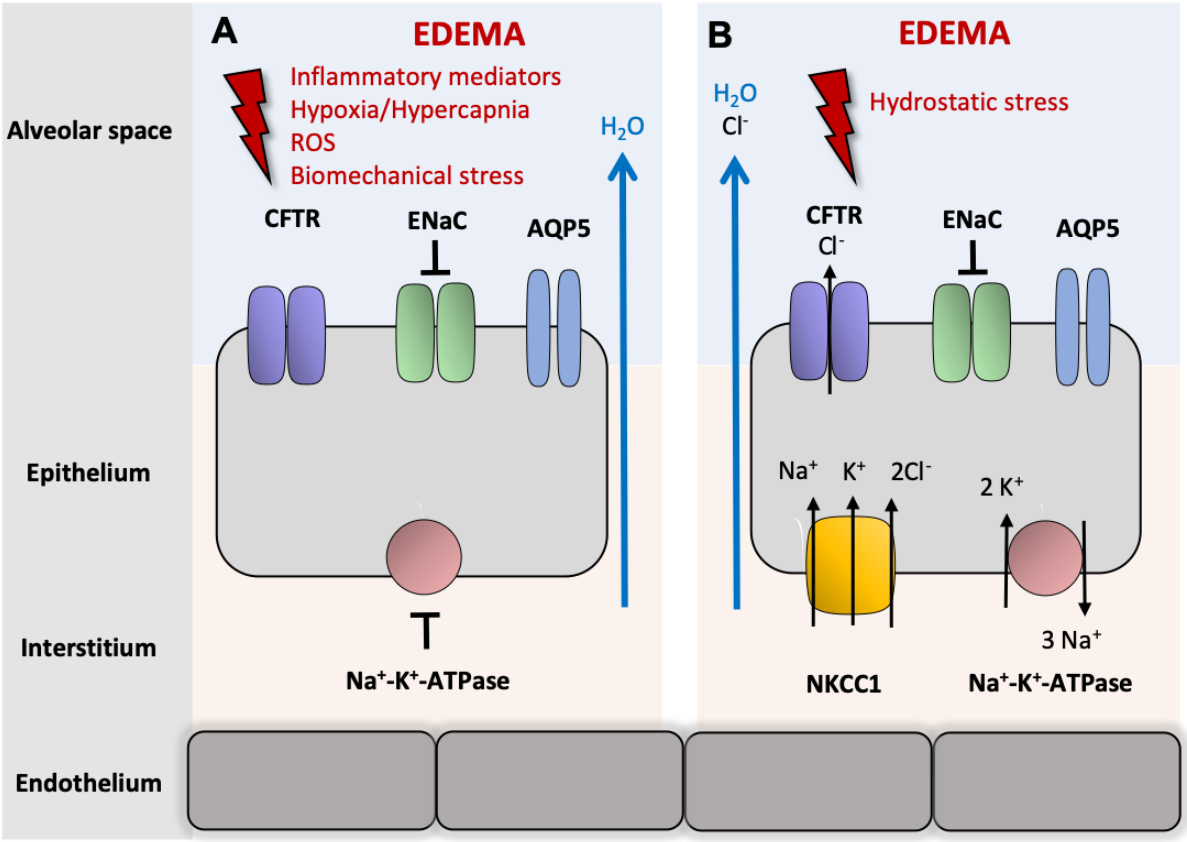

Figure 1-3: Factors impairing alveolar fluid clearance.

(A) In ARDS inflammatory mediators, high CO_2 and low O_2 levels, reactive oxygen species (ROS) or biomechanical stress inhibit AFC by downregulation or inhibition of ion transporters, channels, and pumps like the epithelial sodium channel (ENaC) and Na^+- K^+-ATPase. Additionally, a loss of alveolar junctional proteins leads to barrier disruption and fluid can leak into the alveolar space. (B) Furthermore, inhibition of apical Na^+ uptake results in basolateral Na^+ transport via Na^+-K^+-Cl^- co-transporter 1 (NKCC1), leading to a reversal of transepithelial Cl^- flux and the subsequent active secretion of fluid into the alveolar space.

1.2.3 Epithelial cell apoptosis in acute lung injury

In ARDS, apoptosis, a process of controlled cell death, can be induced in epithelial cells (80) by a number of factors including pro-inflammatory cytokines, ROS and hypoxia (144), and an increased number of apoptotic markers and ligands are present in the alveolar epithelium as well as the pulmonary edema fluid of patients with ARDS (2). The functional relevance of apoptosis as a pathophysiological factor in lung injury is highlighted by the fact that mice treated with the bacterial endotoxin lipopolysaccharide (LPS) show increased epithelial cell apoptosis (35), whereas mice treated with an inhibitor of apoptosis are protected from LPS-induced lung injury (59).

In general, apoptosis is a homeostatic mechanism in the development, maintenance and remodeling of tissues. A wide variety of stimuli and conditions induce regulated cell death as a defense mechanism to maintain physiological tissue function (24). However, when excessively activated, this process becomes pathogenic; accordingly, dysregulated apoptosis

contributes relevantly to disease processes including autoimmune diseases as well as pulmonary and cardiovascular disorders (30, 144).

Initiation of apoptosis involves a complex series of intracellular signaling events linking the initial extra- or intracellular stimuli to the final demise of the cell. In general, apoptosis is induced via two main pathways: i) the death receptor or extrinsic pathway, and ii) the mitochondrial or intrinsic pathway. The extrinsic pathway is initiated by extracellular binding of ligands to death receptors on the cell surface, like Fas (FasR) and the tumor necrosis factor (TNFR) receptor. Receptor binding initiates the activation of a group of cysteine proteases, named caspases, leading to the induction of signaling cascades that in turn cause cell death. The intrinsic pathway can be triggered by deprivation of factors (e.g. growth factors, hormones, cytokines) that suppress apoptotic death programs, or by pro-apoptotic stimuli including DNA damage, toxins, hypoxia, viral infections (24), ROS (101) as well as processes like autophagy (71) and endoplasmic reticulum (ER) stress (63). These diverse stimuli cause so-called mitochondrial outer membrane permeabilization (MOMP) leading to the release of cytochrome c into the cytosol, which activates caspase signaling cascades and ultimately causes the demise of the cell (53). Both pathways have been linked to epithelial cell death in response to lung injury (41, 119). For instance, in a mouse model of indirect lung injury by hemorrhagic shock and sepsis, FasR-deficient mice showed decreased caspase 3 activation and less severe lung injury as compared to wild type controls (105). Soluble Fas ligand (FasL) is present in bronchoalveolar lavage fluid (BALF) from ARDS patients, and BALF concentration of FasL correlates with increased epithelial apoptosis as well as mortality rate (88). Other studies reported that alveolar epithelial cells undergo apoptosis via the intrinsic pathway, which is induced by hyperoxia through increased ROS production and also by hypoxia (16, 65). Additionally, elevated expression of the pro-apoptotic CCAAT-enhancer-binding protein (C/EBP) homologous protein (CHOP), which is initiated in response to severe ER stress (115), was found in the lungs of LPS-treated mice (25). CHOP has been associated with activation of both the extrinsic and intrinsic apoptotic pathways and functions as the key mediator in ER stress-induced apoptosis (118).

1.2.4 ER stress-induced epithelial apoptosis

ER stress-induced apoptosis was identified as an important pathophysiologic factor in lung injury (25). The ER stress response is a highly conserved intracellular regulator, which serves as a homeostatic self-defense mechanism under physiological conditions.

Dysregulation or increased activation of the ER stress response can induce cell apoptosis (Figure 1-4), and it has been linked to several disease scenarios including inflammation, ischemic heart disease, and viral infections (147).

Generally, upon accumulation of misfolded proteins, the unfolded protein response (UPR) is activated in the ER lumen and UPR-signaling cascades are initiated. The UPR includes three major signaling pathways mediated by three key regulators located in the ER membrane: i) inositol-requiring enzyme 1 (IRE1), ii) protein kinase-like ER kinase (PERK), and iii) activating transcription factor 6 (ATF6). Immunoglobulin binding protein (BiP), an ER chaperone, inactivates these sensor proteins by binding to their luminal domain under physiological conditions. Accumulation of unfolded proteins in the ER causes release of BiP from these sensors, resulting in their activation (113). Activated PERK, IRE1α and ATF6 induce signaling pathways that reduce accumulation of misfolded proteins in the ER by increasing expression of ER chaperones, blocking mRNA translation, and stimulating export of misfolded proteins from the ER into the cytosol for ubiquitination as well as ER-assisted degradation (ERAD) (46). Upon release of BiP, ATF6 translocates to the Golgi apparatus where it is cleaved by site 1 (S1P) and site 2 (S2P) protease. The cleaved cytosolic domain of ATF6 induces the expression of several genes involved in protein folding and degradation (46). Both IRE1 and PERK are activated by dimerization and autophosphorylation. Activated IRE1 processes the mRNA of X-box binding protein 1 (XBP1) generating a spliced form of XBP1 which upregulates UPR target genes that function in ERAD (136). Under chronic ER stress, the kinase domain of IRE1 interacts with TNF receptor-associated factor 2 (TRAF2) leading to downstream activation of apoptosis signal-regulating kinase 1 (ASK1) and c-Jun N-terminal kinase (JNK), which ultimately causes the induction of apoptosis (126). Activation of PERK induces phosphorylation and inactivation of eukaryotic translation initiation factor 2α (eIF2α), which causes inhibition of global mRNA translation by preventing the formation of the ribosomal initiation complex. Furthermore, phosphorylated eIF2a selectively stimulates activating transcription factor 4 (ATF4) leading to enhanced expression of CHOP, which is encoded by the DNA damage-inducible transcript 3 (*DIDT3*) gene and can initiate apoptotic pathways via several mechanisms. One well-described mechanism of CHOP-induced apoptosis is the suppression of the anti-apoptotic protein Bcl2. *In vitro* and *in vivo* studies reported a correlation between downregulation of Bcl2, which blocks mitochondrial permeabilization, and elevated CHOP concentrations (34, 90). Additionally, prolonged ER stress and increased CHOP levels cause induction of apoptosis via

oxidative stress, either directly through generation of ROS (22) or indirectly through increased ER oxidoreductase 1α (Ero1α) expression, which hyperoxidizes the ER and promotes cell death (72). Moreover, CHOP initiates the extrinsic apoptotic pathway by expression of death receptor 5 (DR5), also known as TRAIL receptor 2 (TRAILR2), a caspase-activating cell-surface receptor of the TNFR family (145).

Of relevance for this study, bacterial airway infection leads to the activation of toll-like receptors, which in turn can induce phosphorylation and activation of eIF2α, resulting in upregulation of ATF4 and CHOP expression (74). Furthermore, CHOP-deficient mice were protected from cell apoptosis in LPS-induced lung injury (25).

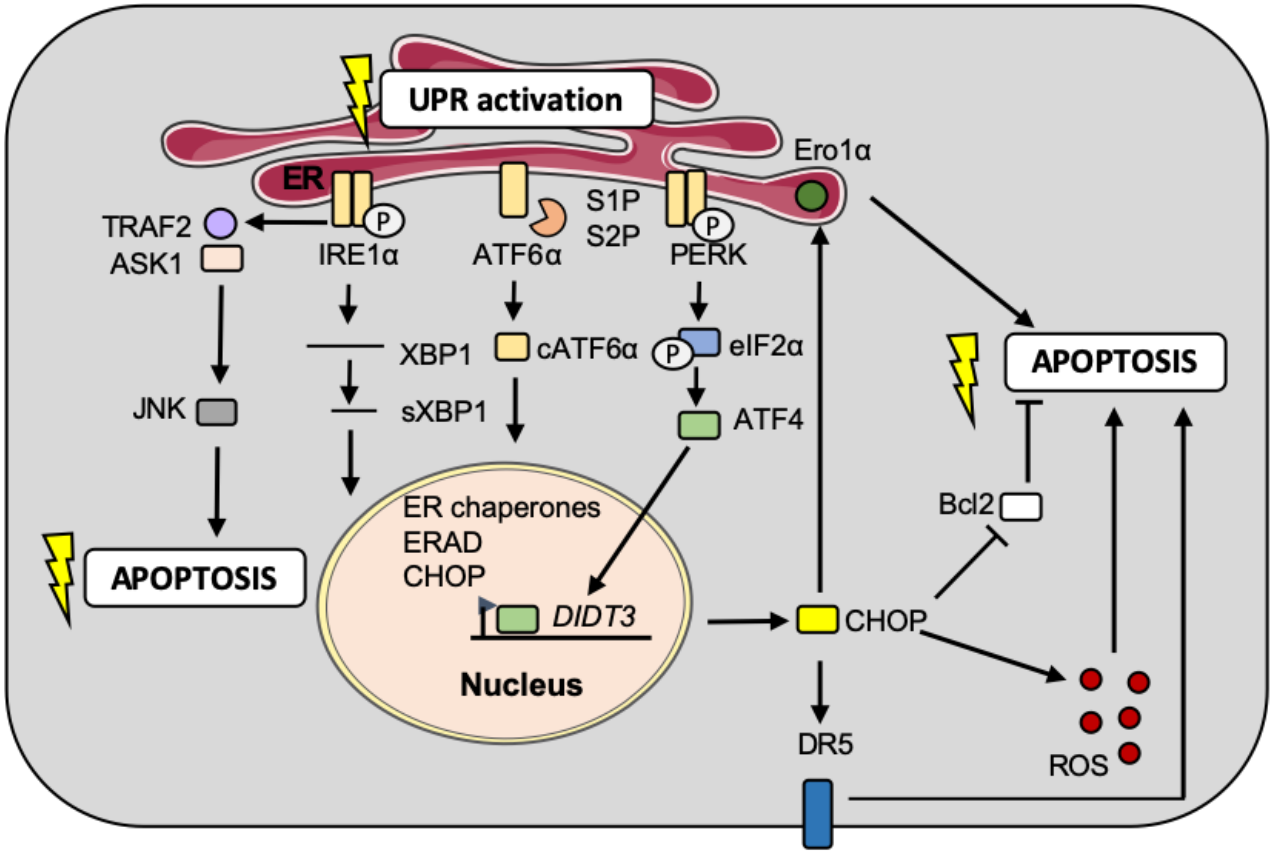

Figure 1-4: Mechanisms of ER stress-induced apoptosis.

The ER stress response is initiated by activation of the three sensor proteins: inositol-requiring enzyme 1 (IRE1), protein kinase-like ER kinase (PERK), and activating transcription factor 6 (ATF6). Upon dimerization and phosphorylation, IRE1α splices X-box binding protein 1 (sXBP1) mRNA, which upregulates UPR genes encoding ER chaperones and the ER-assisted degradation (ERAD) machinery. IRE1α also recruits TNF receptor-associated factor 2 (TRAF2) and apoptosis signal-regulating kinase 1 (ASK1), leading to downstream activation of c-Jun N-terminal kinase (JNK), which can induce apoptosis. Activated ATF6 is cleaved by the proteases S1P (site 1 protease) and S2P (site 2 protease), and the cleaved ATF6 (cATF6) fragment forms an active transcriptional factor that mediates expression of several components important for protein folding and degradation. PERK phosphorylates eukaryotic translation initiation factor 2α (eIF2α) and enhances ATF4-dependent protein translation, including expression of pro-apoptotic C/EBP homologous protein (CHOP), which is encoded by the DNA damage-inducible transcript 3 (*DIDT3*) gene. CHOP stimulates generation of reactive oxygen species (ROS) and induces expression of proteins that contribute to cell death, including ER oxidoreductase 1 α (Ero1α) and death receptor (DR5). Additionally, CHOP suppresses the expression of anti-apoptotic protein Bcl2.

1.3 Amino acid (AA) signaling pathways in ARDS

Amino acids (AAs) are not only the main building blocks of proteins, hormones and metabolites - they also serve as an energetic source and act as signaling molecules and regulators of gene expression. Consequently, efficient regulatory mechanisms to ensure homeostatic intracellular and extracellular AA composition are mandatory for normal cell function. In line with this notion, nutritional deprivation, particularly the unavailability of essential AAs, has been shown to be associated with more severe clinical outcomes in critically ill patients (47). Specifically, in acute respiratory failure, mortality in malnourished patients who required mechanical ventilation was significantly higher than in well-nourished patients requiring mechanical ventilation (106), suggesting a direct link between nutritional depletion and lung function. Notably, a study from 1983 showed both beneficial and adverse effects of AAs supplementation on lung function during mechanical ventilation (142). This paradox stresses the need to identify molecular mechanisms that control stress responses to nutritional deprivation in critically ill patients. Although little research has been done so far to address the role of AA bioavailability in the context of lung injury, lack of AAs may cause increased epithelial apoptosis via AA-sensitive mechanisms like mammalian target of rapamycin (mTOR)-dependent- and general control non-derepressible 2 (GCN2) kinase pathways, which will be the focus of the following chapters.

1.3.1 The mammalian target of rapamycin (mTOR) pathway and autophagy

The mTOR complex is a well-described AA sensor and central control hub that integrates a wide array of extracellular and intracellular signals to regulate metabolism and cell growth. Two distinct macromolecular protein complexes are formed by mTOR, in which mTOR acts as catalytic subunit. mTOR complex 1 (mTORC1) contains the protein Raptor (regulatory-associated protein of mTOR), is inhibited by rapamycin, and controls mitogen- and nutrient-sensitive cell growth, whereas mTOR complex 2 (mTORC2) contains the protein Rictor (rapamycin-insensitive companion of mTOR) and is rapamycin-insensitive. While it is well known that intracellular AA availability controls mTORC1 activity, the role of mTORC2 in AA sensing has not been defined (62). In the presence of AAs, mTORC1 is activated and then phosphorylates translational effector proteins such as ribosomal S6 kinase (S6K) and eIF4E-binding protein 1 (4E-BP1) to enhance translation of targets involved in cell growth (40). The mTOR complex functions as a negative regulator of autophagy, as mTOR inhibits the autophagy initiating complex by interacting with Unc-51-like autophagy activating kinase 1

(ULK1). Inactivation of mTORC1 by stress including AA starvation causes activation of the ULK1-containing pro-autophagic complex, promoting a signaling cascade to induce formation, elongation and maturation of autophagosomes. Activation of the autophagic response has been linked to the development of various forms of lung injury, including ALI following cigarette smoke exposure, acute viral and bacterial infection, or ventilator-induced lung injury (95). Accordingly, in a murine model of ALI induced by intra-tracheal administration of LPS, lung injury and epithelial apoptosis was aggravated by the mTORC1 inhibitor rapamycin (31). Conversely, in influenza-induced lung inflammation, blocking of autophagy not only reduced epithelial cell death, but also attenuated lung injury and mortality (123). Analogously, autophagy was shown to mediate influenza-induced production of pro-inflammatory cytokines and chemokines in epithelial cells, while inhibition of autophagy ameliorated lung inflammation (103). In contrast, however, activated autophagic protein LC3B may play a protective role in hyperoxia-induced lung injury via interaction with Fas-mediated apoptosis pathways (127). This seeming contradiction is in line with the dual role of autophagy as a physiological pro-survival mechanism, while excessive autophagy leads to programmed cell death via a complex crosstalk between autophagic and apoptotic pathways (71).

1.3.2 The general control non-derepressible 2 (GCN2) kinase pathway

Another important AA sensing pathway is the GCN2 kinase pathway, which plays a major role in cellular homeostasis and is initiated upon AA deprivation. GCN2, a serine/threonine-protein kinase, measures AA abundance through binding to uncharged transfer RNA (tRNA) (37, 143). Depletion of even a single AA can lead to GCN2 phosphorylation and activation. Following activation, GCN2 phosphorylates eIF2α, converging with the PERK limb of the ER stress response and inducing selective gene expression via ATF4. As described in Chapter 1.2.4, transcription mediated by ATF4 leads to expression of CHOP, which in turn induces apoptotic pathways (Figure 1-4). Additional ATF4 targets include members of the solute carrier 38 (*SLC38*) family of AA transporters, which contain, besides a C/EBP motif, an amino acid response (AAR) element (102) and are the topic of the next chapter.

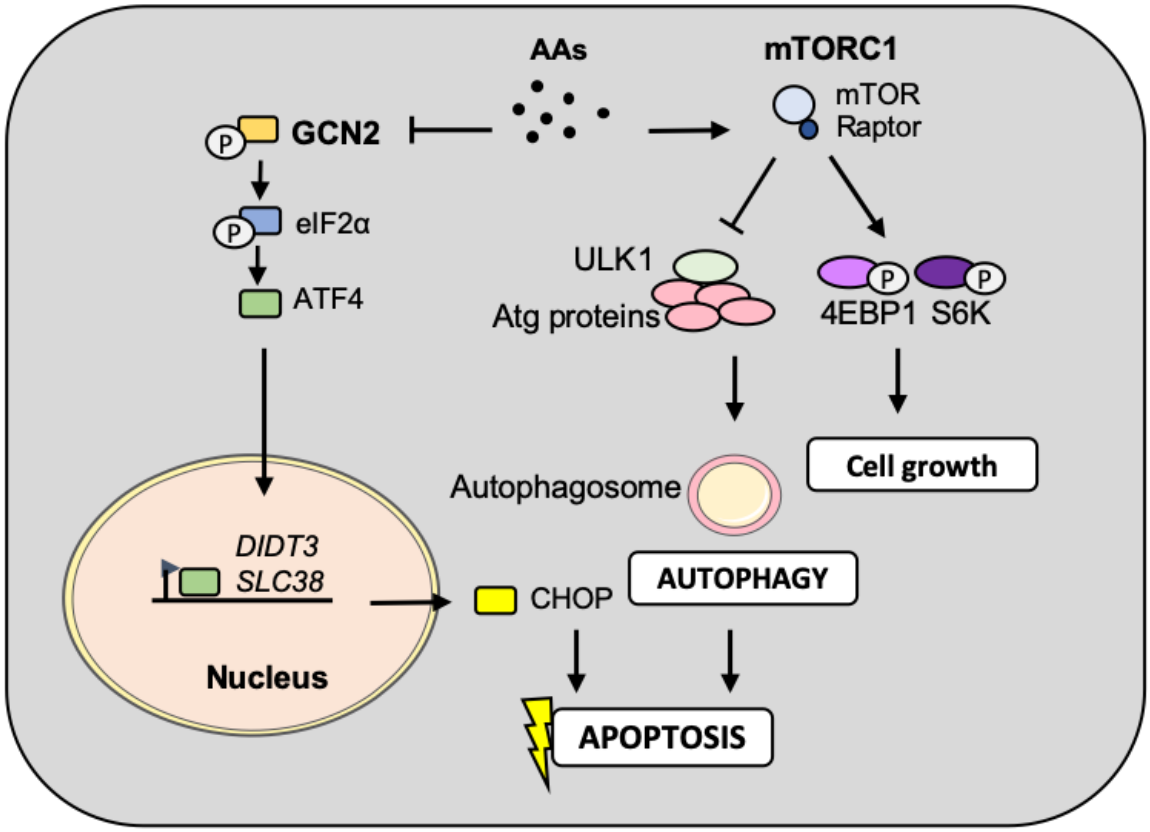

Figure 1-5: Intracellular AA-signaling pathways.

Intracellular AA abundance leads to activation of mammalian target of rapamycin complex 1 (mTORC1), which phosphorylates and activates ribosomal S6 kinase (S6K) and eIF4E-binding protein 1 (4E-BP1) to enhance cell growth. In parallel, mTOR inhibits activation of autophagy by binding to Unc-51-like autophagy activating kinase 1 (ULK1). Deprivation of AAs inhibits mTOR causing activation of autophagy, which can in turn induce cell apoptosis. Lack of intracellular AAs also initiates the GCN2 pathway with GCN2 phosphorylating eukaryotic translation initiation factor 2α (eIF2α) that stimulates ATF4-dependent protein translation, including expression of pro-apoptotic C/EBP homologous protein (CHOP) and members of the solute carrier family 38 (*SLC38*) of AA transporters.

1.4 Sodium-coupled Neutral amino Acid Transporters (SNATs)

SNATs are transmembrane transporters which maintain intracellular homeostasis by mediating the co-transport of small neutral AAs along with a single Na^+ ion. SNATs are encoded by the *SLC38* gene family that comprises 11 members with 6 functional characterized isotypes (Table 1-1). Characterized members are subdivided based on their functional properties into System A or System N transporters (78). SNAT1, SNAT2 and SNAT4 are System A transporters, which mediate the uptake of one neutral AA (AA) with one Na^+ ion. System A SNATs are characterized by a broad substrate profile of small zwitterionic aliphatic AA including alanine, asparagine, serine, glutamine, glycine, methionine, and cysteine. The transporter function of System A SNATs can be blocked by the substrate analogue N-methyl-aminoisobutyric acid (MeAIB) leading to reduced intracellular AA concentrations (12, 91). On the basis of early studies on AA co-transport (20, 44, 60), System A transport can be defined as AA uptake

coupled to the Na^+ electrochemical potential gradient generated by Na^+-K^+-ATPase with a 1:1 stoichiometry. In contrast, the System N subtypes SNAT3 and SNAT5 transport Na^+ and a neutral AA in an antiport against H^+, only accept glutamine, histidine, and asparagine as substrates, and are MeAIB insensitive (12).

Table 1-1: SLC38 family of System A and System N transporters (modified from Bröer 2014)

Gene	Protein	Alias	Substrates	System	Expression
SLC38A1	SNAT1	GlnT, SAT1, ATA1, SA2, NAT2	(G),A,S,C,N,Q,H,(M)	A	ubiquitous
SLC38A2	SNAT2	SAT2, ATA2, SA1	G,P,A,S,C,N,Q,H,M	A	ubiquitous
SLC38A3	SNAT3	SN1, NAT	Q,N,H	N	eye, liver, brain, pancreas
SLC38A4	SNAT4	ATA3, NAT3, SAT3, PAAT	G,(P),A,S,C,N,(M),R,K	A	liver, bladder
SLC38A5	SNAT5	SN2	Q,N,H,A,S	N	mouth, cervix, bladder, bone, intestine, lung, kidney, eye esophagus
SLC38A6	SNAT6		Unknown		esophagus, cervix, mouth, lung, kidney, muscle
SLC38A7	SNAT7		Q,N,H,A,S	N	ubiquitous
SLC38A8	SNAT8		Unknown		testis
SLC38A9	SNAT9		Unknown		parathyroid, testis, adrenal gland, thyroid
SLC38A10	SNAT10		Unknown		ubiquitous
SLC38A11	SNAT11		Unknown		spleen, eye, bone marrow, pharynx

1.4.1 Regulation of SNAT2

While System A transporters share significant sequence homologies, SNAT2 (*SLC38A2*) is the most ubiquitously expressed System A transporter, while SNAT1 is preferentially found in the nervous system and SNAT4 in the liver (78). Additionally, SNAT2 is described as one of the most extensively regulated System A transporters, thus potentially reflecting its important contribution to cellular Na^+ absorption and AA signaling, controlling various cellular functions. In general, transport activity is often regulated by recruitment of transporters from intracellular vesicles to the plasma membrane (66, 97). Accordingly, SNAT2 trafficking from intracellular compartments to the cell surface and subsequent activation can be induced upon appropriate cellular stimulation (51). Factors leading to increased SNAT2 activity include

hormones like glucocorticoids, estrogen and insulin, as well as growth factors, in particular, epidermal growth factor (91). Furthermore, increased pH in the physiological range of pH 6 – pH 8 strongly activates SNAT2-mediated transport, whereas low extracellular pH inhibits transporter activity (78). SNAT2 was also shown to be upregulated in cells exposed to hyperosmotic stress, leading to elevated cellular intake of Na^+ and organic osmolytes (AAs) to help establish an osmotic driving force for water uptake to restore both intracellular volume and ionic strength (10, 17, 48). Another major mechanism of SNAT2 regulation which has been described for all System A transporters and observed in numerous cell types is its ability to undergo adaptive regulation in response to changes in cellular AA availability (49). SNAT2 gene expression is induced by AA deprivation via the GCN2-eIF2α-ATF4 axis (see 1.3.2). The adaptive increase in SNAT2 gene expression is paralleled by an enhanced protein stabilization via a process that involves its reduced ubiquitination and degradation (52). SNAT2 surface stability is negatively regulated by the ubiquitin proteasome system, in particular the ubiquitin E3 ligase Nedd4-2, which binds the transporter and decreases its surface expression by catalyzing its degradation (42). A potential regulatory concept was found for ENaC, where phosphorylation of Nedd4-2 interfered with its binding ability to ENaC, resulting in decreased internalization and, consequently, stabilized ENaC surface expression leading to increased sodium uptake (94, 120). Analogously, previous studies in mice with tissue-specific Nedd4-2 knockout revealed a critical role for Nedd4-2 in regulating salt and fluid transport in epithelia of the lung (112). Similarly, loss of Nedd4-2 in rat lungs by RNA interference reduced extravascular lung fluid (73). The protective effect of Nedd4-2 inhibition on fluid transport has been predominantly attributed to the inhibition of ENaC degradation. However, other Nedd4-2 targets like SNAT2 may be involved but have not been investigated so far.

1.4.2 AA signaling through SNAT2

SNAT2-mediated AA signaling is mainly mediated via the mTOR signaling pathway [93,101,102]. The AAs leucine and arginine are potent activators of mTOR(40), but are not substrates of SNAT2. However, an indirect activation pathway has been described, whereby AAs like glutamine are transported by SNAT2 into the cytosol, which then serve as exchange substrates for general AA antiporter LAT1 (leucine-preferring amino acid transporter 1), resulting in the exchange of intracellular glutamine for leucine (29). Accordingly, depletion or inhibition of System A transporter SNAT2 reduced intracellular AA concentration and impaired mTOR activation (27).

Hence, loss of SNAT2 may lead to intracellular nutritional deprivation, inhibition of mTOR signaling and an increased autophagic response.

Besides indirect activation of the mTOR pathway regulating intracellular AA concentration, a more direct signaling function by SNAT2 has been proposed where SNAT2 acts as an extracellular AA sensor or so-called transceptor (49, 107). This concept proposes that AA ligand binding may directly alter intracellular signaling cascades. There is evidence that SNAT2 may be able to signal directly to mTOR, as MeAIB was found to promote phosphorylation of the mTOR downstream target S6K, independently to changes in intracellular AA concentration (128).

1.4.3 SNAT2-mediated Na^+ transport

Besides functioning as AA transporter, SNAT2 facilitates the cellular uptake of Na^+. However, the functional relevance of SNAT-mediated Na^+ transport has not been addressed so far and relatively little is known regarding the potential role of SNAT2 in lung fluid balance. In freshly isolated ATII cells, Brown and colleagues identified a Na^+ AA co-transport system which accounted for 13% of total sodium entry (13). Their data indicates that System A co-transport uptake may present an important pathway for Na^+ uptake into type II alveolar epithelial cells, and thereby contribute to the maintenance of lung fluid balance. The findings by Brown and colleagues were independently confirmed by a second study demonstrating an alanine-dependent Na^+ co-transport in ATII cells (19). Though there is no evidence to date that SNAT2 is involved in alveolar epithelial Na^+ uptake and alveolar fluid transport in the intact lung, these studies raise the possibility that the co-transport mediated by SNAT2 may play a relevant role in AFC, and thus may protect the lung from excessive fluid accumulation and pulmonary edema.

2 Aims of the project

As ARDS is the most frequent cause of death in critical care medicine, there is an urgent need for a better understanding of its underlying pathophysiology and the mechanisms that maintain alveolar homeostasis and repair. In this context, the aim of the present project was to elucidate the functional role of sodium-coupled neutral amino acid transporter SNAT2 in i) alveolar fluid transport and ii) epithelial cell homeostasis in the intact and injured lung. In the healthy lung, SNAT2-mediated Na^+ uptake may protect the alveolus from edema and injury, in that it drives AFC. In parallel, through its AA transporter function, SNAT2 may maintain adequate intracellular AA levels, and thus sustain homeostatic levels of ER stress, autophagy and apoptosis. Conversely, loss of SNAT2 may drive epithelial apoptosis in lung injury, and prevent resolution of lung edema, thus contributing to the hallmarks of ALI/ARDS.

The following hypotheses were specifically addressed in this thesis:

1. SNAT2-mediated Na^+ uptake maintains alveolar fluid balance and protects the lung from edema formation.
2. SNAT2 is lost under infectious or inflammatory conditions characteristic for ARDS.
3. In the context of lung injury, loss of SNAT2-mediated AA transport leads to increased epithelial apoptosis through a mechanism involving the eIF2α-ATF4 limb of the ER stress response.

3 Methods

3.1 *Ex vivo* studies

3.1.1 Animals

Animal experiments were performed in prospective, randomized and controlled studies in male Sprague-Dawley rats (Charles River Laboratories) with body weights (BW) of 330-400 g, C57BL/6J mice (Charles Rivers Laboratories) of 25-30 g BW, and a SNAT2 (*Slc38a2*) knockout (KO) mouse strain. *Slc38a2*$^{tm1a(KOMP)Wtsi}$ mice (Wellcome Trust Sanger Institute) were generated by reporter-tagged insertion mutagenesis between exon 1 and 2 on a C57BL/6N background. As *Slc38a2* homozygous mice (*Slc38a2*$^{-/-}$) are subviable, experiments were conducted in heterozygous-deficient SNAT2 mice (*Slc38a2*$^{+/-}$) with a BW of 18-25 g and their corresponding wild type (WT).

Animal experiments were in conformity to institutional and governmental guidelines and designed according to the 3R principle (reduction, refinement, replacement). All procedures were approved by the responsible governmental body (Landesamt für Gesundheit und Soziales, LAGeSo) under the registration numbers T0279/13 and G0404/17.

3.1.2 Isolated perfused mouse lung (IPL)

Lungs from C57BL/6J, *Slc38a2*$^{+/-}$ and corresponding WT mice were isolated, placed in a 37°C water-jacketed chamber (Hugo Sachs Elektronik HAVARD apparatus), and constantly inflated with a gas mixture of 21% O_2 ,5%C O_2, and 74% N_2 at a positive airway pressure of 5 cmH_2O. The pulmonary artery and the left atrium were cannulated, and the lungs were continuously pump-perfused at 1 ml/min with Hank's balanced salt solution (HBSS) containing 20% fetal calf serum (FCS) in a circulating system at 37°C and a baseline left atrial pressure (P_{LA}) of 2 cmH_2O, as described previously (15, 121, 132). Edema formation was induced by increased hydrostatic pressure (PLA 7 cmH2O) or simulated by intratracheal instillation of 100 µL HBSS with or without 2 mMol/L L-alanine or 10 mMol/L SNAT inhibitor N-methyl-aminoisobutyric acid (MeAIB). As SNAT2-dependent fluid absorption may be masked by other Na^+ channels, particularly ENaC, 10 µMol/L amiloride was added to the instillate in some experiments. The pulmonary artery pressure (P_{AP}) in isolated lungs was monitored continuously via differential low-pressure transducers and PULMODYN Data Acquisition Software (HAVARD Apparatus).

After 30 min, the experiment was terminated and the lungs were collected for quantification of the wet-to-dry lung weight (wet/dry) ratio as a measure of lung edema.

3.1.3 Double indicator dilution technique (DIDT) in the isolated perfused rat lung

To differentiate between alveolar fluid shifts as a consequence of passive fluid filtration and active alveolar fluid transport, a previously established two-compartmental double-indicator dilution technique (DIDT) in the isolated perfused rat lung was applied (121). To this end, lungs from Sprague-Dawley rats were isolated and pump-perfused at 37°C with 14 mL/min perfusion buffer (see 3.6.1) containing 3% bovine serum albumin (BSA). The lungs were continuously ventilated with a tidal volume of 10 mL/kg BW and a respiratory rate of 80 breaths/min. For measurements of alveolar fluid transport, 0.15 mg/mL of the fluorescent high-molecular mass tracer Texas red dextran (70 kDa, excitation/emission wavelengths 595/615 nm; Life Technologies), which cannot cross the intact alveolocapillary barrier, was diluted in 5 mL of Ringer´s solution and instilled into the distal air space. In parallel, 0.02 mg/mL of the low-molecular mass tracer Na^+- fluorescein (360 Da, excitation/emission wavelength 460/515 nm; Sigma-Aldrich), which reflects passive paracellular fluid filtration, was added to the lung perfusate. Samples of both the alveolar instillate and the lung perfusate were drawn after 0, 10 and 60 min of perfusion. Tracer concentrations in the instillate and perfusate were assessed by fluorescence measurements of each sample using a spectrophotometer (SpectraMax M5e micro plate reader, Molecular Devices). Active fluid transport (net fluid shift) in and out the alveolar space was calculated from the change in concentration of Texas Red Dextran in the alveolar instillate. The fluid filtration rate was determined from the Na^+- fluorescein concentration in the alveolar space. Active alveolar fluid transport reflecting osmotically driven fluid shifts between the distal air spaces and the interstitial space in the form of alveolar fluid clearance (AFC) or secretion (AFS), respectively, and was calculated as the difference between net fluid shift into the alveolar space and fluid filtration rate. Positive values (> 0mL/h) reflect AFS and values <0 mL/h reflect AFC.

3.2 *In vivo* studies

3.2.1 LPS-induced acute lung injury (LPS-ALI) in mice

For induction of lung injury by LPS, *Slc38a2*$^{+/-}$ and corresponding WT mice were anesthetized by isoflurane inhalation and 5 mg/kg BW LPS (*E.coli* 0111:B4) diluted in 30 µL of 0.9%-isotonic NaCl was applied intranasally. Control mice received 30 µL of pure 0.9%-isotonic NaCl. After

24 h, mice were anesthetized by intraperitoneal application of a mixture of 100 mg/kg BW ketamine and 20 mg/kg BW xylazine and placed in a supine position on a heating pad. The trachea was cannulated, and mice were mechanically ventilated with a tidal volume of 7 mL/kg BW and a respiratory rate of 150 breaths/min using a MiniVent mouse ventilator (Hugo Sachs Electronic HAVARD apparatus). Next, mice were sacrificed by exsanguination and the lungs were excised for post hoc analyses. Lung edema was estimated as wet/dry ratio from the superior lobe of the right lung. The lower lobe and accessory lobe of the right lung were frozen in liquid nitrogen and utilized for analyses of protein and RNA expression profiles. The left lung was washed three times with 100 µL of ice-cold phosphate-buffered saline (PBS) to obtain bronchoalveolar lavage fluid (BALF). Protein concentration in BALF as an indicator of alveolo-capillary barrier failure was quantified by colorimetric bicinchoninic acid assay (BCA, see section 3.4.1). The experimental protocol for the *in vivo* lung injury model is schematically shown in Figure 3-1.

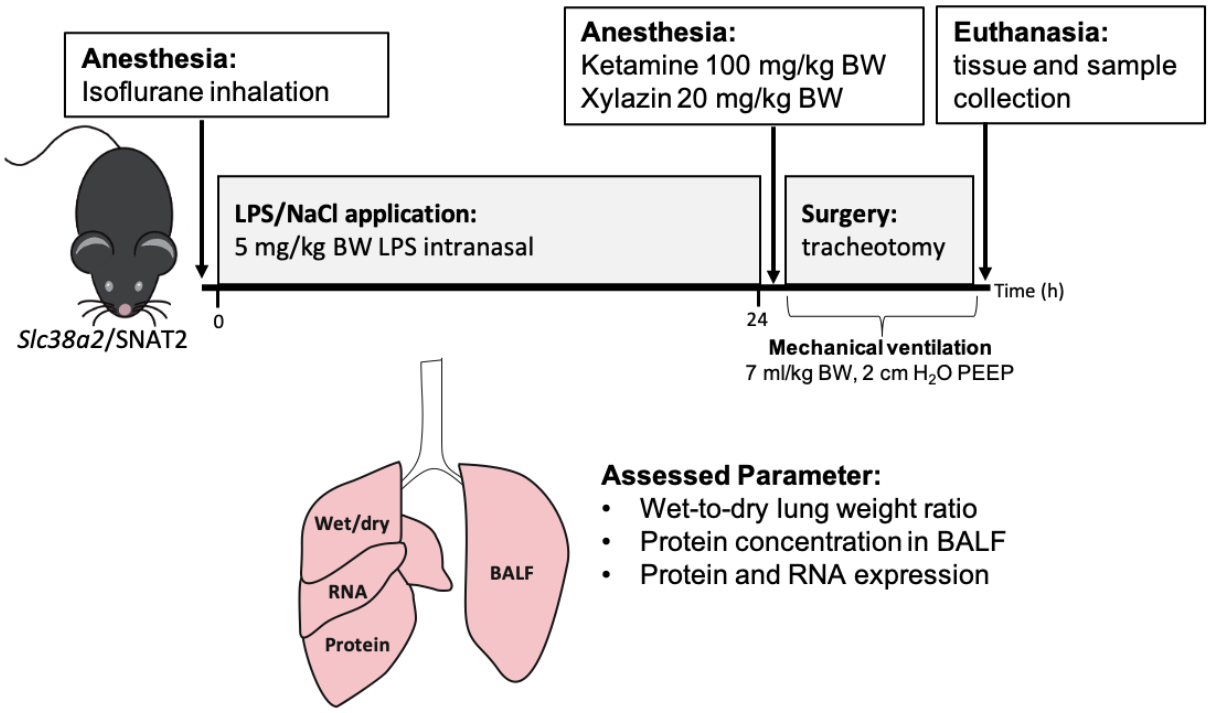

Figure 3-1: Experimental protocol of the LPS-ALI model in mice.

3.2.2 Acid-induced acute lung injury (HCl-ALI) in mice

Slc38a2$^{+/-}$ and the corresponding WT mice were anesthetized as described above and placed in supine position on a thermostatically controlled electric heating blanket to maintain body temperature at 37.5° C. Following tracheotomy, mice were ventilated with room air at 150 breath/min, positive end-expiratory pressure (PEEP) of 2 cmH_2O, and a tidal volume of 7 mL/kg BW. The right jugular vein was cannulated for a continuous infusion of 200 µL/h anesthetic

mixture of 100 mg/kg BW ketamine and 20 mg/kg BW xylazine in 0.9%-isotonic NaCl. After surgical preparation and a stabilization period of 15 min, lung injury was induced by intratracheal application of 2 mL/kg BW hydrochloric acid (HCl; pH 1.5). After 2 h, mice were euthanized by exsanguination and the lungs were excised for analysis of edema formation (wet/dry ratio) and changes in protein and RNA expression profiles as described above. The experimental protocol for the acid-induced lung injury model is schematically presented in Figure 3-2.

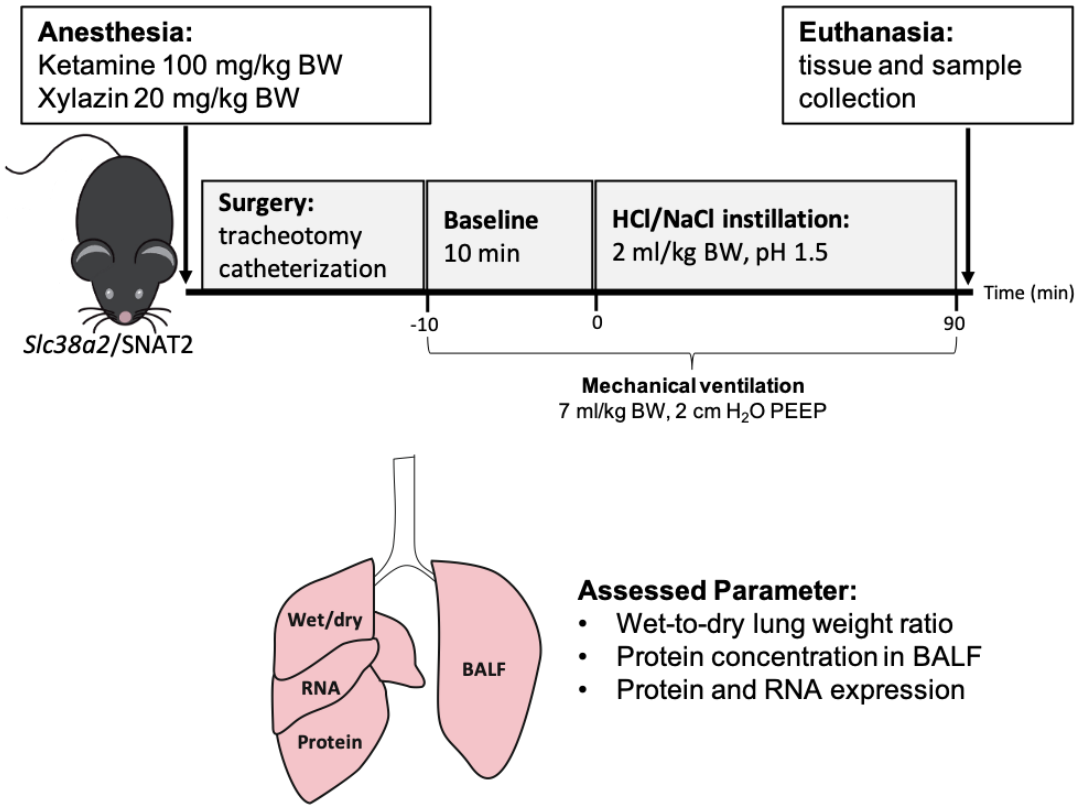

Figure 3-2: Experimental protocol of the HCl-ALI model in mice.

3.3 *In vitro* studies

3.3.1 Cell culture

Pulmonary epithelial cell lines A549 and NCI-H441 were propagated in T75 cell culture flasks in appropriate media (Table 3-1) containing 10% FCS and 1% penicillin/streptomycin. Human primary epithelial cells (hPAEpCs) were cultured in complete human epithelial cell culture medium (Cell Biologics) as recommended by the manufacturer. Cells were kept in a humidified atmosphere at 37°C and 5% CO_2 in a standard cell incubator. At 80% confluence, cells were detached and singularized with Trypsin-EDTA after washing with Dulbecco´s PBS (DPBS). Trypsinization was stopped by resuspension in standard medium and cells were seeded at the desired dilution into culture dishes containing fresh medium.

Table 3-1: List of pulmonary epithelial cells

Cells	Origin	Culture medium
A549	human alveolar epithelial adenocarcinoma cell line	High Glucose DMEM (Gibco)
NCI-H441	human lung adenocarcinoma epithelial cell line	RPMI – 1640 (Gibco)
hPAEpCs	human primary alveolar epithelial cells	Complete human epithelial cell culture medium (Cell Biologics)

***Cryopreservation*:** To preserve cells for longer periods, aliquots of each cell line were stored in liquid nitrogen at -196°C. After trypsinization, cells were resuspended in 1.5 mL serum-free cryo medium (cryo-SFM, PromoCell) and transferred into cryo vials (1x 10^6 cells/vial). Before storage in liquid nitrogen, cells were kept in a freezing container at -80°C overnight. To thaw frozen cells, cryo vials were warmed in a water bath at 37°C and the contents were immediately dissolved in pre-warmed standard medium. Cells were transferred to a culture flask and the media was changed the next day.

Cell counting: The number of viable cells was counted by trypan blue dye exclusion using a hemocytometer. Cells were harvested as described above and 10 µL of cell suspension was mixed with 10 µL of 0.4% trypan blue. A quantity of 10 µL of the mixture was added to the hemocytometer. Dead cells incorporating trypan blue appear blue under the microscope due to their injured cell membrane and were accordingly excluded from cell counts.

3.3.2 Gene silencing

NCI-H441 cells were seeded at a density of 50,000 cells/cm^2 on a 6-well culture plate and grown for 2 days until confluence was reached. To specifically knockdown SNAT2 gene expression, cells were treated with small interfering RNA (siRNA) targeting SNAT2 (SantaCruz) and a scrambled control siRNA (SantaCruz). Prior to siRNA treatment, cells were incubated in basal culture medium containing only 1% FCS for 2 h at 37°C and 5% CO_2. Transfection was performed using the Effectene Transfection Reagent (Qiagen) according to the manufacturer's protocol. Successful downregulation of SNAT2 gene expression was confirmed by quantitative real time PCR (qRT-PCR, see 3.4.2).

3.3.3 Stimulation of cell lines

To test for the effects of infectious or inflammatory mediators on SNAT2 expression, epithelial cells NCI-H441 were cultured to confluence on 12-well plates at a density of 50,000 cells/ cm^2. After incubation in basal medium for 2 h, cells were treated for 24 h with 0.2 µg/mL

pneumolysin (PLY), a toxin released by *Streptococcus pneumoniae*, or 50 ng/mL of a cytokine cocktail containing TNF-α, IFN-γ, IL-1β and LPS (Cytomix). For analysis of changes in SNAT2 expression, cells were lysed and protein or RNA was extracted for western blot analysis (3.4.1) or qRT-PCR (see 3.4.2), respectively.

3.3.4 AA deprivation

To test for the effects of AA deprivation on SNAT2 expression, NCI-H441 cells were seeded on 12-well plates as described above. At confluence, cells were incubated in basal culture medium for 2h. To deprive cells of AAs, the medium was replaced with Earl´s balanced salt solution (EBSS), a starvation medium (114), and cells were incubated for further 4h or 8h, respectively, followed by cell lysis for protein and RNA extraction.

3.3.5 L-alanine transport assay

L-alanine transport through lung epithelial cells was measured in a transwell assay system (Figure 3-3) in the epithelial cell line NCI-H441 and in hPAEpCs. Cells were grown at a density of 450,000 cells/cm^2 on a 3 µm pore polycarbonate membrane insert (Corning®). After 48 h, the complete medium was changed to basal medium containing only 1% FCS and cells were preincubated either with 10 mMol/L of the SNAT inhibitor MeAIB or 100 µMol/L of mercury chloride ($HgCl_2$) (a non-specific inhibitor of SNATs) for 4 h, or treated with siRNA targeting SNAT2 or scrambled siRNA (see 3.3.2). To start the experiment, the medium was replaced with 500 µL buffer (PBS + 0.2% BSA) in the lower well and 100 µL buffer containing 2 mMol/L L-alanine was added to the upper well. After 2h of incubation at 37°C, 50 µL solution was collected from the lower well. Alanine concentration was quantified by a colorimetric alanine detection kit (Sigma) according to the manufacturer´s protocol and absorbance was measured at 570 nm using a 96-well microplate reader (Sunrise™, TECAN or SpectraMax M5e, Molecular Devices).

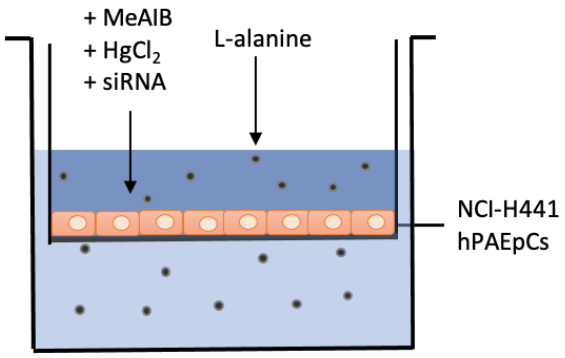

Figure 3-3: L-alanine transwell assay in NCI-H441 cells.

3.4 Biochemical and molecular biological methods

3.4.1 Western blotting

To analyze changes in protein expression profiles, proteins from mouse lung tissue and lung epithelial cells (A549, NCI-H441, hPAEpCs) were extracted. Cells were directly lysed in 250 µL radioimmunoprecipitation assay (RIPA) buffer (3.6.1), whereas mouse lung tissue was first cut into small pieces and then homogenized for 30-50 s in 500 µL RIPA buffer using an IKA® T10 basic Ultra Turrax disperser. To remove cellular debris, the lysed cells and lung tissues were centrifuged (12,000 g, 10 min, 4°C) and protein concentrations of the supernatants were determined by BCA (Pierce™ BCA protein assay kit, Thermo Fisher Scientific). Colorimetric quantification was performed using a 96-well microplate reader (Sunrise™, TECAN) at a wavelength of 562 nm. For protein separation by sodium dodecyl sulfate polyacrylamide gel electrophoresis (SDS-PAGE), 10-20 µg of protein was mixed with dithiothreitol (DTT) containing reducing loading buffer (Laemmli sample buffer, Bio-Rad) and incubated for 5 min at 95°C. Subsequently, protein lysates were separated in a 10% SDS-polyacrylamide gel (Table 3-2) under reducing conditions at 120 V for 90 min (67) using a Mini-PROTEAN electrophoresis system (Bio-Rad). Following separation, proteins were transferred to a nitrocellulose membrane (Bio-Rad) over 90 min at 100 V using a wet blotting system (129). Non-specific epitopes were blocked by incubating membranes in tris buffered saline (TBS) containing 0.1% Tween 20 (TBS-T) and 5% milk powder for 60 min. Specific primary antibodies (see 3.6.3) were dissolved in TBS-T containing 3% BSA, added to the membranes and stored overnight at 4°C. After washing three times for 5 min with TBS-T, membranes were incubated with the appropriate horseradish peroxidase (HRP)-conjugated secondary antibody (see 3.6.3) at room temperature for 60 min, followed by three additional washing steps. Proteins of interest were visualized using the reaction of HRP with a chemiluminescent substrate (ECL™ Prime Western

blotting detection reagent, Amersham) and protein bands were captured by a Celvin® chemiluminescence imaging system.

To remove all bound antibodies from the PVDF membrane, blots were incubated in stripping buffer (CANDOR) for 40 min at room temperature, followed by three washing steps with TBS-T (5 min). After blocking for 30 min with TBS-T containing 5% milk powder, the membrane was stained with a primary antibody detecting glycerinaldehyd-3-phosphat dehydrogenase (GAPDH), which was used as loading control, and staining was performed as described above.

Table 3-2: Composition of the polyacrylamide gels

Reagent	Stacking gel (5 ml)	Separation gel (10 ml)
0.5 Mol/L Tris/HCl, pH 6.8	0.325 ml	-
1.5 Mol/L Tris/HCl, pH 8.8	-	2.5 ml
30% acrylamide mix	0.25 ml	3.3 ml
10 % SDS	5 µl	100 µl
10% ammonium persulfate (APS)	5 µl	100 µl
tetramethylethylenediamine (TEMED)	2 µl	5 µl
Aqua bidest	1.4 ml	4 ml

3.4.2 Quantitative real-time polymerase chain reaction (qRT-PCR)

Changes in gene expression profiles in mouse lung tissue and epithelial cells (A549, NCI-H441, hPAEpCs) were examined by qRT-PCR. For RNA isolation, cells were lysed in 350 µL RLT buffer provided by the RNeasy RNA isolation Kit (Qiagen). Lung tissue was homogenized as described above in 500 µL RLT buffer. Samples were further processed following the instructions of the kit's manufacturer. RNA concentrations of each sample were measured using a NanoDrop™ Lite Spectrophotometer (Thermo Fisher Scientific). Subsequently, 200-500 ng of RNA was transcribed into cDNA using a First Strand cDNA Synthesis Kit (Thermo Fisher Scientific) according to the manufacturer's protocol. Quantitative RT-PCR was performed with the QuantStudio 5 Real-Time PCR System (Applied Biosytems) using the QuantiFast SYBR Green PCR Kit (Qiagen). Reactions were set up according to the manufacturer's instructions with the following primers:

SLC38A2/SNAT2 (human) for 5´- GTGTTAATGGCTGTGACCCTGAC -3´

	rev 5´- GAGACTATGACGCCACCAACTGA -3´
Slc38a2/SNAT2 (mouse)	for 5´- TCACCGTGACCATCTTGTCC-3´
	rev 5´- TGCACGGATCTCATTGGTTC-3´
SLC38A1/SNAT1 (human)	for 5´- GTGTATGCTTTACCCACCATTGC -3´
	rev 5´- GCACGTTGTCATAGAATGTCAAGT-3´
SLC38A4/SNAT4 (human)	for 5´- TTGCCGCCCTCTTTGGTTAC -3´
	rev 5´- GAGGACAATGGGCACAGTTAGT -3´
Ddit3/CHOP (mouse)	for 5´- CCACCACACCTGAAAGCAGAA-3´
	rev 5´- AGGTGAAAGGCAGGGACTCA-3´
ATF4 (mouse)	for 5´- GGGTTCTGTCTTCCACTCCA-3´
	rev 5´- AAGCAGCAGAGTCAGGCTTTC-3´
GAPDH (human+ mouse)	for 5´- TCACCACCATGGAGAAGGC-3´
	rev 5´- GCTAAGCAGTTGGTGGTGCA-3´
RPL13 (mouse)	for 5´- CCCTCCACCCTATGACAAGA-3´
	rev 5´- CTGCCTGTTTCCGTAACCTC-3´

For quantification of qRT-PCR data the comparative 2-$\Delta\Delta C_T$ (cycle threshold) method (76) was used, with ribosomal protein L13a (RPL13) as housekeeping control for mouse lung samples and GAPDH for cell lysates, respectively.

3.4.3 Genotyping

For genotyping of *Slc38a2* mice, DNA was extracted from tail biopsies or ear punches using the REDExtract-N-Amp™ Tissue PCR Kit (Sigma-Aldrich). In brief, samples were incubated with 100 µL extraction solution containing 25 µL tissue preparation solution for 15 min at room temperature. After boiling samples for 7 min at 95°C, 100 µL neutralization solution was added to stop the reaction. PCR mix was prepared according to the manufacturer's instructions using 0.5 µMol/L of one of the following primers:

*Slc38a2*_common	for 5´-CAGTGTCACCCCAGAACCAG-3´
*Slc38a2*_KO	rev 5´-TCGTGGTATCGTTATGCGCC-3´

*Slc38a2*_WT rev 5´-AAGGAAGGCAGGTAGAGGTGG-3´

Extracted DNA was amplified in a standard PCR cycler (MJ Research PTC-200 Thermal Cycler, Marshall Scientific) using the following PCR settings:

Initial denaturation	94°C	5 min	
Denaturation	94°C	30 sec	35 cycles
Annealing	58°C	30 sec	
Elongation	72°C	45 sec	
Final elongation	72°C	7 min	

After amplification, 10 µL of DNA was loaded on a 1% agarose gel containing 1x GelRed® nucleic acid gel stain (Biotium) and separated by gel electrophoresis at 100 V with Tris-Acetate-EDTA (TAE) as running buffer. Finally, DNA was visualized using a UV-transilluminator (Dark Hood DH-50, Biostep).

3.5 Statistical Analysis

All results were analyzed using the statistical software GraphPad Prism 8 (GraphPad Inc.). Groups were compared using the one-sample t-test (hypothetical value = 1), one-way analysis of variance (ANOVA) or two-way ANOVA followed by Bonferroni post hoc test. Data were considered significantly different at probability values < 0.05. In all figures, data are shown as mean ± standard error of the mean (SEM).

3.6 Materials and solutions

3.6.1 Buffer

Buffer	Components
Perfusion buffer (rat IPL)	130 mMol/L NaCl 1.4 mMol/L $CaCl_2$ 4 mMol/L KCl 1 mMol/L Mg $Cl_2 \bullet 6H_2O$ 28 mMol/L Na-lactate 8.3 mMol/L D-glucose
RIPA lysis buffer	150 mMol/L NaCl 50 mMol/L Tris/HCl 1% Nonidet P-40 0.1% SDS 1x phosphatase and protease inhibitor pH adjusted to 7.5
10x SDS PAGE running buffer	0.25 Mol/L Tris 1.92 Mol/L Glycine 1% SDS pH adjusted to 7.5
10x Transfer buffer	0.25 Mol/L Tris 1.92 Mol/L Glycine 0.1% SDS (20% Ethanol added to 1x buffer)
10x TBS	0.05 Mol/L Tris 0.1 Mol/L NaCl pH adjusted to 7.4
50x TAE buffer	2 Mol/L Tris 1 Mol/L acetic acid 50 mMol/L EDTA

3.6.2 Stimulants and inhibitors

Name	Catalog No.	Manufacturer
Amiloride hydrochloride hydrate	A7410	Sigma Aldrich
$HgCl_2$	1044190050	Sigma Aldrich
IFN-γ recombinant human protein	PHC4031	Thermo Fisher Scientific
IL1-β recombinant human protein	10139HNAE5	Thermo Fisher Scientific
L-alanine	A7627	Sigma Aldrich
LPS, *E.coli* 0111:B4	LPS25	Sigma Aldrich
MeAIB	M2383	Sigma Aldrich
TNF-α recombinant human protein	10602HNAE5	Thermo Fisher Scientific

3.6.3 Antibodies

Primary antibodies	Catalog No.	Manufacturer
Anti-CHOP mouse	2895	Cell Signaling
Anti-GAPDH rabbit	ab9485	Abcam
Anti SNAT2 rabbit	LS-C179270	LSBio
Anti SNAT2 rabbit	ab90677	Abcam

Secondary antibodies	Catalog No.	Manufacturer
Anti-mouse IgG HRP	7076	Cell Signaling
Anti-rabbit IgG HRP	ab205718	Abcam

3.6.4 Commercially available kits

Name	Catalog No.	Manufacturer
Alanine assay kit	MAK001	Sigma Aldrich
Pierce™ BCA protein assay kit	23227	Thermo Fisher Scientific
RNeasy Mini Kit	74106	Qiagen
First strand cDNA synthesis kit	K1622	Thermo Fisher Scientific
QuantiFast SYBR green PCR kit	20456	Qiagen
Effectene Transfection Reagent	301425	Qiagen
REDExtract-N-Amp™ Tissue PCR Kit	XNAT	Sigma Aldrich

4 Results

4.1 SNATs mediate Na^+ transport in isolated perfused lungs (IPL)

Under physiological conditions active movement of ions and fluid across the epithelial barrier maintains normal lung function and protects the lung from the development of edema. Dysregulation of fluid transport due to loss of activity and/or expression of ion channels and pumps including ENaC and the Na^+-K^+-ATPase leads to accumulation of fluid in the alveolar space. By use of a double indicator dilution assay in the rat IPL model (see 3.1.3), our group previously showed that inhibition of ENaC by amiloride blocks AFC (121), which was replicated herein in new DIDT experiments (Figure 4-1). However, as only 50% of fluid transport is amiloride-sensitive (36), and thus ENaC-dependent, we focused in the present study on amiloride-insensitive SNATs. To test the functional relevance of SNATs in alveolar fluid transport, the SNAT substrate L-alanine (5 mMol/L) was added to the instillate, which partially reversed amiloride-induced inhibition of fluid transport and, as such, rescued AFC (Figure 4-1). This rescue by L-alanine in amiloride-treated lungs was both Na^+-dependent and sensitive to $HgCl_2$, a non-specific inhibitor of SNATs. In fact, application of $HgCl_2$ or a Na^+ free alveolar instillate not only blocked AFC, but further reduced alveolar fluid flux to negative values (reflecting AFS) significantly below those of amiloride alone, highlighting the functional relevance of amiloride-insensitive, $HgCl_2$-sensitive Na^+ (co-) transport in alveolar fluid transport.

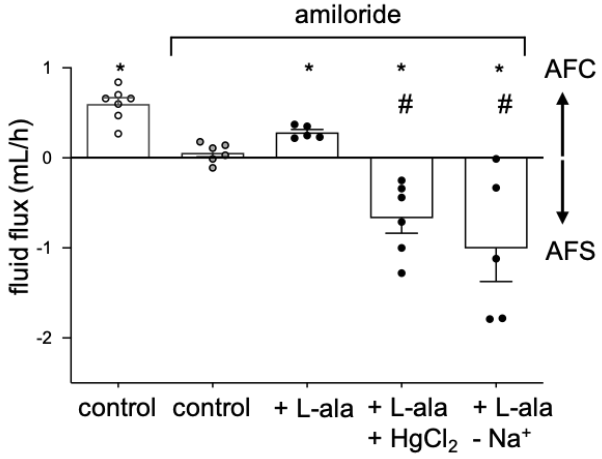

Figure 4-1: SNATs mediate alveolar fluid transport in isolated perfused rat lungs.

Fluid flux was determined by a double-indicator dilution technique (DIDT) in isolated perfused rat lungs. Negative values represent alveolar fluid secretion (AFS), positive values represent alveolar fluid clearance (AFC). Intratracheal administration of 10 µMol/L amiloride inhibited basal AFC. Addition of 5 mMol/L L-alanine (L-ala) to the alveolar instillate restored AFC, which was blocked in turn by Na^+-free instillate or 100 µMol/L of the non-specific SNAT inhibitor $HgCl_2$. Data are mean ± SEM. *p<0.05 vs. control + amiloride and #p<0.05 vs. L-ala + amiloride.

The functional importance of SNATs in AFC was further validated by measuring wet/dry ratios in isolated perfused lungs of C57BL/6J mice. Edema formation was induced by intratracheal instillation of fluid (100 µL HBSS). Addition of amiloride to the instillate increased wet/dry ratios in the lungs of C57BL/6 mice (Figure 4-2 A). This effect was again rescued by addition of L-alanine and blocked by the SNAT inhibitor MeAIB. Moreover, inhibition of SNAT alone in the absence of amiloride sufficed to increase W/D ratio in fluid-instilled murine lungs.

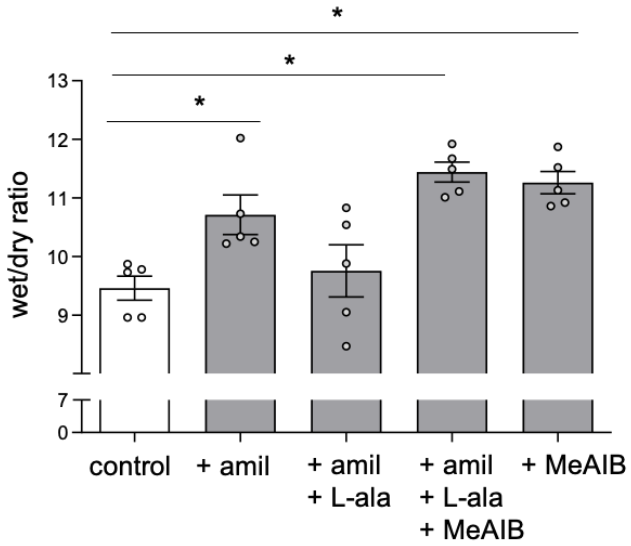

Figure 4-2: SNATs contribute to edema resolution in isolated perfused mouse lungs.

After 5 min of baseline perfusion and mechanical ventilation, pulmonary edema was simulated in isolated perfused lungs of C57BL/6J mice by intratracheal administration of 100 µL HBSS with or without 10 µMol/L amiloride (amil), 2 mMol/L L-alanine (L-ala), or 10 mMol/L of the SNAT inhibitor MeAIB in the instillate. The lungs were continuously perfused with HBSS containing 20% FCS and ventilated for 30 min. Wet-to-dry (wet/dry) lung weight ratio was increased by amiloride. This effect was prevented by L-alanine and again blocked by MeAIB. Data are ± SEM. *p<0.05

Taken together, results from the independently performed rat and mouse IPL experiments identify SNAT-mediated Na^+ transport as an important mechanism of AFC, which may protect the lungs from fluid accumulation and the formation of pulmonary edema.

4.2 Expression profile of System A transporters in alveolar epithelial cells

As the previously described functional data point to a potential role of SNATs in AFC, we next probed for the expression of System A subtypes in alveolar epithelial cells.

Initial PCR analyses identified expression of SNAT1 - SNAT6 isotypes in rat lung tissue (Figure 4-3 A). In subsequent analyses, we focused specifically on system A SNATs because of their inhibitability by MeAIB on the one hand, and their broad expression profile and restriction to Na^+ and AA, yet not to H^+ transport, on the other. In line with previous reports that SNAT1 and SNAT2 are ubiquitously expressed, while SNAT4 is restricted to the liver and bladder (12), SNAT1 and in particular SNAT2 mRNA - yet not SNAT4 mRNA - were detected in the lung

epithelial cell lines A549 (Figure 4-3 B), NCI-H441 (Figure 4-3 C) and hPAEpCs (Figure 4-3 D). Based on its prominent expression at the mRNA level, SNAT2 protein expression was analyzed, and was again verified in A549, NCI-H441 and hPAEp cells (Figure 4-3 E). These data indicate that SNAT2 is the most abundantly expressed System A transporter in the pulmonary epithelium.

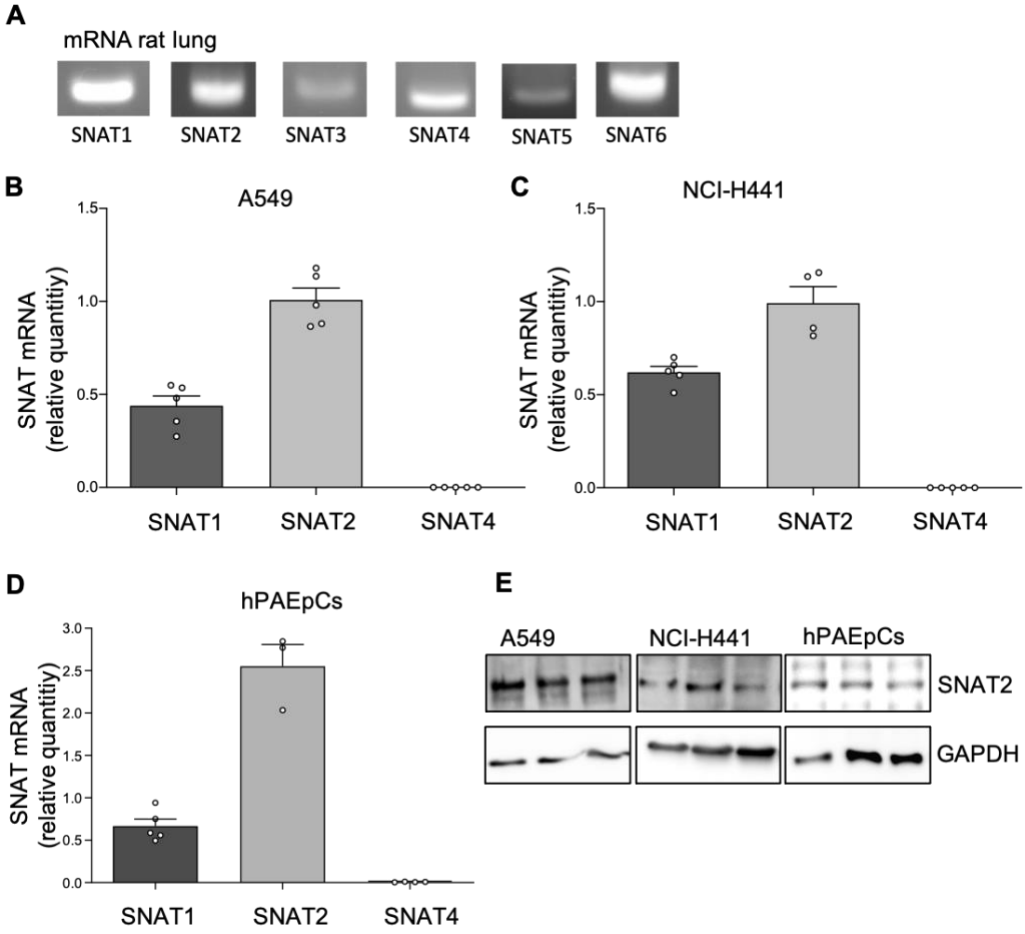

Figure 4-3: Expression of SNATs in alveolar epithelial cells.

(A) Expression of mRNA for all SNAT isotypes was determined by PCR in rat lung homogenates. In A549 cells (B), NCI-H441 cells (C) and hPAEpCs (D), mRNA expression of System A SNATs was quantified by qRT-PCR, and SNAT2 mRNA was identified as the most highly expressed System A SNAT. Data are mean ± SEM. (D) SNAT2 protein expression was demonstrated by western blot in A549, NCI-H441 and hPAEpCs. Specificity of the antibody for western blot analysis was confirmed in mice with a heterozygous deficiency for SNAT2 (please see Figure 4-6).

4.3 SNAT2 expression increases in response to AA deprivation in lung epithelial cells

A prominent characteristic of system A transporters is their dual function as transporters and receptors (“transceptors”) for AAs (49). As such, system A transceptors not only facilitate AA transport but also respond to changes in free extra- and intracellular AA pools. Specifically, AA deprivation has been shown to upregulate SNAT2 in L6 myotubes and HeLa cells, respectively (52, 96).

To test for a similar AA-dependent regulation of SNAT2 in lung epithelial cells, SNAT2 expression in response to AA deficiency was analyzed. In NCI-H441 cells, incubation in AA-free medium for 4h caused an upregulation of SNAT2 protein expression (Figure 4-4 A). Similarly, mRNA expression of SNAT2 was significantly increased after 4 h. Upregulation of SNAT2 gene expression was similarly detected after 8 and 24 h of AA deprivation (Figure 4-4 B).

Taken together, these results confirm an adaptive regulation of SNAT2 gene and protein expression by its substrate in pulmonary epithelial cells.

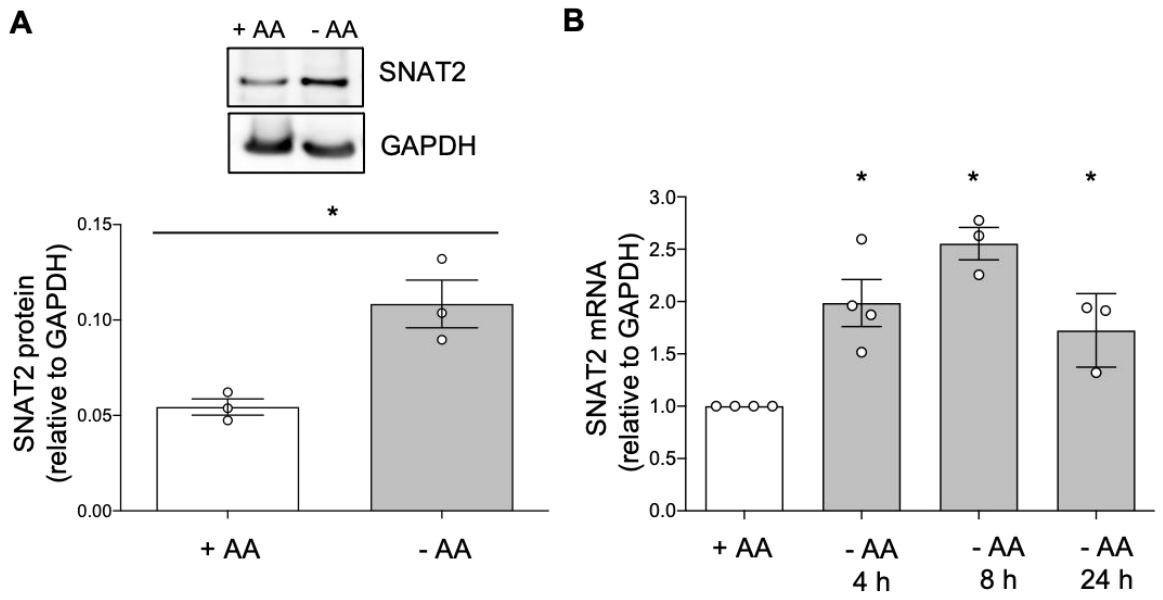

Figure 4-4: SNAT2 expression in response to AA deprivation in alveolar epithelial cells.

NCI-H441 cells were incubated in complete- (+AA) or AA-free (-AA) medium. (A) Representative immunoblots (top) and quantitative densitometric data (bottom) show significantly increased SNAT2 protein expression after 4 h of AA deprivation. Data are mean ± SEM. *p<0.05. (B) SNAT2 mRNA levels were elevated in cells deprived of AA for 4, 8, and 24 h. Data are mean ± SEM. *p<0.05 vs. +AA control.

4.4 SNAT2 mediates L-alanine transport in alveolar epithelial cells

To test whether SNAT2 mediates AA transport in alveolar epithelial cells, we next measured transepithelial transport of L-alanine across NCI-H441 cells and hPAEpCs in a transwell assay. Pre-treatment of NCI-H441 cells with the non-specific SNAT inhibitor $HgCl_2$ reduced translocation of L-alanine from the upper to the lower well (Figure 4-5 A). Similarly, the addition of MeAIB resulted in decreased L-alanine transport in hPAEpCs (Figure 4-5 B). To specifically probe for the role of SNAT2 in AA transport, experiments were repeated in NCI-H441 cells after downregulation of SNAT2 by siRNA (Figure 4-5 C). Consistently, gene knockdown of SNAT2 resulted in significantly decreased L-alanine transport (Figure 4-5 D) demonstrating that SNAT2 is functionally relevant for AA transport in alveolar epithelial cells.

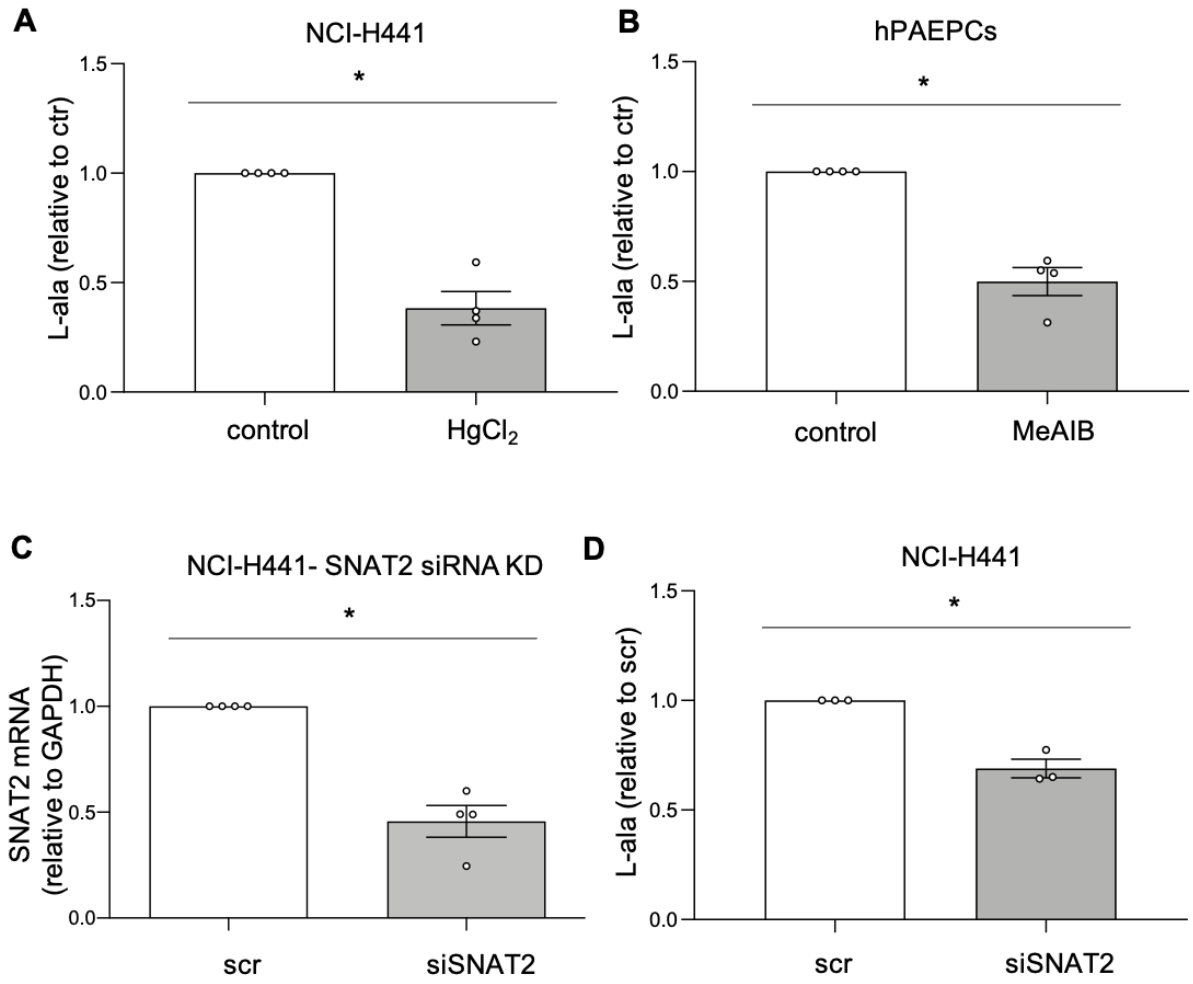

Figure 4-5: Transepithelial L-alanine transport in alveolar epithelial cells.

NCI-H441 cells and hPAEpCs were grown to confluence on a transwell filter and pre-treated with $HgCl_2$ (100 µMol/L) and MeAIB (10 mMol/L), respectively. L-alanine (2 mMol/L) was added to the upper well, and its concentration in the lower well was measured after 2 h of incubation. (A) In NCI-H441, $HgCl_2$ markedly reduced L-ala transport into the lower chamber. (B) In hPAEpCs, pre-incubation with MeAIB markedly decreased L-ala transport into the lower chamber. (C) NCI-H441 cells were pre-treated with siRNA targeting SNAT2 or a scrambled siRNA (scr). Efficiency of SNAT2 knockdown was determined by qRT-PCR and cells treated with SNAT2 siRNA show significantly reduced SNAT2 mRNA expression. (D) In NCI-H441 cells, downregulation of SNAT2 by siRNA reduced L-ala transport into the lower chamber. Data are mean ± SEM, *p<0.05.

4.5 *Slc38a2* knockout mice die shortly after birth

To specifically test for a functional role of SNAT2 in alveolar fluid transport and edema formation, the following *in situ* and *in vivo* analyses were performed in a *Slc28a2*/SNAT2 knockout mouse strain. Notably, and in line with a critical role for SNAT2 in AFC, homozygous *Slc38a2*$^{-/-}$ mice proved to be subviable and were found at sub-Mendelian ratios (approx. 2% of the total litter), suggesting that *Slc38a2*$^{-/-}$ die either during fetal development or immediately after birth (in which case they are typically cannibalized by their mothers) (140). In the few cases in which *Slc38a2*$^{-/-}$ neonates could be monitored immediately after birth, these mice showed marked dyspnea and cyanosis and died shortly after birth (please see

https://figshare.com/articles/media/Slc28a2_SNAT2_KO_pup_mp4/13650686). Due to the subviable phenotype of *Slc38a2*$^{-/-}$ mice, the subsequent analyses were done in heterozygous *Slc38a2*$^{+/-}$ mice, in which SNAT2 expression is markedly reduced at both the mRNA and protein level (Figure 4-6).

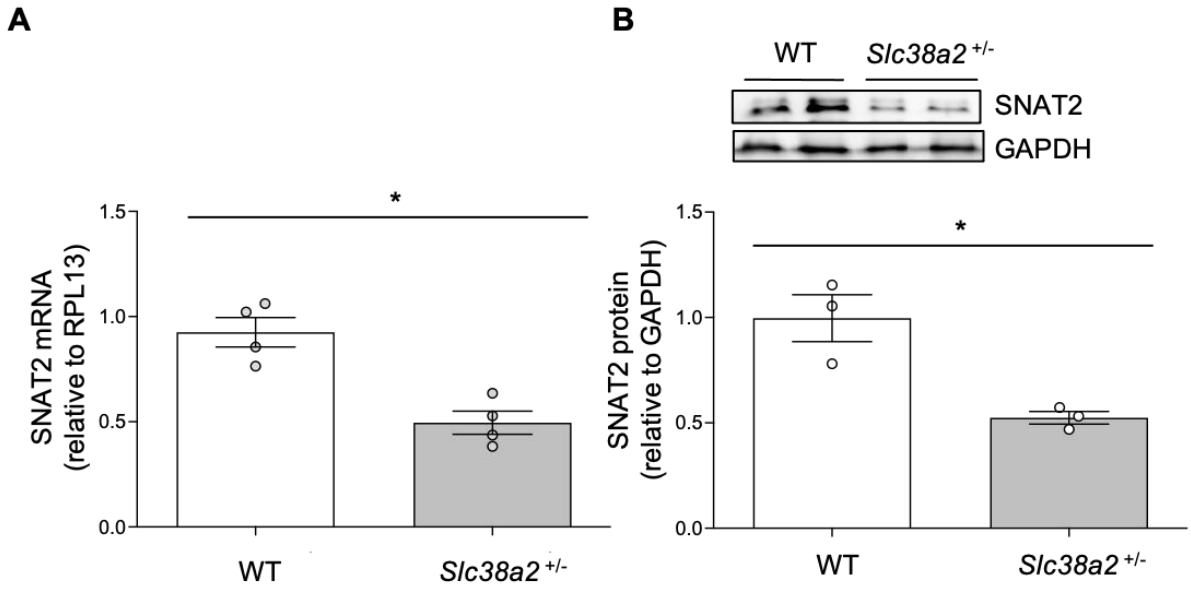

Figure 4-6: Expression of SNAT2 in *Slc38a2*$^{+/-}$ mice**.**

Protein and mRNA were isolated from the lungs of *Slc38a2*$^{+/-}$ and corresponding WT mice, and quantified by qRT-PCR and western blot, respectively. (A) SNAT2 mRNA expression is decreased in the lungs of *Slc38a2*$^{+/-}$ as compared to WT mice. (B) Similarly, SNAT2 protein was reduced in *Slc38a2*$^{+/-}$ mice. Data shown are ± SEM. *p<0.05.

4.6 Reduced SNAT2 expression impairs alveolar fluid transport *ex vivo*

The functional relevance of SNAT2 in edema formation was elucidated in isolated lungs of *Slc38a2*$^{+/-}$ and corresponding WT mice. After 5 min of perfusion, pulmonary edema was simulated by intratracheal administration of fluid (100 µL HBSS) with or without amiloride or L-alanine, and the lungs were perfused and mechanically ventilated for 30 min. Intratracheal administration of amiloride increased the wet/dry ratios in the lungs of WT mice (Figure 4-7 A). This effect was rescued by the addition of L-alanine. In *Slc38a2*$^{+/-}$ mice, wet/dry ratios were significantly higher following intratracheal administration of HBSS as compared to WT control, consistent with an impaired AFC. This effect was not attributable to loss of ENaC in heterozygous mice, as expression of the β-subunit tended to be increased rather than decreased in the lungs of *Slc38a2*$^{+/-}$ mice as compared to WT (Figure 4-7 B). Notably, L-alanine did not rescue AFC in the amiloride-treated lungs of *Slc38a2*$^{+/-}$ mice, further consolidating a functional role for SNAT2-mediated Na^+/AA co-transport in AFC.

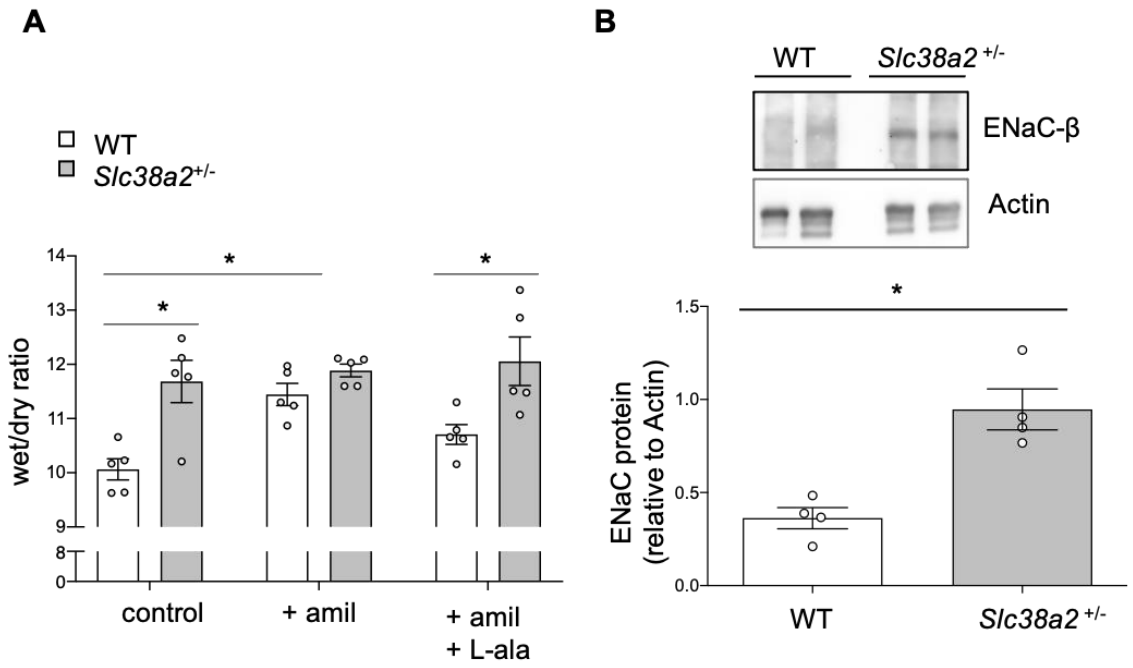

Figure 4-7: Reduced SNAT2 expression in the lungs of *Slc38a2*/SNAT2 mice impairs alveolar fluid clearance.
After 5 min at baseline perfusion and mechanical ventilation, pulmonary edema was simulated in isolated perfused lungs of *Slc38a2*$^{+/-}$ and corresponding WT mice by intratracheal administration of 100 µL HBSS with or without 10 µMol/L amiloride (amil) or 2 mMol/L L-alanine (L-ala) in the instillate. The lungs were continuously perfused with HBSS containing 20% FCS and ventilated for 30 min. (A) The lungs of *Slc38a2*$^{+/-}$ mice show elevated wet/dry ratios as compared to control WT lungs after fluid instillation and no rescue effect of L-alanine after amiloride treatment. Data are mean ± SEM. *p<0.05. (B) Expression of the β-subunit of ENaC is increased in the lungs of *Slc38a2*$^{+/-}$ mice as compared to WT. Data are mean ± SEM.

Next, in the isolated perfused mouse lungs, left atrial pressures (P_{LA}) were elevated to mimic cardiogenic pulmonary edema. After 5 min at baseline perfusion, P_{LA} was increased from 2 to 7 cmH_2O. In the lungs of WT mice, P_{LA} elevation only caused a moderate increase in W/D ratio which failed to reach significance. In contrast, in the lungs of *Slc38a2*$^{+/-}$ mice, the W/D ratio increased markedly in response to PLA elevation, resulting in significantly higher values as compared to corresponding WT mice (Figure 4-8). Taken together, these results point to a crucial role for SNAT2 in alveolar fluid transport. Loss of SNAT2 impairs fluid clearance and causes edema formation as demonstrated by increased wet/dry ratios in different IPL models.

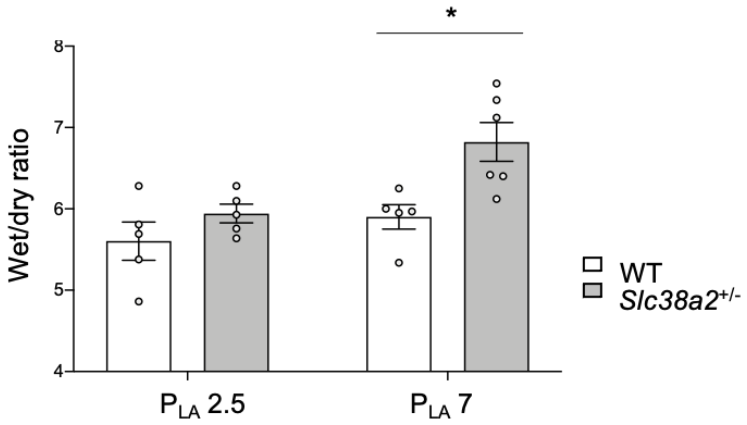

Figure 4-8: Cardiogenic pulmonary edema formation is increased in isolated lungs of *Slc38a2*$^{+/-}$ as compared to WT mice.

After 5 min at baseline perfusion and mechanical ventilation, cardiogenic pulmonary edema was induced in isolated lungs of *Slc38a2*$^{+/-}$ and corresponding WT mice by increasing left atrial pressures (P_{LA}) from 2 to 7 cmH_2O. The lungs were continuously perfused with HBSS containing 20% FCS and ventilated for 25 min. (A) Hydrostatic stress caused a pronounced increase in wet-to-dry lung weight ratio in *Slc38a2*$^{+/-}$ mice that was not detectable in WT controls. Data are mean ± SEM. *p<0.05.

4.7 Partial loss of SNAT2 promotes pulmonary edema formation in acid-induced ALI

To further elucidate the role of SNAT2 in permeability-type lung edema *in vivo,* preliminary experiments were performed in *Slc38a2*$^{+/-}$ mice and corresponding WT mice using the hydrochloric acid (HCl)-induced lung injury model as described in 3.2.2.

Our pilot data show that intratracheal instillation of HCl followed by mechanical ventilation for 2 h increases wet/dry ratios in *Slc38a2*$^{+/-}$ relative to corresponding WT mice (Figure 4-9 A). Analysis of CHOP expression in the lung lysates of HCl-challenged mice showed increased CHOP levels in the lungs of *Slc38a2*$^{+/-}$ mice as compared to WT (Figure 4-9 B), indicating a dual role for SNAT2 in epithelial fluid transport and ER stress regulation in ALI/ARDS.

Taken together, the elevated wet/dry ratios in *Slc38a2*$^{+/-}$ mice with HCl-induced lung injury confirmed a critical role for SNAT2 in AFC and permeability-type lung edema formation *in vivo*. Additionally, increased CHOP expression in *Slc38a2*$^{+/-}$ mice suggests a potential additional role for SNAT2 in ER-stress induced apoptosis. However, these preliminary results need to be confirmed in future experiments and compared to appropriate NaCl-treated controls.

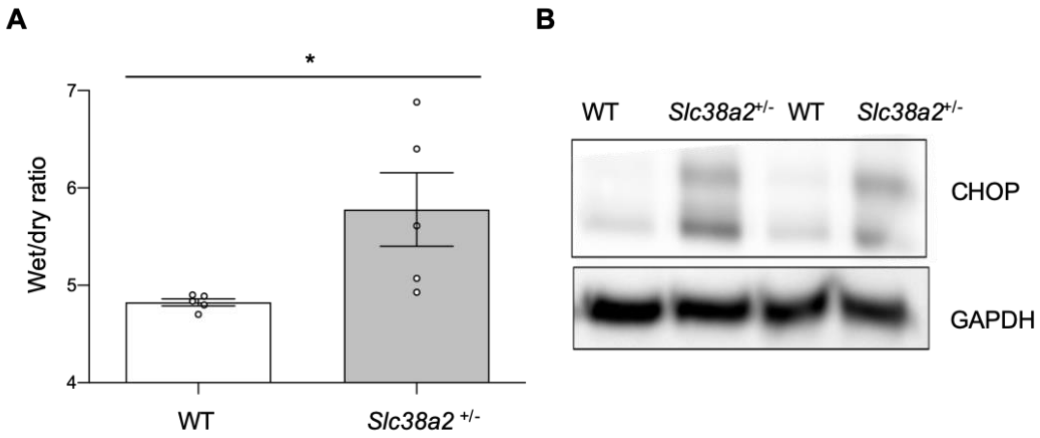

Figure 4-9: Partial loss of SNAT2 aggravates edema formation and ER stress in hydrochloric acid (HCl)-induced lung injury.

WT and *Slc38a2*$^{+/-}$ mice were anesthetized and HCl (pH 1.5) was instilled intratracheally. After 2 h of mechanical ventilation, the lungs were collected for measurement of wet-to-dry weight ratio and protein extraction. (A) Wet-to-dry lung weight ratio was increased in the lungs of HCl-instilled *Slc38a2*$^{+/-}$ as compared to WT mice. Data are mean ± SEM. *p<0.05. (B) CHOP protein expression was elevated in the lungs of HCl-instilled *Slc38a2*$^{+/-}$ as compared to WT mice.

4.8 SNAT2 expression is decreased after treatment with Cytomix or PLY

A hallmark of ARDS is the increased release of pro-inflammatory mediators into the alveolar space, which not only causes direct epithelial injury but also inhibits activity and gene expression of ion channels and pumps involved in AFC such as ENaC or Na^+-K^+-ATPase (50).

To assess a potential similar regulation of SNAT2 expression in scenarios of infection and/or inflammation, we tested for the effects of cytokines and pneumolysin (PLY), a bacterial exotoxin released by *Streptococcus pneumoniae*, on SNAT2 expression in pulmonary epithelial cells. NCHI-H441 cells were incubated for 24 h with either PLY or a Cytomix consisting of TNF-α, IL-1β IFN-γ and LPS which mimics the pro-inflammatory environment of ARDS/ALI *in vitro.* Incubation with Cytomix markedly downregulated SNAT2 protein expression in NCI-H441 cells (Figure 4-10 A), a finding that was reproduced by treatment with PLY (Figure 4-10 B). These data suggest that SNAT2 may be lost under infectious or inflammatory conditions characteristic for ARDS, thus potentially aggravating impaired alveolar fluid transport and formation of permeability-type lung edema.

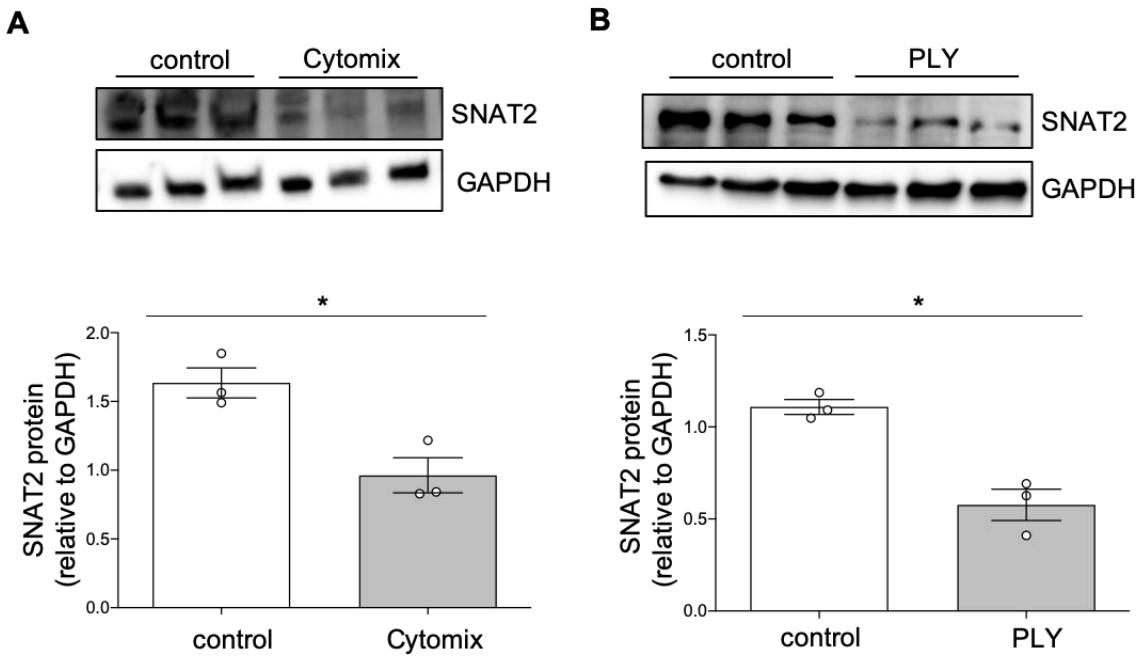

Figure 4-10: SNAT2 protein expression is downregulated in inflammatory or infectious conditions.

NCI-H441 cells were incubated with 0.2 µg/mL pneumolysin (PLY) or 50 ng/mL of a cocktail of TNF-α, IFN-γ, IL-1β and LPS (Cytomix) medium for 24 h. (A) Representative immunoblots (top) and quantitative densitometric data (bottom) show decreased expression of SNAT2 in NCI-H441 following treatment with Cytomix. (B) Similarly, stimulation with PLY reduced SNAT2 protein expression. Data are mean ± SEM. *p≤0.05.

4.9 Partial loss of SNAT2 increases expression of ATF4 and CHOP in LPS-induced ALI

As SNAT2 is downregulated in inflammatory or infectious conditions mimicking ARDS *in vitro*, we next analyzed the effects of SNAT2 loss in an experimental model of LPS-induced lung injury (as described in 3.2.1.) *in vivo* in *Slc38a2*$^{+/-}$ and corresponding WT mice. Intranasal challenge with LPS 24 h prior to euthanasia resulted in elevated protein concentrations in BALF in WT mice, yet it caused an even more pronounced increase in *Slc38a2*$^{+/-}$ mice (Figure 4-11 A). In contrast, LPS did not cause the formation of pulmonary edema in either genotype, indicated by unchanged wet/dry ratios in LPS versus NaCl-treated lungs (Figure 4-11 B).

To test whether SNAT2 loss may activate AA-sensitive intracellular signaling pathways, LPS-treated lungs were further analyzed for changes in mRNA expression of ATF4, which can be induced by AA depletion via either the PERK pathway, the ER stress response, or GCN2. Additionally, lung lysates were tested for expression of the pro-apoptotic protein CHOP, the transcription of which is induced by ATF4. LPS challenge increased ATF4 mRNA expression only in the lungs of *Slc38a2*$^{+/-}$ mice, yet not in WT (Figure 4-11 C). Similarly, LPS increased the expression of the pro-apoptotic transcription factor CHOP only in *Slc38a2*$^{+/-}$ but not in the corresponding WT mice (Figure 4-11 D).

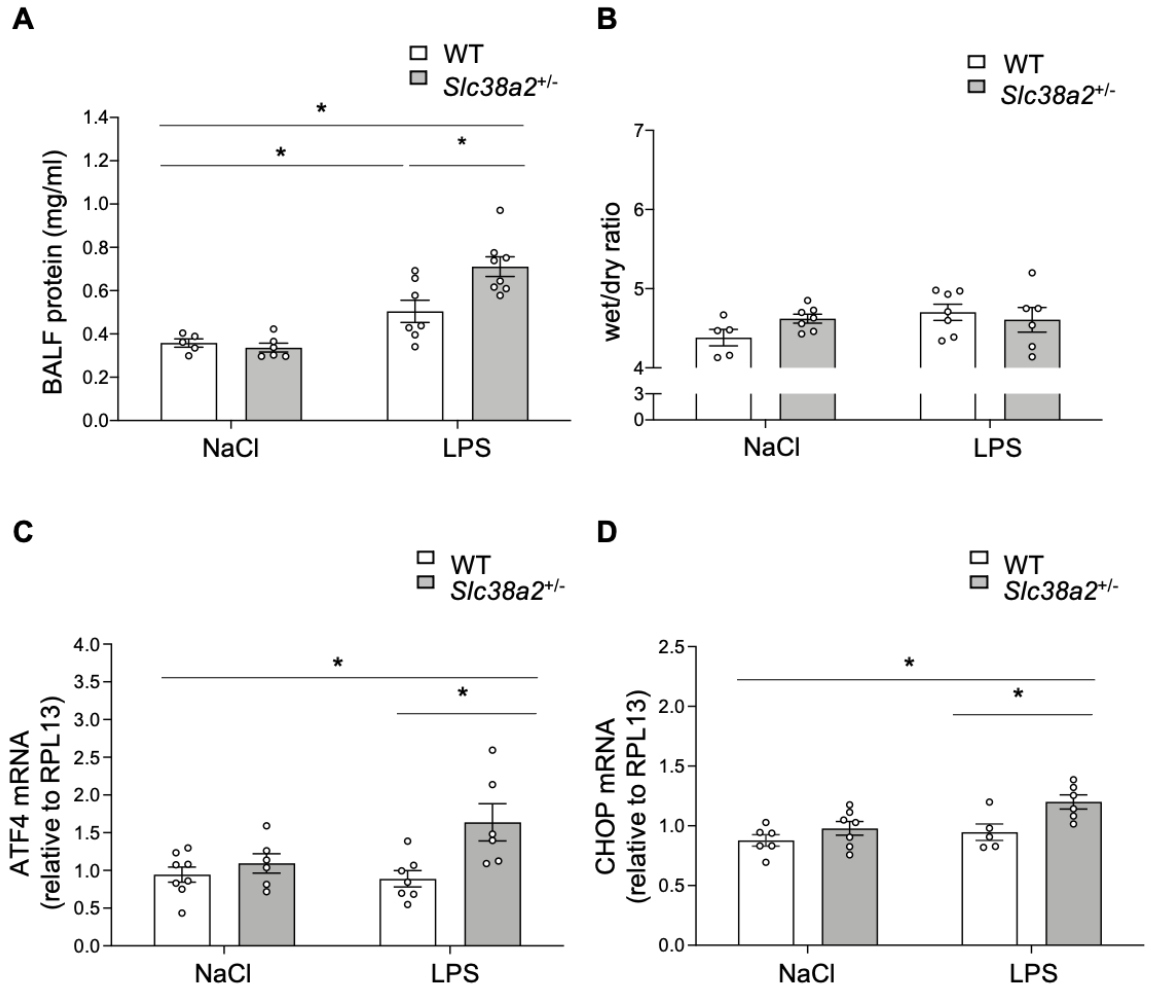

Figure 4-11: Partial SNAT2 deficiency increases the expression of the downstream targets of AA-sensitive pathways ATF4 and CHOP in LPS-induced lung injury.

WT and *Slc38a2*$^{+/-}$ mice were anesthetized and LPS (5 mg/kg) or NaCl was instilled intranasally. After 24h mice were euthanized, and the lungs were collected for measurement of wet/dry ratio, measurement of bronchoalveolar lavage fluid (BALF) protein concentration and RNA extraction. (A) Protein concentration in BALF was increased in both *Slc38a2*$^{+/-}$ and WT mice, with an even higher increase in *Slc38a2*$^{+/-}$ compared to LPS-treated WT. (B) No differences in wet-to-dry lung weight ratios were observed in response to LPS or between genotypes. (C) ATF4 mRNA expression was increased in the lungs of LPS-treated *Slc38a2*$^{+/-}$ as compared to WT mice. (D) CHOP mRNA expression was increased in the lungs of LPS-treated *Slc38a2*$^{+/-}$ as compared to WT mice. Data are mean ± SEM. *p<0.05.

In addition to mediating alveolar fluid transport, these data suggest a crucial role for SNAT2 in cell homeostasis, as partial loss of SNAT2 induces the upregulation of AA-sensitive apoptotic genes and pathways.

4.10 Statement of Contribution

Rat IPL experiments (Figure 4-1) were performed at the Keenan Research Institute of St. Michael's, Toronto, Canada, by Simon Rozowsky as part of his master's thesis. PCR analyses of the SNAT expression profile in rat lung lysates were performed by Cecile Chupin at the Keenan Research Institute of St. Michael's, Toronto, Canada. Delia Isabel Langner performed the qRT-PCR on SNAT expression in A549 cells. Tamador Zetoun provided help with the western blots in Figure 4-3 and the genotyping of the mice. Manuela Schläfereit and Ramona Warnke provided valuable technical assistance with animal breeding and care.

5 Discussion

Despite ARDS being the most frequent cause of death in intensive care, effective approved treatments are still lacking. Hence, a better understanding of the pathomechanisms is crucial for developing novel therapeutic strategies. This work identifies SNAT2 as potential therapeutic target to counteract edema formation and alleviate lung injury. The findings of this study point to a functional relevance of i) SNAT2-mediated Na^+ transport in AFC and the protection from pulmonary edema, and ii) SNAT2-mediated AA transport in alveolar epithelial hemostasis.

Primarily, SNAT2 was found as the most highly expressed System A transporter in alveolar epithelial cells that effectively transports L-ala across the epithelial cell layer. The importance of SNAT2-mediated Na^+ uptake in AFC was confirmed in isolated perfused lungs and a murine model of HCl-induced ALI, in which genetic loss of SNAT2 resulted in impaired fluid clearance and aggravated edema formation. Moreover, increased expression of pro-apoptotic genes and pathways was found in SNAT2-partially deficient mice in a model of LPS-induced lung injury, suggesting a role for SNAT2 in cell hemostasis. Lastly, in cultured epithelial cells SNAT2 expression was decreased under inflammatory or infectious conditions characteristic for ARDS.

5.1 SNAT2 mediated Na^+ transport is critical for AFC and resolution of lung edema

A tight regulation of alveolar fluid volume is essential for normal lung function and protection of the lung from pulmonary edema. Vectorial Na^+ and fluid transport is a tightly coordinated process that is driven by the electrochemical gradient provided by the Na^+-K^+-ATPase. Besides Na^+-K^+-ATPase activity, the rate of Na^+ uptake from the alveolar space depends on the expression and activation of Na^+ channels and transporters in the luminal membrane of alveolar epithelial cells. Although a number of different channels and transporters are involved in the regulation of fluid transport, AFC has so far been predominantly attributed to the amiloride-sensitive ENaC. Consequently, pharmacological activation of ENaC by β-adrenergic-stimulation was tested as a therapeutic intervention to improve fluid clearance in patients with pulmonary edema in two randomized multicentric clinical trials - the beta-agonist lung injury (BALTI) trials (38, 82). Although prior clinical studies demonstrated the clinical potential of inhaled β_2-adrenergic agonists to reduce high altitude edema and to decrease lung water content after lung resection (75, 116), respectively, the β2-agonist

salbutamol failed to reverse edema formation and did not improve overall survival in both BALTI trials. The reasons why β_2-adrenergic agonists did not prove similarly effective in these trails remain speculative and are likely multifactorial. While the negative BALTI trails do not question the importance of ENaC in AFC in general, the potential functional relevance of apical Na^+ channels and transporters other than ENaC in fluid homeostasis should be considered, however. Notably, since 40% of AFC is amiloride-insensitive (100), sodium channels other than ENaC may provide for alternative therapeutic targets. Functional studies indicate the expression and relevance of an amiloride-independent Na^+-coupled co-transporter system in alveolar epithelial cells, namely a Na^+-coupled neutral AA co-transport (13, 19). Isolated perfused rat lung experiments revealed the functional relevance of Na^+-coupled AA transport in lungs following ENaC inhibition by amiloride. Specifically, addition of the neutral AA L-alanine to the alveolar space partially antagonized the effect of amiloride and, as such, promoted AFC. This rescue of AFC by L-alanine, which was also Na^+-dependent, indicated a so far largely unrecognized amiloride-insensitive mechanism of alveolar epithelial ion and fluid transport. In IPL models, alveolar fluid instillation for measurement of AFC is typically performed with crystalloid solutions like 0.9% NaCl, Ringer´s solution, or HBSS allowing for Na^+ uptake via ENaC. Crystalloid solutions, however, lack non-ionic components like AA that may be required as substrates for amiloride-independent Na^+-co-transporters, which explains the previously unrecognized role of Na^+-AA co-transport in AFC.

In additional rat IPL experiments, the rescue by L-alanine in amiloride-treated lungs was not only blocked by Na^+ but also sensitive to $HgCl_2$, a non-specific inhibitor of Na^+-coupled AA transport, which even reversed AFC to AFS. As $HgCl_2$ may also affect alveolar fluid transport by blocking water channels (33, 134), the functional relevance of SNAT inhibition on amiloride-insensitive fluid transport was further investigated in isolated mouse lungs where pulmonary edema was mimicked by intratracheal fluid instillation and MeAIB was used as specific inhibitor of System A SNATs. Again, AFC decreased in response to amiloride but could be largely rescued by the addition of physiological levels of L-ala to the alveolar instillate. The latter effect was blocked effectively by MeAIB. Moreover, SNAT inhibition by MeAIB in the absence of amiloride was sufficient to increase pulmonary edema formation. These findings provide proof-of-principle for a previously unrecognized relevance of SNAT-mediated Na^+ transport in the regulation of alveolar fluid balance.

As these findings only indicate a general involvement of System A transporter in AFC, the next goal of this study was to identify which SNAT subtype is primarily involved in lung fluid balance. Previous publications had reported that SNAT1 and SNAT2 are ubiquitously expressed, while SNAT4 is limited to the liver, pancreas and kidney (12, 78). In line with these reports, only SNAT1 and SNAT2 - yet not SNAT4 - mRNA was detected in the lung epithelial cell lines A549 and NCI-H441. Notably, gene expression of SNAT2 was particularly high in comparison to SNAT1. These data align with previous studies which showed high expression of SNAT1 in the brain and neuronal system, whereas only weak levels of SNAT1 were detected in lung, skeletal muscle, spleen and intestines (18, 79, 137). In contrast, expression of SNAT2 was more widespread and SNAT2 was accordingly found at higher expression levels in most tissues including the heart, adrenal gland, skeletal muscle, stomach, brain, spinal cord, colon, and lung (43, 122, 146). These findings, combined with the expression data from this study, which also detected SNAT2 protein in the epithelial cell lines A549 and NCI-H441, identify System A transporter SNAT2 as potential candidate involved in Na^+/AA co-transport in the lung.

To specifically probe for the role of SNAT2-mediated Na^+ transport in alveolar fluid transport, a *Slc38a2*/SNAT2 deficient mouse strain was obtained by the Sanger Institute. Unexpectedly, mice with a homozygous loss of SNAT2 were found to be subviable and died either during fetal development or immediately after birth. Newborn *Slc38a2*$^{-/-}$ pups typically succumbed to cyanotic dyspnea. Notably, this phenotype is reminiscent of newborn mice deficient for the α-subunit of ENaC (*Scnn1α*$^{-/-}$), which die shortly after delivery due to their inability to clear their lungs from fluid. Strikingly, α-ENaC-deficient mice died within 40 h postnatally, while *Slc38a2*$^{-/-}$ mice survived less than one hour, stressing the critical role of SNAT2 in alveolar fluid homeostasis.

As *Slc38a2*$^{-/-}$ mice were subviable, the effect of partial SNAT2 loss on AFC and edema formation was studied in *Slc38a2*$^{+/-}$ mice in which SNAT2 mRNA and protein expression were markedly reduced. In fluid-instilled isolated lungs, the partial loss of SNAT2 reduced efficient removal of liquid from the alveolar space. Notably, the lungs´ ability to clear fluid was also severely impaired in *Slc38a2*$^{+/-}$ mice under control conditions. As these mice should have functional ENaC, it was considered that the loss of SNAT2 may potentially negatively regulate ENaC expression. The immunoblot data of this study, however, found that expression of the ENaC β-subunit was increased, rather than decreased, in the lungs of *Slc38a2*$^{+/-}$ mice. As such, these findings indicate a critical role of SNAT2 in AFC, which is further supported by the

effective inhibition of AFC by the System A inhibitor MeAIB in fluid-instilled lungs as well as the subviable and cyanotic phenotype of the *Slc38a2*$^{-/-}$ pups.

As impaired AFC has not only been described for permeability-type lung edema, which develops in ARDS, but also in cardiogenic-type edema, which occurs as major complication of left-sided heart failure, the role of SNAT2-mediated Na^+ transport in response to hydrostatic stress was evaluated. In isolated lungs of *Slc38a2*$^{+/-}$ mice, the wet-to-dry weight ratios were markedly increased relative to WT when perfused at elevated hydrostatic pressures. These findings further consolidate the functional relevance of SNAT2-mediated Na^+ transport in AFC and edema formation.

Lastly, the functional relevance of partial SNAT2 loss for fluid transport *in vivo* was tested in an experimental murine model of HCl-induced ALI. The HCl-ALI model is widely used to mimic lung injury due to the aspiration of gastric contents, an important risk factor for ARDS in human patients (1). Low pH acid aspiration leads to direct damage to the airway and alveolar epithelium and causes a disruption of the alveolar-capillary barrier with neutrophilic infiltration (87). More importantly for this study, HCl has been described to not only cause increased epithelial apoptosis but also to affect alveolar epithelial fluid transport, resulting in impaired AFC and edema formation independent from pulmonary blood flow or vascular filtration (89, 93). Herein, preliminary data in SNAT2-deficient mice show that partial loss of SNAT2 aggravated edema formation, further confirming a functional role for SNAT2 in AFC. However, these findings need further validation, as the appropriate control experiments with NaCl instillation as compared to HCl are lacking at this stage.

5.2 SNAT2 expression is regulated by AA availability and lost under inflammatory conditions

In addition to their functional importance for Na^+- uptake, system A transporters are known to modulate intracellular AA signaling by exhibiting dual transporter/receptor (“transceptor”) functions. As such, these transporters not only mediate AA transport but also sense changes in AA availability, and with that modulate their own expression (49). The present study confirmed this concept by demonstrating an upregulation of SNAT2 protein and RNA expression following incubation in AA free medium in cells of the lung epithelial cell line NCI-H441. These results are in line with previous reports, where an increased SNAT2 expression in response to AA deprivation was found in L6 myotubes and HeLa cells, respectively (52, 96).

While these findings verify an adaptive regulation of SNAT2 by AAs, it remains unclear how the increase in SNAT2 expression is triggered. A potential regulatory mechanism inducing SNAT2 transcription is the GCN2/ATF4 pathway. Low intracellular AA pools activate GCN2 by phosphorylation, which in turn phosphorylates eIF2α, leading to downstream activation of ATF. Binding of ATF4 to the C/EBP-ATF composite genomic element in the *Slc38a2* gene has been shown to increase gene expression of SNAT2 (102). Alternatively, SNAT2 may be regulated via the PERK pathway of the ER stress response. Similarly to GCN2, activation of PERK phosphorylates eIF2α, resulting in ATF4-mediated gene expression. In a study by Gjymishka and colleagues, elevated ATF4 protein levels and increased binding of ATF4 to the SNAT2 C/EBP-ATF composite site were observed after induction of ER stress in human hepatoma cells (39). Transcriptional activity of SNAT2 remained, however, at basal level in these experiments, suggesting that activation of the UPR may simultaneously generate a suppressive signal which blocks SNAT2 transcription downstream of ATF4 binding. In the context of lung injury, this concept is of particular importance as overactivation of the UPR, which has been demonstrated in LPS-induced lung injury (61), may inhibit SNAT2 expression rather than initiating its transcription, even though ATF4 is activated. Thus, the loss of SNAT2 expression may not only block SNAT2-mediated Na^+ transport and AFC but also SNAT2-mediated AA uptake, and therefore further aggravate ER stress.

Although molecular mechanisms leading to increased ER stress are not fully understood, there is evidence that inflammatory cytokines like TNF-α, IL-1β and IFN-γ can trigger ER-stress (14). Accordingly, the inflammatory response in ARDS may activate the ER stress response, blocking the expression of SNAT2. In line with this concept, a downregulation of SNAT2 protein expression in the lung epithelial cell line NCI-H441 was observed after incubation with Cytomix (containing TNF-α, IL-1β, IFN-γ and LPS) or PLY, which can also induce the ER stress response (3). In addition to the downregulation of SNAT2 gene expression, the pro-inflammatory response may also modulate SNAT2 transporter stability. Such a regulatory mechanism could involve ubiquitination of SNAT2 by the E3 ligase Nedd4-2, which mediates degradation not only of ENaC, but similarly of SNAT2 (42). In line with this view, Nedd4-2 was found to be upregulated in LPS-induced ALI, resulting in decreased AFC and increased edema formation (42). The authors attributed this effect to the loss of ENaC, yet it may be equally or synergistically attributed to increased degradation of SNAT2 resulting in impaired AFC.

5.3 Loss of SNAT2-mediated AA signaling aggravates lung injury

To date, little is known about the functional role of SNAT2-medited AA transport in the lungs. In the present study, it has been confirmed that SNAT2 is functionally relevant for transepithelial AA transport in NCI-H441 cells, as inhibition of SNAT2 impaired L-alanine transport across the cell layer.

The aims of this study were to examine the role of SNAT2 in alveolar hemostasis and to elucidate the consequences of SNAT2 loss under inflammatory or infectious pathological conditions like ARDS. A potential importance of SNAT2 in alveolar repair and hemostasis was first hinted at in a study from 2000 by Berk and colleagues, in which the authors reported that hypoxia reduced System A transporter activity in human lung fibroblasts (7). The resulting decrease in AA uptake via System A transporters suppressed selective mRNA expression of extracellular matrix genes, like tropoelastin and collagen type I, which are essential for tissue regeneration. Intriguingly, the findings by Berk and colleagues suggest that System A-mediated AA uptake is required for the repair of alveolar structures, and that inhibition of System A transporters may thus prolong and potentially aggravate alveolar injury.

In the present work, partial loss of SNAT2-mediated AA transport not only prevented lung repair but also aggravated alveolar epithelial injury, as demonstrated in a mouse model of LPS-induced lung injury. LPS challenge resulted in a more severe injury of the alveolar capillary barrier in heterozygous SNAT2 deficient as compared to WT mice, as indicated by increased BALF protein concentrations. However, no changes in wet/dry ratios were detected in this model. This finding is in line with other studies, which additionally reported that LPS treatment did not cause formation of pulmonary edema (99). LPS is a potent activator of the innate immune response and induces a neutrophilic inflammatory response, with elevated levels of intrapulmonary cytokines and increased apoptosis (35). However, by itself, LPS does not cause severe epithelial injury and edema formation as seen in humans with ARDS (87). As this part of the study was primarily focused on the functional relevance of SNAT2 in AA-signaling and epithelial cell homeostasis rather than fluid transport, the LPS model was nevertheless chosen to analyze the effects of partial loss of SNAT2-mediated AA signaling in the context of lung injury. In particular, this study aimed to address the induction of AA-sensitive pathways which may drive or contribute to epithelial apoptosis in response to LPS. One key AA-signaling pathway is the GCN2 kinase pathway, which has previously been shown to be modulated by SNAT2 signaling (92). As such, AA insufficiency due to the loss of SNAT2 can activate GCN2 and

induce the translation of selected cellular stress response proteins, such as the transcription factors ATF4 and the pro-apoptotic protein CHOP, which in turn induce the expression of selected genes promoting the recovery of AA homeostasis (131). If, however, cellular stress persists and cannot be resolved, CHOP induces cell death by activating apoptotic pathways via several mechanisms (see Figure 1-4). In line with this concept, Endo and colleagues demonstrated that apoptosis in various pulmonary cells of LPS challenged mice was caused by increased activation of ATF-mediated CHOP expression (25). In the present study, however, LPS increased the expression of ATF4 and its downstream target CHOP only in *Slc38a2*$^{+/-}$ mice, but not in WT. The divergence between the results of Endo and colleagues and our study is likely to relate to the fact that the LPS concentration in the present study was 10x lower, and as such not sufficient to induce CHOP expression in WT mice. The increased gene expression of ATF4 and CHOP in LPS challenged mice, as well as the increased CHOP protein expression in *Slc38a2*$^{+/-}$ mice challenged by HCl-induced lung injury, suggest that SNAT2-mediated AA signaling may be particularly relevant in the injured lung.

As these experiments were conducted to provide basic proof-of-principle for a role of SNAT2 in alveolar epithelial homeostasis, the precise signaling pathway that underlies increased ATF4 gene expression in response to partial SNAT2 loss remains to be elucidated. Since lack of nutrients and AAs can induce the ER stress response (6, 11), loss of SNAT2-mediated AA signaling may potentially drive CHOP expression in parallel by GCN2 and increased activation of the UPR, specifically PERK.

Limitations

The present study has several limitations, which should be considered in the interpretation of the data. First, it cannot be fully excluded that the applied pharmacological inhibitors have off-target effects. In particular, $HgCl_2$ is highly non-specific as it is also a well-known inhibitor of aquaporins (33), namely Na^+-K^+ ATPase (4) or the Na^+-K^+-$2Cl^-$ cotransporter (64). MeAIB, on the other hand, is so far rather considered to be specific for System A SNATs. The effects of MeAIB on neutral AA cotransporters have been shown to be dose-dependent (26), and MeAIB has accordingly been used extensively at concentrations similar to those in the present study (10 mMol/L) to suppress uptake of System A substrates (58, 107, 149). Importantly, the effects of MeAIB on L-alanine transport mimicked those of siRNA-mediated SNAT2 silencing in alveolar epithelial cells *in vitro* and replicated impaired AFC from the lungs of *Slc38a2*$^{+/-}$ mice in the isolated perfused lung preparation. As such, it seems reasonable to conclude that the

observed effects were attributable to inhibition of SNAT2 rather than non-specific off-target effects.

Furthermore, the present study did not analyze the differing SNAT2 expression profile in the various alveolar epithelial cell types as well as in basolateral versus apical membranes. These analyses were hampered by the quality of the available antibodies, which did not suffice for immunohistochemistry or immuno-electron microscopy.

The findings of the present study provide a first insight into the functional relevance of SNAT2-mediated AA signaling in the context of alveolar epithelial homeostasis. In lung injury, sufficient SNAT2 expression and activity may maintain alveolar homeostasis by warranting appropriate intracellular AA levels, and may thus block the induction of pro-apoptotic signaling cascades including the GCN2 pathway, the ER stress response, or autophagy. The exact mechanisms and pathways of SNAT2-mediated AA signaling in this scenario remain, however, to be elucidated in future follow-up studies. In particular, the potential role of SNAT2 loss on mTOR and autophagy has not been addressed in this study. Inhibition of SNAT2 signaling reduces intracellular AA concentration, and thus impairs mTOR signaling (28). Since mTOR is a major negative regulator of autophagy, the inhibition of mTOR by loss of SNAT2-mediated AA signaling could be an activator of autophagy, which in turn can induce apoptotic pathways (71).

Furthermore, further analyses on the regulation of SNAT2 expression and/or activity in the alveolar epithelium are required. The findings of the present study on pulmonary epithelia cells i) confirm an adaptive regulation in response to substrate availability of SNAT2, and ii) suggest a loss of SNAT2 expression/activity under infectious or inflammatory conditions characteristic for ARDS, but do not, however, identify the regulatory mechanisms and pathways involved.

Lastly, the translatability of the present findings from mice and rats to the human scenario, which could be tested in isolated perfused human lungs, needs to be addressed in future studies.

Conclusion and outlook

As ARDS is a life-threatening disease in critically ill patients and the most frequent cause of death in intensive care, understanding its pathophysiological mechanisms as well as identifying methods for pharmacological intervention are in dire need. The accumulation of fluid in the alveolar space is a major pathophysiological factor of ARDS that drives impaired

gas exchange, and consequently respiratory failure and death. Factors leading to pulmonary edema in ARDS include: i) inhibition of vectorial water and ion transport due to the loss of ion channels and transporters, and ii) disruption of the alveolo-capillary barrier integrity due to dysregulated cellular homeostasis resulting in epithelial apoptosis. Ideally, therapeutic approaches should thus aim to improve alveolar fluid reabsorption, while restoring alveolar barrier function by inhibiting epithelial apoptosis.

This study identifies SNAT2 as a functionally relevant Na^+ transporter with a critical role in alveolar fluid transport (Figure 5-1 A). In different animal models, the inhibition or genetic deficiency of SNAT2 impaired AFC, promoting the formation of pulmonary edema. In addition to mediating Na^+-absorption and alveolar fluid transport, SNAT2 may also be involved in the regulation of cellular homeostasis via its role as an AA transporter (Figure 5-1 B). In LPS-induced ALI, loss of SNAT2 resulted in increased gene expression of ATF4 and its downstream target CHOP, which may drive epithelial apoptosis in lung injury, presumably via activation of the GCN2 pathway, the ER stress response and/or autophagy. Further analyses of SNAT2-medited AA-signaling are required to delineate the exact pathways triggering epithelial apoptosis via AA-sensitive signaling cascades. Although the results of our present study demonstrate that SNAT2 is lost under inflammatory conditions, regulatory mechanisms leading to the loss of SNAT2 so far remain unclear. Future studies should hence also focus on the cellular mechanisms of SNAT2 regulation in the intact and injured alveolus, which may identify novel and promising therapeutic targets to maintain alveolar fluid transport and epithelial cell homeostasis in lung injury by sustaining SNAT2 expression and/or activity in the injured alveolus.

In summary, the findings of the present study identify a functional role for SNAT2-mediated Na^+ transport in AFC and the protection from pulmonary edema. In this regard, dysregulated fluid transport has predominantly been attributed to an inhibition of amiloride-sensitive Na^+ transport due to the loss of activity and expression of ENaC. In this study, a critical role for the amiloride-insensitive transporter SNAT2 in epithelial Na^+ uptake and transepithelial fluid transport was confirmed.

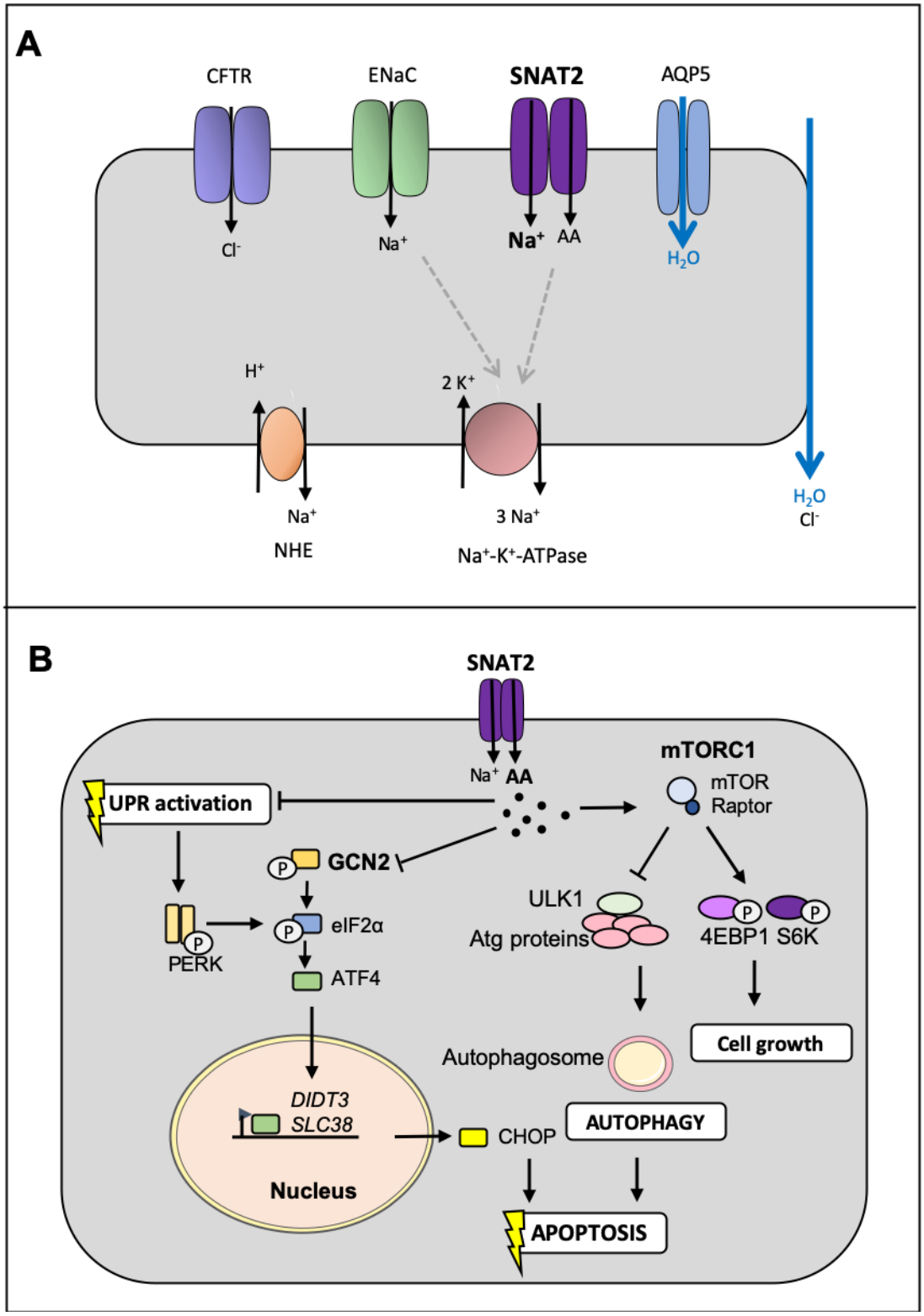

Figure 5-1: Dual function of SNAT2 in alveolar fluid transport and cell homeostasis.

(A) In addition to ENaC, SNAT2 emerges as critical epithelial transporter for Na^+-driven alveolar fluid absorption. (B) SNAT2-mediated AA transport maintains epithelial cell homeostasis by regulating ER stress, autophagy and apoptosis.

References

1. **Aeffner F**, **Bolon B**, **Davis IC**. Mouse Models of Acute Respiratory Distress Syndrome: A Review of Analytical Approaches, Pathologic Features, and Common Measurements. .
2. **Albertine KH**, **Soulier MF**, **Wang Z**, **Ishizaka A**, **Hashimoto S**, **Zimmerman GA**, **Matthay MA**, **Ware LB**. Fas and fas ligand are up-regulated in pulmonary edema fluid and lung tissue of patients with acute lung injury and the acute respiratory distress syndrome. *Am J Pathol* 161: 1783–96, 2002. doi: 10.1016/S0002-9440(10)64455-0.
3. **Alhamdi Y**, **Neill DR**, **Abrams ST**, **Malak HA**, **Yahya R**, **Barrett-Jolley R**, **Wang G**, **Kadioglu A**, **Toh C-H**. Circulating Pneumolysin Is a Potent Inducer of Cardiac Injury during Pneumococcal Infection. *PLOS Pathog* 11: e1004836, 2015. doi: 10.1371/journal.ppat.1004836.
4. **Anner BM**, **Moosmayer M**, **Imesch E**. Mercury blocks Na-K-ATPase by a ligand-dependent and reversible mechanism. *Am J Physiol - Ren Fluid Electrolyte Physiol* 262, 1992. doi: 10.1152/ajprenal.1992.262.5.f830.
5. **Ashbaugh D**, **Boyd Bigelow D**, **Petty T**, **Levine B**. Acute respiratory distress in adults. *Lancet* 290: 319–323, 1967. doi: 10.1016/S0140-6736(67)90168-7.
6. **Balsa E**, **Soustek MS**, **Thomas A**, **Cogliati S**, **García-Poyatos C**, **Martín-García E**, **Jedrychowski M**, **Gygi SP**, **Enriquez JA**, **Puigserver P**. ER and Nutrient Stress Promote Assembly of Respiratory Chain Supercomplexes through the PERK-eIF2α Axis. *Mol Cell* 74: 877-890.e6, 2019. doi: 10.1016/j.molcel.2019.03.031.
7. **Berk JL**, **Hatch CA**, **Goldstein RH**. Hypoxia inhibits amino acid uptake in human lung fibroblasts. *J Appl Physiol* 89: 1425–1431, 2000. doi: 10.1152/jappl.2000.89.4.1425.
8. **Bernard GR**, **Artigas A**, **Brigham KL**, **Carlet J**, **Falke K**, **Hudson L**, **Lamy M**, **Legall JR**, **Morris A**, **Spragg R**. Report of the American-European consensus conference on ARDS: definitions, mechanisms, relevant outcomes and clinical trial coordination. *Intensive Care Med* 20: 225–232, 1994.
9. **BéruBé K**, **Prytherch Z**, **Job C**, **Hughes T**. Human primary bronchial lung cell constructs: The new respiratory models. *Toxicology* 278 Elsevier: 311–318, 2010.
10. **Bevilacqua E**, **Bussolati O**, **Dall'Asta V**, **Gaccioli F**, **Sala R**, **Gazzola GC**, **Franchi-Gazzola R**. SNAT2 silencing prevents the osmotic induction of transport system A and hinders cell recovery from hypertonic stress. *FEBS Lett* 579: 3376–3380, 2005. doi: 10.1016/j.febslet.2005.05.002.
11. **Bobak Y**, **Kurlishchuk Y**, **Vynnytska-Myronovska B**, **Grydzuk O**, **Shuvayeva G**, **Redowicz MJ**, **Kunz-Schughart LA**, **Stasyk O**. Arginine deprivation induces endoplasmic reticulum stress in human solid cancer cells. *Int J Biochem Cell Biol* 70: 29–38, 2016. doi: 10.1016/j.biocel.2015.10.027.
12. **Bröer S**. The SLC38 family of sodium-amino acid co-transporters. *Pflugers Arch* 466: 155–72,

2014. doi: 10.1007/s00424-013-1393-y.

13. **Brown SE**, **Kim KJ**, **Goodman BE**, **Wells JR**, **Crandall ED**. Sodium-amino acid cotransport by type II alveolar epithelial cells [Online]. *J Appl Physiol* 59: 1616–1622, 1985. http://www.ncbi.nlm.nih.gov/pubmed/4066594 [30 Jan. 2017].
14. **Brozzi F**, **Nardelli TR**, **Lopes M**, **Millard I**, **Barthson J**, **Igoillo-Esteve M**, **Grieco FA**, **Villate O**, **Oliveira JM**, **Casimir M**, **Bugliani M**, **Engin F**, **Hotamisligil GS**, **Marchetti P**, **Eizirik DL**. Cytokines induce endoplasmic reticulum stress in human, rat and mouse beta cells via different mechanisms. *Diabetologia* 58: 2307–2316, 2015. doi: 10.1007/s00125-015-3669-6.
15. **Brueckl C**, **Kaestle S**, **Kerem A**, **Habazettl H**, **Krombach F**, **Kuppe H**, **Kuebler WM**. Hyperoxia-induced reactive oxygen species formation in pulmonary capillary endothelial cells in situ. *Am J Respir Cell Mol Biol* 34: 453–463, 2006. doi: 10.1165/rcmb.2005-0223OC.
16. **Buccellato LJ**, **Tso M**, **Akinci OI**, **Chandel NS**, **Budinger GRS**. Reactive oxygen species are required for hyperoxia-induced Bax activation and cell death in alveolar epithelial cells. *J Biol Chem* 279: 6753–60, 2004. doi: 10.1074/jbc.M310145200.
17. **Bussolati O**, **Dall'Asta V**, **Franchi-Gazzola R**, **Sala R**, **Rotoli BM**, **Visigalli R**, **Casado J**, **Lopez-Fontanals M**, **Pastor-Anglada M Al**, **Gazzola GC**. The role of system A for neutral amino acid transport in the regulation of cell volume. In: *Molecular Membrane Biology*. Taylor and Francis Ltd, 2001, p. 27–38.
18. **Chaudhry FA**, **Schmitz D**, **Reimer RJ**, **Larsson P**, **Gray AT**, **Nicoll R**, **Kavanaugh M**, **Edwards RH**. Glutamine uptake by neurons: Interaction of protons with system a transporters. *J Neurosci* 22: 62–72, 2002. doi: 10.1523/jneurosci.22-01-00062.2002.
19. **Clerici C**, **Soler P**, **Saumon G**. Sodium-dependent phosphate and alanine transports but sodium-independent hexose transport in type II alveolar epithelial cells in primary culture. *Biochim Biophys Acta - Biomembr* 1063: 27–35, 1991. doi: 10.1016/0005-2736(91)90349-D.
20. **Dall'asta V**, **Franchi-Gazzola R**, **Bussolati O**, **Sala R**, **Rotoli BM**, **Rossi PA**, **Uggeri J**, **Belletti S**, **Visigalli R**, **Gazzola GC**. Emerging roles for sodium dependent amino acid transport in mesenchymal cells. *Amino Acids* 11: 117–33, 1996. doi: 10.1007/BF00813856.
21. **Derwall M**, **Martin L**, **Rossaint R**. The acute respiratory distress syndrome: pathophysiology, current clinical practice, and emerging therapies. *Expert Rev Respir Med* 12: 1021–1029, 2018. doi: 10.1080/17476348.2018.1548280.
22. **Di S**, **Fan C**, **Ma Z**, **Li M**, **Guo K**, **Han D**, **Li X**, **Mu D**, **Yan X**. PERK/eIF-2α/CHOP Pathway Dependent ROS Generation Mediates Butein-induced Non-small-cell Lung Cancer Apoptosis and G2/M Phase Arrest. *Int J Biol Sci* 15: 1637–1653, 2019. doi: 10.7150/ijbs.33790.
23. **Eaton AF**, **Yue Q**, **Eaton DC**, **Bao HF**. ENaC activity and expression is decreased in the lungs of protein kinase C-α knockout mice. *Am J Physiol - Lung Cell Mol Physiol* 307: L374, 2014. doi:

10.1152/ajplung.00040.2014.

24. **Elmore S**. Apoptosis: A Review of Programmed Cell Death. *Toxicol Pathol* 35: 495–516, 2007. doi: 10.1080/01926230701320337.

25. **Endo M**, **Oyadomari S**, **Suga M**, **Mori M**, **Gotoh T**. The ER Stress Pathway Involving CHOP Is Activated in the Lungs of LPS-Treated Mice. *J Biochem* 138: 501–507, 2005. doi: 10.1093/jb/mvi143.

26. **Erickson JD**. Functional identification of activity-regulated, high-affinity glutamine transport in hippocampal neurons inhibited by riluzole. *J Neurochem* 142: 29–40, 2017. doi: 10.1111/jnc.14046.

27. **Evans K**, **Nasim Z**, **Brown J**, **Butler H**, **Kauser S**, **Varoqui H**, **Erickson JD**, **Herbert TP**, **Bevington A**. Acidosis-sensing glutamine pump SNAT2 determines amino acid levels and mammalian target of rapamycin signalling to protein synthesis in L6 muscle cells. *J Am Soc Nephrol* 18: 1426–36, 2007. doi: 10.1681/ASN.2006091014.

28. **Evans K**, **Nasim Z**, **Brown J**, **Clapp E**, **Amin A**, **Yang B**, **Herbert TP**, **Bevington A**. Inhibition of SNAT2 by Metabolic Acidosis Enhances Proteolysis in Skeletal Muscle. *J Am Soc Nephrol* 19: 2119–2129, 2008. doi: 10.1681/ASN.2007101108.

29. **Fan S-J**, **Goberdhan DCI**. PATs and SNATs: Amino Acid Sensors in Disguise. *Front Pharmacol* 9: 640, 2018. doi: 10.3389/fphar.2018.00640.

30. **Favaloro B**, **Allocati N**, **Graziano V**, **Ilio C Di**, **Laurenzi V De**. Role of Apoptosis in disease. *Aging (Albany NY)* 4: 330, 2012. doi: 10.18632/AGING.100459.

31. **Fielhaber JA**, **Carroll SF**, **Dydensborg AB**, **Shourian M**, **Triantafillopoulos A**, **Harel S**, **Hussain SN**, **Bouchard M**, **Qureshi ST**, **Kristof AS**. Inhibition of Mammalian Target of Rapamycin Augments Lipopolysaccharide-Induced Lung Injury and Apoptosis. *J Immunol* 188: 4535–4542, 2012. doi: 10.4049/jimmunol.1003655.

32. **Folkesson HC**, **Matthay MA**. Alveolar epithelial ion and fluid transport: Recent progress. *Am. J. Respir. Cell Mol. Biol.* 35: 10–19, 2006.

33. **Folkesson HG**, **Matthay MA**, **Hasegawa H**, **Kheradmand F**, **Verkman AS**. Transcellular water transport in lung alveolar epithelium through mercury- sensitive water channels. *Proc Natl Acad Sci U S A* 91: 4970–4974, 1994. doi: 10.1073/pnas.91.11.4970.

34. **Fu HY**, **Okada K**, **Liao Y**, **Tsukamoto O**, **Isomura T**, **Asai M**, **Sawada T**, **Okuda K**, **Asano Y**, **Sanada S**, **Asanuma H**, **Asakura M**, **Takashima S**, **Komuro I**, **Kitakaze M**, **Minamino T**. Ablation of C/EBP homologous protein attenuates endoplasmic reticulum-mediated apoptosis and cardiac dysfunction induced by pressure overload. *Circulation* 122: 361–9, 2010. doi: 10.1161/CIRCULATIONAHA.109.917914.

35. **Fujita M**, **Kuwano K**, **Kunitake R**, **Hagimoto N**, **Miyazaki H**, **Kaneko Y**, **Kawasaki M**, **Maeyama**

T, **Hara N**. Endothelial cell apoptosis in lipopolysaccharide-induced lung injury in mice. [Online]. *Int Arch Allergy Immunol* 117: 202–8, 1998. http://www.ncbi.nlm.nih.gov/pubmed/9831808.

36. **Fukuda N**, **Folkesson HG**, **Matthay MA**. Relationship of interstitial fluid volume to alveolar fluid clearance in mice: Ventilated vs. in situ studies. *J Appl Physiol* 89: 672–679, 2000. doi: 10.1152/jappl.2000.89.2.672.
37. **Gallinetti J**, **Harputlugil E**, **Mitchell JR**. Amino acid sensing in dietary-restriction-mediated longevity: roles of signal-transducing kinases GCN2 and TOR. *Biochem J* 449: 1–10, 2013. doi: 10.1042/BJ20121098.
38. **Gates S**, **Perkins GD**, **Lamb SE**, **Kelly C**, **Thickett DR**, **Young JD**, **McAuley DF**, **Snaith C**, **McCabe C**, **Hulme CT**, **Gao Smith F**. Beta-agonist lung injury TrIal-2 (BALTI-2): A multicentre, randomised, double-blind, placebo-controlled trial and economic evaluation of intravenous infusion of salbutamol versus placebo in patients with acute respiratory distress syndrome. *Health Technol Assess (Rockv)* 17: 1366–5278, 2013. doi: 10.3310/hta17380.
39. **Gjymishka A**, **Palii SS**, **Shan J**, **Kilberg MS**. Despite increased ATF4 binding at the C/EBP-ATF composite site following activation of the unfolded protein response, system a transporter 2 (SNAT2) transcription activity is repressed in HepG2 cells. *J Biol Chem* 283: 27736–27747, 2008. doi: 10.1074/jbc.M803781200.
40. **Hara K**, **Yonezawa K**, **Weng QP**, **Kozlowski MT**, **Belham C**, **Avruch J**. Amino acid sufficiency and mTOR regulate p70 S6 kinase and eIF-4E BP1 through a common effector mechanism. *J Biol Chem* 273: 14484–14494, 1998. doi: 10.1074/jbc.273.23.14484.
41. **Hashimoto S**, **Kobayashi A**, **Kooguchi K**, **Kitamura Y**, **Onodera H**, **Nakajima H**. Upregulation of Two Death Pathways of Perforin / Granzyme and FasL / Fas in Septic [Online]. *Am J Physiol Lung Cell Mol Physiol* 275: L1040-1050, 1998. http://ajplung.physiology.org/content/275/6/L1040.
42. **Hatanaka T**, **Hatanaka Y**, **Setou M**. Regulation of amino acid transporter ATA2 by ubiquitin ligase Nedd4-2. *J Biol Chem* 281: 35922–35930, 2006. doi: 10.1074/jbc.M606577200.
43. **Hatanaka T**, **Huang W**, **Wang H**, **Sugawara M**, **Prasad PD**, **Leibach FH**, **Ganapathy V**. Primary structure, functional characteristics and tissue expression pattern of human ATA2, a subtype of amino acid transport system A. *Biochim Biophys Acta - Biomembr* 1467: 1–6, 2000. doi: 10.1016/S0005-2736(00)00252-2.
44. **Heinz E**, **Geck P**, **Pfeiffer B**. Energetic problems of the transport of amino acids in Ehrlich cells. *J Membr Biol* 57: 91–4, 1980. doi: 10.1007/bf01868995.
45. **Herridge MS**, **Tansey CM**, **Matté A**, **Tomlinson G**, **Diaz-Granados N**, **Cooper A**, **Guest CB**, **Mazer CD**, **Mehta S**, **Stewart TE**, **Kudlow P**, **Cook D**, **Slutsky AS**, **Cheung AM**. Functional disability 5 years after acute respiratory distress syndrome. *N Engl J Med* 364: 1293–1304, 2011. doi: 10.1056/NEJMoa1011802.

46. **Hetz C**. The unfolded protein response: controlling cell fate decisions under ER stress and beyond. *Nat Rev Mol Cell Biol* 13: 89–102, 2012. doi: 10.1038/nrm3270.

47. **Hoffer LJ**, **Bistrian BR**. Appropriate protein provision in criticai illness : a systematic and narrative review. *Am J Clin Nutr* 96: 591–600, 2012. doi: 10.3945/ajcn.l.

48. **Horio M**, **Yamauchi A**, **Matsuoka Y**, **Moriyama T**, **Fukunaga M**, **Imai E**, **Orita Y**. Effect of hypertonic stress on amino acid levels and system A activity in rat peritoneal mesothelial cells [Online]. *Perit Dial Int* 19: 124–130, 1999. http://www.ncbi.nlm.nih.gov/pubmed/10357182 [4 Jan. 2020].

49. **Hundal HS**, **Taylor PM**. Amino acid transceptors: gate keepers of nutrient exchange and regulators of nutrient signaling. *Am J Physiol Metab* 296: E603–E613, 2009. doi: 10.1152/ajpendo.91002.2008.

50. **Huppert LA**, **Matthay MA**. Alveolar Fluid Clearance in Pathologically Relevant Conditions: In Vitro and In Vivo Models of Acute Respiratory Distress Syndrome. *Front Immunol* 8, 2017. doi: 10.3389/fimmu.2017.00371.

51. **Hyde R**, **Christie GR**, **Litherland GJ**, **Hajduch E**, **Taylor PM**, **Hundal HS**. Subcellular localization and adaptive up-regulation of the System A (SAT2) amino acid transporter in skeletal-muscle cells and adipocytes. *Biochem J* 355: 563–568, 2001. doi: 10.1042/bj3550563.

52. **Hyde R**, **Cwiklinski EL**, **MacAulay K**, **Taylor PM**, **Hundal HS**. Distinct sensor pathways in the hierarchical control of SNAT2, a putative amino acid transceptor, by amino acid availability. *J Biol Chem* 282: 19788–19798, 2007. doi: 10.1074/jbc.M611520200.

53. **Ichim, Gabriel; Tait SWG**. A fate worse than death: apoptosis as an oncogenic process. *Nat Rev Cancer* 16: 539–548, 2016. doi: 10.1038/nrc.2016.58.

54. **Ingbar DH**, **Bhargava M**, **O'Grady SM**. Mechanisms of alveolar epithelial chloride absorption. *Am. J. Physiol. - Lung Cell. Mol. Physiol.* 297 American Physiological Society Bethesda, MD: L813–L815, 2009.

55. **Jain L**, **Eaton DC**. Physiology of fetal lung fluid clearance and the effect of labor. In: *Seminars in Perinatology*, p. 34–43.

56. **Johnson ER**, **Matthay MA**. Acute lung injury: epidemiology, pathogenesis, and treatment. *J Aerosol Med Pulm Drug Deliv* 23: 243–52, 2010. doi: 10.1089/jamp.2009.0775.

57. **Johnson MD**, **Bao H-F**, **Helms MN**, **Chen X-J**, **Tigue Z**, **Jain L**, **Dobbs LG**, **Eaton DC**. Functional ion channels in pulmonary alveolar type I cells support a role for type I cells in lung ion transport. *Proc Natl Acad Sci U S A* 103: 4964–4969, 2006. doi: 10.1073/pnas.0600855103.

58. **Kate M**, **Evans F**. The Effects of Acidosis, Glutamine Starvation and Inhibition of the pH Sensitive SNAT2 Amino Acid Transporter on Protein Metabolism in L6 Muscle Cells. , 2008.

59. **Kawasaki M**, **Kuwano K**, **Hagimoto N**, **Matsuba T**, **Kunitake R**, **Tanaka T**, **Maeyama T**, **Hara N**.

Protection from lethal apoptosis in lipopolysaccharide-induced acute lung injury in mice by a caspase inhibitor. *Am J Pathol* 157: 597–603, 2000. doi: 10.1016/S0002-9440(10)64570-1.

60. **Kilberg MS**, **Christensen HN**. The relation between membrane potential and the transport activity of system A and L in plasma membrane vesicles of the Ehrlich cell. *Membr Biochem* 3: 155–68, 1980. doi: 10.3109/09687688009063883.
61. **Kim HJ**, **Jeong JS**, **Kim SR**, **Park SY**, **Chae HJ**, **Lee YC**. Inhibition of endoplasmic reticulum stress alleviates lipopolysaccharide-induced lung inflammation through modulation of NF-κB/HIF-1α signaling pathway. *Sci Rep* 3: 1142, 2013. doi: 10.1038/srep01142.
62. **Kim J**, **Guan K-L**. Amino Acid Signaling in TOR Activation. *Annu Rev Biochem* 80: 1001–1032, 2011. doi: 10.1146/annurev-biochem-062209-094414.
63. **Kim R**, **Emi M**, **Tanabe K**, **Murakami S**. Role of the unfolded protein response in cell death. .
64. **Kinne-Saffran E**, **Kinne RKH**. Inhibition by mercuric chloride of Na-K-2Cl cotransport activity in rectal gland plasma membrane vesicles isolated from Squalus acanthias. *Biochim Biophys Acta - Biomembr* 1510: 442–451, 2001. doi: 10.1016/S0005-2736(00)00375-8.
65. **Krick S**, **Eul BG**, **Hänze J**, **Savai R**, **Grimminger F**, **Seeger W**, **Rose F**. Role of Hypoxia-Inducible Factor-1α in Hypoxia-Induced Apoptosis of Primary Alveolar Epithelial Type II Cells. *Am J Respir Cell Mol Biol* 32: 395–403, 2005. doi: 10.1165/rcmb.2004-0314OC.
66. **Krokowski D**, **Guan BJ**, **Wu J**, **Zheng Y**, **Pattabiraman PP**, **Jobava R**, **Gao XH**, **Di XJ**, **Snider MD**, **Mu TW**, **Liu S**, **Storrie B**, **Pearlman E**, **Blumental-Perry A**, **Hatzoglou M**. GADD34 Function in Protein Trafficking Promotes Adaptation to Hyperosmotic Stress in Human Corneal Cells. .
67. **Laemmli UK**. Cleavage of structural proteins during the assembly of the head of bacteriophage T4. *Nature* 227: 680–685, 1970. doi: 10.1038/227680a0.
68. **Laffey JG**, **Kavanagh BP**, **Ney L**, **Kuebler WM**, **Oba Y**, **Salzman GA**, **Brower RG**, **Matthay MA**, **Wheeler A**. Ventilation with lower tidal volumes as compared with traditional tidal volumes for acute lung injury. *N. Engl. J. Med.* 343 Massachusetts Medical Society: 812–814, 2000.
69. **Lee DF**, **Salguero FJ**, **Grainger D**, **Francis RJ**, **MacLellan-Gibson K**, **Chambers MA**. Isolation and characterisation of alveolar type II pneumocytes from adult bovine lung. *Sci Rep* 8: 11927, 2018. doi: 10.1038/s41598-018-30234-x.
70. **Lee JW**, **Fang X**, **Dolganov G**, **Fremont RD**, **Bastarache JA**, **Ware LB**, **Matthay MA**. Acute lung injury edema fluid decreases net fluid transport across human alveolar epithelial type II cells. *J Biol Chem* 282: 24109–19, 2007. doi: 10.1074/jbc.M700821200.
71. **Levine B**, **Yuan J**. Autophagy in cell death: An innocent convict? *J. Clin. Invest.* 115: 2679–2688, 2005.
72. **Li G**, **Mongillo M**, **Chin K-T**, **Harding H**, **Ron D**, **Marks AR**, **Tabas I**. Role of ERO1-alpha-mediated stimulation of inositol 1,4,5-triphosphate receptor activity in endoplasmic reticulum stress-

induced apoptosis. *J Cell Biol* 186: 783–92, 2009. doi: 10.1083/jcb.200904060.

73. **Li T**, **Koshy S**, **Folkesson HG**. Involvement of αENaC and Nedd4-2 in the conversion from lung fluid secretion to fluid absorption at birth in the rat as assayed by RNA interference analysis. *Am J Physiol - Lung Cell Mol Physiol* 293: 1069–1078, 2007. doi: 10.1152/ajplung.00151.2007.
74. **Liao Y**, **Fung TS**, **Huang M**, **Fang SG**, **Zhong Y**, **Liu DX**. Upregulation of CHOP/GADD153 during Coronavirus Infectious Bronchitis Virus Infection Modulates Apoptosis by Restricting Activation of the Extracellular Signal-Regulated Kinase Pathway. *J Virol* 87: 8124–8134, 2013. doi: 10.1128/jvi.00626-13.
75. **Licker M**, **Tschopp JM**, **Robert J**, **Frey JG**, **Diaper J**, **Ellenberger C**. Aerosolized salbutamol accelerates the resolution of pulmonary edema after lung resection. *Chest* 133: 845–852, 2008. doi: 10.1378/chest.07-1710.
76. **Livak KJ**, **Schmittgen TD**. Analysis of Relative Gene Expression Data Using Real-Time Quantitative PCR and the 2−ΔΔCT Method. *Methods* 25: 402–408, 2001. doi: 10.1006/METH.2001.1262.
77. **Ma T**, **Fukuda N**, **Song Y**, **Matthay MA**, **Verkman AS**. Lung fluid transport in aquaporin-5 knockout mice. *J Clin Invest* 105: 93–100, 2000. doi: 10.1172/JCI8258.
78. **Mackenzie B**, **Erickson JD**. Sodium-coupled neutral amino acid (System N/A) transporters of the SLC38 gene family. *Pflugers Arch* 447: 784–95, 2004. doi: 10.1007/s00424-003-1117-9.
79. **Mackenzie B**, **Schäfer MKH**, **Erickson JD**, **Hedige MA**, **Weihe E**, **Varoqui H**. Functional properties and cellular distribution of the system A glutamine transporter SNAT1 support specialized roles in central neurons. *J Biol Chem* 278: 23720–23730, 2003. doi: 10.1074/jbc.M212718200.
80. **Martin TR**, **Nakamura M**, **Matute-Bello G**. The role of apoptosis in acute lung injury. *Crit Care Med* 31: S184–S188, 2003. doi: 10.1097/01.CCM.0000057841.33876.B1.
81. **Matthay M a**, **Folkesson HG**, **Clerici C**. Lung epithelial fluid transport and the resolution of pulmonary edema. *Physiol Rev* 82: 569–600, 2002. doi: 10.1152/physrev.00003.2002.
82. **Matthay MA**, **Brower RG**, **Carson S**, **Douglas IS**, **Eisner M**, **Hite D**, **Holets S**, **Kallet RH**, **Liu KD**, **MacIntyre N**, **Moss M**, **Schoenfeld D**, **Steingrub J**, **Thompson BT**. Randomized, placebo-controlled clinical trial of an aerosolized β2-agonist for treatment of acute lung injury. *Am J Respir Crit Care Med* 184: 561–568, 2011. doi: 10.1164/rccm.201012-2090OC.
83. **Matthay MA**, **Robriquet L**, **Fang X**. Alveolar epithelium: Role in lung fluid balance and acute lung injury. In: *Proceedings of the American Thoracic Society*, p. 206–213.
84. **Matthay MA**, **Ware LB**, **Zimmerman GA**. The acute respiratory distress syndrome. *J Clin Invest* 122: 2731–2740, 2012. doi: 10.1172/JCI60331.on.
85. **Matthay MA**, **Zemans RL**. The acute respiratory distress syndrome: pathogenesis and treatment. *Annu Rev Pathol* 6: 147–63, 2011. doi: 10.1146/annurev-pathol-011110-130158.

86. **Matthay MA**, **Zimmerman GA**. Acute lung injury and the acute respiratory distress syndrome: Four decades of inquiry into pathogenesis and rational management. *Am J Respir Cell Mol Biol* 33: 319–327, 2005. doi: 10.1165/rcmb.F305.

87. **Matute-Bello G**, **Frevert CW**, **Martin TR**. Animal models of acute lung injury. .

88. **Matute-Bello G**, **Liles WC**, **Steinberg KP**, **Kiener PA**, **Mongovin S**, **Chi EY**, **Jonas M**, **Martin TR**. Soluble Fas ligand induces epithelial cell apoptosis in humans with acute lung injury (ARDS). *J Immunol* 163: 2217–25, 1999. doi: ji_v163n4p2217 [pii].

89. **McAuley DF**, **Frank JA**, **Fang X**, **Matthay MA**. Clinically relevant concentrations of β2-adrenergic agonists stimulate maximal cyclic adenosine monophosphate-dependent airspace fluid clearance and decrease pulmonary edema in experimental acid-induced lung injury. *Crit Care Med* 32: 1470–1476, 2004. doi: 10.1097/01.CCM.0000129489.34416.0E.

90. **McCullough KD**, **Martindale JL**, **Klotz LO**, **Aw TY**, **Holbrook NJ**. Gadd153 sensitizes cells to endoplasmic reticulum stress by down-regulating Bcl2 and perturbing the cellular redox state. *Mol Cell Biol* 21: 1249–59, 2001. doi: 10.1128/MCB.21.4.1249-1259.2001.

91. **McGivan JD**, **Pastor-Anglada M**. Regulatory and molecular aspects of mammalian amino acid transport. *Biochem J* 299: 321–334, 1994. doi: 10.1042/bj2990321.

92. **Menchini RJ**, **Chaudhry FA**. Multifaceted regulation of the system A transporter Slc38a2 suggests nanoscale regulation of amino acid metabolism and cellular signaling. *Neuropharmacology* 161: 2019.

93. **Modelska K**, **Pittet JF**, **Folkesson HG**, **Broaddus VC**, **Matthay MA**. Acid-induced lung injury: Protective effect of anti-interleukin-8 pretreatment on alveolar epithelial barrier function in rabbits. *Am J Respir Crit Care Med* 160: 1450–1456, 1999. doi: 10.1164/ajrccm.160.5.9901096.

94. **Nagaki K**, **Yamamura H**, **Shimada S**, **Saito T**, **Hisanaga S**, **Taoka M**, **Isobe T**, **Ichimura T**. 14-3-3 Mediates Phosphorylation-Dependent Inhibition of the Interaction between the Ubiquitin E3 Ligase Nedd4-2 and Epithelial Na $^{+}$ Channels. *Biochemistry* 45: 6733–6740, 2006. doi: 10.1021/bi052640q.

95. **Nakahira K**, **Porras MAP**, **Choi AMK**. Autophagy in pulmonary diseases. *Am J Respir Crit Care Med* 194: 1196–1207, 2016. doi: 10.1164/rccm.201512-2468SO.

96. **Nardi F**, **Hoffmann TM**, **Stretton C**, **Cwiklinski E**, **Taylor PM**, **Hundal HS**. Proteasomal modulation of cellular SNAT2 (SLC38A2) abundance and function by unsaturated fatty acid availability. *J Biol Chem* 290: 8173–8184, 2015. doi: 10.1074/jbc.M114.625137.

97. **Nissen-Meyer LSH**, **Chaudhry FA**. Protein Kinase C Phosphorylates the System N Glutamine Transporter SN1 (Slc38a3) and Regulates Its Membrane Trafficking and Degradation. *Front Endocrinol (Lausanne)* 4, 2013. doi: 10.3389/fendo.2013.00138.

98. **Nord EP**, **Brown SE**, **Crandall ED**. Characterization of Na+-H+ antiport in type II alveolar

epithelial cells [Online]. *Am J Physiol* 252: C490-498, 1987. http://www.ncbi.nlm.nih.gov/pubmed/3034070 [30 Jan. 2017].

99. **Nowak D**, **Pietras T**, **Antczak A**, **Kr61 M**, **Piasecka G**. *Effect of bacterial lipopolysaccharide on the content of lipid peroxidation products in lungs and other organs of mice*. 1993.

100. **O'Brodovich H**, **Yang P**, **Gandhi S**, **Otulakowski G**. Amiloride-insensitive Na + and fluid absorption in the mammalian distal lung. *Am J Physiol Cell Mol Physiol* 294: L401–L408, 2008. doi: 10.1152/ajplung.00431.2007.

101. **Ott M**, **Gogvadze V**, **Orrenius S**, **Zhivotovsky B**. Mitochondria, oxidative stress and cell death. *Apoptosis* 12: 913–922, 2007.

102. **Palii SS**, **Thiaville MM**, **Pan Y-X**, **Zhong C**, **Kilberg MS**. Characterization of the amino acid response element within the human sodium-coupled neutral amino acid transporter 2 (SNAT2) System A transporter gene. *Biochem J* 395: 517–27, 2006. doi: 10.1042/BJ20051867.

103. **Pan H**, **Zhang Y**, **Luo Z**, **Li P**, **Liu L**, **Wang C**, **Wang H**, **Li H**, **Ma Y**. Autophagy mediates avian influenza H5N1 pseudotyped particle-induced lung inflammation through NF- B and p38 MAPK signaling pathways. *AJP Lung Cell Mol Physiol* 306: L183–L195, 2014. doi: 10.1152/ajplung.00147.2013.

104. **Pastor-Anglada M**, **Ciarimboli G**, **Broer S**, **Goberdhan DCI**, **Fan S-J**. PATs and SNATs: Amino Acid Sensors in Disguise. *Front Pharmacol | www.frontiersin.org* 1: 640, 2018. doi: 10.3389/fphar.2018.00640.

105. **Perl M**, **Chung C-S**, **Perl U**, **Lomas-Neira J**, **de Paepe M**, **Cioffi WG**, **Ayala A**. Fas-induced Pulmonary Apoptosis and Inflammation during Indirect Acute Lung Injury. *Am J Respir Crit Care Med* 176: 591–601, 2007. doi: 10.1164/rccm.200611-1743OC.

106. **Pingleton SK**, **Harmon GS**. Nutritional management in acute respiratory failure [Online]. *Jama* 257: 3094–3099, 1987. http://www.ncbi.nlm.nih.gov/pubmed/3295313.

107. **Pinilla J**, **Aledo JC**, **Cwiklinski E**, **Hyde R**, **Taylor PM**, **Hundal HS**. SNAT2 transceptor signalling via mTOR: a role in cell growth and proliferation? *Front Biosci (Elite Ed)* 3: 1289–1299, 2011. doi: 10.2741/332.

108. **Ranieri VM**, **Rubenfeld GD**, **Thompson BT**, **Ferguson ND**, **Caldwell E**, **Fan E**, **Camporota L**, **Slutsky AS**. Acute respiratory distress syndrome: The Berlin definition. *JAMA - J Am Med Assoc* 307: 2526–2533, 2012. doi: 10.1001/jama.2012.5669.

109. **Ricard JD**, **Dreyfuss D**, **Saumon G**. Ventilator-induced lung injury. *Curr. Opin. Crit. Care* 8: 12–20, 2002.

110. **Ridge KM**, **Olivera WG**, **Saldias F**, **Azzam Z**, **Horowitz S**, **Rutschman DH**, **Dumasius V**, **Factor P**, **Sznajder JI**. Alveolar type 1 cells express the alpha2 Na,K-ATPase, which contributes to lung liquid clearance. *Circ Res* 92: 453–460, 2003. doi: 10.1161/01.RES.0000059414.10360.F2.

111. **Riordan JR**. ASSEMBLY OF FUNCTIONAL CFTR CHLORIDE CHANNELS. *Annu Rev Physiol* 67: 701–718, 2005. doi: 10.1146/annurev.physiol.67.032003.154107.

112. **Rotin D**, **Staub O**. Nedd4-2 and the regulation of epithelial sodium transport. *Front. Physiol.* 3 JUN: 2012.

113. **Rutkowski DT**, **Kaufman RJ**. A trip to the ER: Coping with stress. *Trends Cell Biol.* 14: 20–28, 2004.

114. **Sadasivan S**, **Waghray A**, **Larner SF**, **Dunn WA**, **Hayes RL**, **Wang KKW**. Amino acid starvation induced autophagic cell death in PC-12 cells: Evidence for activation of caspase-3 but not calpain-1. *Apoptosis* 11: 1573–1582, 2006. doi: 10.1007/s10495-006-7690-6.

115. **Sano R**, **Reed JC**. ER stress-induced cell death mechanisms. *Biochim. Biophys. Acta - Mol. Cell Res.* 1833: 3460–3470, 2013.

116. **Sartori C**, **Allemann Y**, **Duplain H**, **Lepori M**, **Egli M**, **Lipp E**, **Hutter D**, **Turini P**, **Hugli O**, **Cook S**, **Nicod P**, **Scherrer U**. Salmeterol for the Prevention of High-Altitude Pulmonary Edema. *N Engl J Med* 346: 1631–1636, 2002. doi: 10.1056/nejmoa013183.

117. **Sartori C**, **Matthay M a.** Alveolar epithelial fluid transport in acute lung injury: new insights. *Eur Respir J* 20: 1299–1313, 2002. doi: 10.1183/09031936.02.00401602.

118. **Schroder M**, **Kaufman RJ**. ER stress and the unfolded protein response. *Mutat Res* 569: 29–63, 2005. doi: 10.1016/j.mrfmmm.2004.06.056.

119. **Serrao KL**, **Fortenberry JD**, **Owens ML**, **Harris FL**, **Brown L a**. Neutrophils induce apoptosis of lung epithelial cells via release of soluble Fas ligand. [Online]. *Am J Physiol Lung Cell Mol Physiol* 280: L298-305, 2001. http://ajplung.physiology.org/content/ajplung/280/2/L298.full.pdf [6 Oct. 2017].

120. **Snyder PM**, **Olson DR**, **Thomas BC**. Serum and glucocorticoid-regulated kinase modulates Nedd4-2-mediated inhibition of the epithelial Na+ channel. *J Biol Chem* 277: 5–8, 2002. doi: 10.1074/jbc.C100623200.

121. **Solymosi E a**, **Kaestle-Gembardt SM**, **Vadász I**, **Wang L**, **Neye N**, **Chupin CJA**, **Rozowsky S**, **Ruehl R**, **Tabuchi A**, **Schulz H**, **Kapus A**, **Morty RE**, **Kuebler WM**. Chloride transport-driven alveolar fluid secretion is a major contributor to cardiogenic lung edema. *Proc Natl Acad Sci U S A* 110: E2308-16, 2013. doi: 10.1073/pnas.1216382110.

122. **Sugawara M**, **Nakanishi T**, **Fei YJ**, **Huang W**, **Ganapathy ME**, **Leibach FH**, **Ganapathy V**. Cloning of an amino acid transporter with functional characteristics and tissue expression pattern identical to that of system A. *J Biol Chem* 275: 16473–16477, 2000. doi: 10.1074/jbc.C000205200.

123. **Sun Y**, **Li C**, **Shu Y**, **Ju X**, **Zou Z**, **Wang H**, **Rao S**, **Guo F**, **Liu H**, **Nan W**, **Zhao Y**, **Yan Y**, **Tang J**, **Zhao C**, **Yang P**, **Liu K**, **Wang S**, **Lu H**, **Li X**, **Tan L**, **Gao R**, **Song J**, **Gao X**, **Tian X**, **Qin Y**, **Xu KF**, **Li D**, **Jin**

N, **Jiang C**. Inhibition of autophagy ameliorates acute lung injury caused by avian influenza A H5N1 infection. *Sci Signal* 5: ra16–ra16, 2012. doi: 10.1126/scisignal.2001931.

124. **Sznajder JI**. Alveolar edema must be cleared for the acute respiratory distress syndrome patient to survive. *Am. J. Respir. Crit. Care Med.* 163 American Thoracic SocietyNew York, NY: 1293–1294, 2001.
125. **Sznajder JI**, **Factor P**, **Ingbar DH**. Invited review: Lung edema clearance: Role of Na+-K+-ATPase. *J. Appl. Physiol.* 93 American Physiological SocietyBethesda, MD: 1860–1866, 2002.
126. **Tabas I**, **Ron D**. Integrating the mechanisms of apoptosis induced by endoplasmic reticulum stress. *Nat Cell Biol* 13: 184–190, 2011. doi: 10.1038/ncb0311-184.
127. **Tanaka A**, **Jin Y**, **Lee SJ**, **Zhang M**, **Kim HP**, **Stolz DB**, **Ryter SW**, **Choi AMK**. Hyperoxia-induced LC3B interacts with the Fas apoptotic pathway in epithelial cell death. *Am J Respir Cell Mol Biol* 46: 507–514, 2012. doi: 10.1165/rcmb.2009-0415OC.
128. **Taylor PM**. Amino acid transporters: Éminences grises of nutrient signalling mechanisms? *Biochem Soc Trans* 37: 237–241, 2009. doi: 10.1042/BST0370237.
129. **Towbin H**, **Staehelin T**, **Gordon J**. Electrophoretic transfer of proteins from polyacrylamide gels to nitrocellulose sheets: Procedure and some applications. *Proc Natl Acad Sci U S A* 76: 4350–4354, 1979. doi: 10.1073/pnas.76.9.4350.
130. **Vadász I**, **Raviv S**, **Sznajder JI**. Alveolar epithelium and Na,K-ATPase in acute lung injury. *Intensive Care Med.* 33: 1243–1251, 2007.
131. **Van't Wout EFA**, **Hiemstra PS**, **Marciniak SJ**. The integrated stress response in lung disease. *Am. J. Respir. Cell Mol. Biol.* 50: 1005–1009, 2014.
132. **Vanderpool RR**, **Chesler NC**. Characterization of the isolated, ventilated, and instrumented mouse lung perfused with pulsatile flow. *J Vis Exp* : 3–7, 2011. doi: 10.3791/2690.
133. **Verghese GM**, **Ware LB**, **Matthay BA**, **Matthay MA**. Alveolar epithelial fluid transport and the resolution of clinically severe hydrostatic pulmonary edema. [Online]. *J Appl Physiol* 87: 1301–12, 1999. http://www.ncbi.nlm.nih.gov/pubmed/10517756.
134. **Verkman AS**, **Matthay MA**, **Song Y**. Aquaporin water channels and lung physiology. *Am J Physiol Cell Mol Physiol* 278: L867–L879, 2000. doi: 10.1152/ajplung.2000.278.5.L867.
135. **Vivona ML**, **Matthay M**, **Chabaud MB**, **Friedlander G**, **Clerici C**. Hypoxia Reduces Alveolar Epithelial Sodium and Fluid Transport in Rats. *Am J Respir Cell Mol Biol* 25: 554–561, 2001. doi: 10.1165/ajrcmb.25.5.4420.
136. **Walter P**, **Ron D**. The Unfolded Protein Response: From Stress Pathway to Homeostatic Regulation. *Science (80-)* 334: 1081–1086, 2011. doi: 10.1126/science.1209038.
137. **Wang H**, **Huang W**, **Sugawara M**, **Devoe LD**, **Leibach FH**, **Prasad PD**, **Ganapathy V**. Cloning and functional expression of ATA1, a subtype of amino acid transporter A, from human placenta.

Biochem Biophys Res Commun 273: 1175–1179, 2000. doi: 10.1006/bbrc.2000.3061.

138. **Ware LB**, **Matthay MA**. The acute respiratory distress syndrome. *N Engl J Med* 342: 1334–49, 2000. doi: 10.1056/NEJM200005043421806.

139. **Ware LB**, **Matthay MA**. Alveolar fluid clearance is impaired in the majority of patients with acute lung injury and the acute respiratory distress syndrome. *Am J Respir Crit Care Med* 163: 1376–1383, 2001. doi: 10.1164/ajrccm.163.6.2004035.

140. **Weber EM**, **Olsson AS**, **Algers B**. High mortality rates among newborn laboratory mice - Is it natural and which are the causes? In: *Acta Veterinaria Scandinavica*. BioMed Central, p. S8.

141. **Weidenfeld S**, **Kuebler WM**. Cytokine-Regulation of Na+-K+-Cl− Cotransporter 1 and Cystic Fibrosis Transmembrane Conductance Regulator—Potential Role in Pulmonary Inflammation and Edema Formation. *Front Immunol* 8: 290–6, 2017. doi: 10.3389/fimmu.2017.00393.

142. **Weissman C**, **Askanazi J**, **Rosenbaum S**, **Hyman AI**, **Milic-Emili J**, **Kinney JM**. Amino acids and respiration. *Ann Intern Med* 98: 41–44, 1983. doi: 10.7326/0003-4819-98-1-41.

143. **Wek RC**, **Jiang HY**, **Anthony TG**. Coping with stress: EIF2 kinases and translational control. In: *Biochemical Society Transactions*. Portland Press Ltd, 2006, p. 7–11.

144. **White SR**. Apoptosis and the airway epithelium. *J Allergy* 2011: 948406, 2011. doi: 10.1155/2011/948406.

145. **Yamaguchi H**, **Wang H-G**. CHOP is involved in endoplasmic reticulum stress-induced apoptosis by enhancing DR5 expression in human carcinoma cells. *J Biol Chem* 279: 45495–502, 2004. doi: 10.1074/jbc.M406933200.

146. **Yao D**, **Mackenzie B**, **Ming H**, **Varoqui H**, **Zhu H**, **Hediger MA**, **Erickson JD**. A novel system A isoform mediating Na+/neutral amino acid cotransport. *J Biol Chem* 275: 22790–22797, 2000. doi: 10.1074/jbc.M002965200.

147. **Yoshida H**. ER stress and diseases. *FEBS J.* 274 Blackwell Publishing Ltd: 630–658, 2007.

148. **Zambon M**, **Vincent J-L**. Mortality Rates for Patients With Acute Lung Injury/ARDS Have Decreased Over Time. *Chest* 133: 1120–1127, 2008. doi: 10.1378/chest.07-2134.

149. **Zhang Z**, **Grewer C**. The sodium-coupled neutral amino acid transporter SNAT2 mediates an anion leak conductance that is differentially inhibited by transported substrates. *Biophys J* 92: 2621–2632, 2007. doi: 10.1529/biophysj.106.100776.

Eidesstattliche Erklärung (declaration)

Ich, Sarah Weidenfeld, versichere an Eides statt durch meine eigenhändige Unterschrift, dass ich die vorgelegte Dissertation mit dem Thema: „*Functional relevance of Na^+-coupled neutral amino acid transporter SNAT2 as master regulator of alveolar homeostasis and its critical role in ARDS*“ – „Funktion des Na^+-gekoppelten Aminosäure-Transporters SNAT2 als Masterregulator der alveolären Homöostase und seine kritische Rolle im akuten Lungenschaden“ selbstständig und ohne nicht offengelegte Hilfe Dritter verfasst und keine anderen als die angegebenen Quellen und Hilfsmittel genutzt habe.
Alle Stellen, die wörtlich oder dem Sinne nach auf Publikationen oder Vorträgen anderer Autoren/innen beruhen, sind als solche in korrekter Zitierung kenntlich gemacht. Die Abschnitte zu Methodik (insbesondere praktische Arbeiten, Laborbestimmungen, statistische Aufarbeitung) und Resultaten (insbesondere Abbildungen, Graphiken und Tabellen) werden von mir verantwortet.

Ich versichere ferner, dass ich die in Zusammenarbeit mit anderen Personen generierten Daten, Datenauswertungen und Schlussfolgerungen korrekt gekennzeichnet und meinen eigenen Beitrag sowie die Beiträge anderer Personen korrekt kenntlich gemacht habe (siehe Anteilserklärung).

Meine Anteile an etwaigen Publikationen zu dieser Dissertation entsprechen denen, die in der untenstehenden gemeinsamen Erklärung mit dem/der Erstbetreuer/in, angegeben sind. Für sämtliche im Rahmen der Dissertation entstandenen Publikationen wurden die Richtlinien des ICMJE (International Committee of Medical Journal Editors; www.icmje.og) zur Autorenschaft eingehalten. Ich erkläre ferner, dass ich mich zur Einhaltung der Satzung der Charité – Universitätsmedizin Berlin zur Sicherung Guter Wissenschaftlicher Praxis verpflichte.

Weiterhin versichere ich, dass ich diese Dissertation weder in gleicher noch in ähnlicher Form bereits an einer anderen Fakultät eingereicht habe.

Die Bedeutung dieser eidesstattlichen Versicherung und die strafrechtlichen Folgen einer unwahren eidesstattlichen Versicherung (§§156, 161 des Strafgesetzbuches) sind mir bekannt und bewusst.“

Ort, Datum_____ Unterschrift _____

(Sarah Weidenfeld)

Anteilserklärung an etwaigen erfolgten Publikationen

Publikation: **S. Weidenfeld**, C. Chupin, D.I. Langner, T. Zetoun, S. Rozowsky, W.M. Kuebler. "Sodium coupled neutral amino acid transporter SNAT2 counteracts cardiogenic pulmonary edema by driving alveolar fluid clearance," *Am. J. Physiol. Lung Cell. Mol. Physiol*., Jan. 2021

Frau Weidenfeld hat im Rahmen der oben genannten Publikation folgende experimentelle Arbeiten eigenständig geplant, etabliert und durchgeführt:

- Untersuchungen der Ödembildung durch hydrostatischen Stress oder Flüssigkeitsinstillation in isoliert perfundierte Mauslungen
- SNAT2 Protein und Gen Expressionsprofile in Lungenepithelzellen und Mauslungen mittels Western blot und qRT-PCR
- *In vivo* Modell des Säure-induzierten Lungenschadens
- L-alanin Transport Assay in Lungenepithelzellen

Alle für die oben genannte Publikation relevanten Datenanalysen mit Ausnahme der Analysen des Flüssigkeitstransportes in isoliert perfundierten Rattenlungen wurden von Frau Weidenfeld selbständig durchgeführt. Die entsprechenden Graphen und statistischen Analysen von wurden von Frau Weidenfeld in GraphPad Prism erstellt.

Des Weiteren war Frau Weidenfeld maßgeblich an der Erstellung des Manuskriptes und dem Publikationsprozess beteiligt:

- Eigenständiger Entwurf, einschließlich Abstract, Einleitung, Methoden, Ergebnisse und Diskussion
- Zusammenstellung der endgültigen Manuskriptversion
- Entwurf des Begleitschreibens zum Manuskript
- Entwurf der Manuskriptüberarbeitung einschließlich einer punktuellen Reaktion auf das Feedback der Gutachter

_____

Unterschrift, Datum und Stempel des/der erstbetreuenden Hochschullehrers/in

Unterschrift des Doktoranden/der Doktorandin

Curriculum vitae

Mein Lebenslauf wird aus datenschutzrechtlichen Gründen in der elektronischen Version meiner Arbeit nicht veröffentlicht.

Publication list

Original publications

[1] **S. Weidenfeld**, C. Chupin, D.I. Langner, T. Zetoun, S. Rozowsky, W.M. Kuebler. "Sodium coupled neutral amino acid transporter SNAT2 counteracts cardiogenic pulmonary edema by driving alveolar fluid clearance," *Am. J. Physiol. Lung Cell. Mol. Physiol*., Jan. 2021, doi: 10.1152/ajplung.00461.2020. Online ahead of print.

[2] M.J. McVey, **S. Weidenfeld**, M. Maishan, C. Spring, M. Kim, A. Tabuchi, V. Srbely, A. Takabe-French, S. Simmons, C. Arenz, J.W. Semple, W.M Kuebler. "Platelet extracellular vesicles mediate transfusion-related acute lung injury by imbalancing the sphingolipid rheostat." *Blood*. Nov 2020, doi: 10.1182/blood.2020005985. Online ahead of print.

[3] L. Michalick, **S. Weidenfeld**, B. Grimmer, D. Fatykhova, P.D. Solymosi, F. Behrens, M. Dohmen, M.C. Brack, S. Schulz, E. Thomasch, S. Simmons, H. Müller-Redetzky, N. Suttorp, F. Kurth, J. Neudecker, M. Toennies, T.T. Bauer, S. Eggeling, V.M. Corman, A.C. Hocke, M. Witzenrath, S. Hippenstiel, W.M. Kuebler. "Plasma mediators in patients with severe COVID-19 cause lung endothelial barrier failure." *Eur Respir J*. Nov 2020, doi: 10.1183/13993003.02384-2020. Online ahead of print.

[4] **S. Weidenfeld** and W. M. Kuebler, "Shedding First Light on the Alveolar Epithelial Glycocalyx," *Am. J. Respir. Cell Mol. Biol.*, vol. 59, no. 3, pp. 283–284, Sep. 2018, doi: 10.1165/rcmb.2018-0108ED

[5] **S. Weidenfeld** and W. M. Kuebler, "Cytokine-Regulation of Na^+-K^+-Cl^- -Cotransporter 1 and Cystic Fibrosis Transmembrane Conductance Regulator—Potential Role in Pulmonary Inflammation and Edema Formation," *Front. Immunol.*, vol. 8, no. 2, pp. 290–6, Apr. 2017, doi: 10.3389/fimmu.2017.00393

[6] T. Pasqualon, J. Pruessmeyer, V. Jankowski, A. Babendreyer, E. Groth, J. Schuhmacher, A. Koenen, **S. Weidenfeld,** N. Schwarz, B. Denecke, H. Jahr, D. Dreymueller, J. Jankowski and A. Ludwig "A cytoplasmic C-terminal fragment of syndecan-1 is generated by sequential proteolysis and antagonizes syndecan-1 dependent lung tumor cell migration," *Oncotarget*, vol. 6, no. 31, 2015, doi: 10.18632/oncotarget.5174

[7] T. Pasqualon, J. Pruessmeyer, **S. Weidenfeld,** A. Babendreyer, E. Groth, J. Schuhmacher, N. Schwarz, B. Denecke, H. Jahr, P. Zimmermann, D. Dreymueller and A. Ludwig, "A transmembrane C-terminal fragment of syndecan-1 is generated by the metalloproteinase ADAM17 and promotes lung epithelial tumor cell migration and lung metastasis formation," *Cell. Mol. Life Sci.*, vol. 72, no. 19, pp. 3783–3801, 2015, doi: 10.1007/s00018-015-1912-4

Presentations at scientific conferences

06/2016	Annual Respirology Research Day, University of Toronto, ON, Canada Oral presentation
03/2017	Experimental Biology (EB) 2017 Chicago, Illinois, USA Oral and poster presentation
04/2018	Experimental Biology (EB) 2018 San Diego, California, USA Poster presentation
04/2019	Experimental Biology (EB) 2019 Orlando, Florida, USA Poster presentation
09/2019	98th Meeting of the German Physiological Society (DPG) Ulm, Germany Poster presentation
01/2020	Deutsches Zentrum für Lungenforschung (DZL) – Annual Meeting Travemünde, Germany Poster Presentation

Awards

06/2016	Annual Respirology Research Day, University of Toronto, ON, Canada **Basic Science Award for best oral presentation**
04/2017	Experimental Biology (EB) 2017 – Chicago, Illinois, USA The American Physiological Society, Respiration Section **Usha Award**

04/2018	Experimental Biology (EB) 2018 – San Diego, California, USA
	The American Physiological Society, Respiration Section
	Research Recognition Award
04/2019	Experimental Biology (EB) 2019– Orlando Florida, USA
	The American Physiological Society, Respiration Section
	Research Recognition Award
	Respiration Section Trainee Poster Award

Danksagung (Acknowledgements)

An dieser Stelle möchte ich mich bei den Menschen bedanken, die diese Arbeit ermöglicht haben.

Mein tiefer Dank gilt zuallererst Prof. Dr. Wolfgang Kübler, der mir die Möglichkeit gegeben hat, in seiner Arbeitsgruppe meine Promotion anzufertigen, mich durch die schwierigen, aber auch erfolgreichen Phasen dieses Projektes begleitet hat und mir stets mit Rat und Tat zur Seite stand. Vielen Dank für die exzellente fachliche und engagierte Betreuung.

A very special thanks to my dear lab mates in Toronto. Many thanks to Diana Zabini, Adrienn Krauszman, Maz Maishan, Siegfried Breitling, Mariana Carreira Geralde and Arata Tabuchi for two amazing and adventurous years in and outside the lab.

Ich möchte mich weiterhin ganz herzlich bei allen ehemaligen und derzeitigen Mitgliedern der AG Kübler für die kollegiale und angenehme Arbeitsatmosphäre im Labor, die Grillnachmittage, Weihnachtsfeiern und die gemeinsamen Freizeitaktivitäten bedanken. Mein besonderer Dank gilt hierbei Laura Michalick, Lasti Erfinanda, Jana Grune, Benjamin Grimmer, Szandor Simmons, Niklas Hegemann, Sabrina Schulz und Jasmin Matuszak.

Zum Schluss möchte ich mich ganz herzlich bei meiner Mutter und meiner liebsten Lieblingsschwester Verena für die jahrelange Unterstützung bedanken. Danke, dass ihr immer an mich geglaubt habt. Ein riesengroßes Dankeschön geht an Dirk, der mich insbesondere in der intensiven Schreibphase stets unterstützt und motiviert hat.

Bescheinigung Statistisches Gutachten

CHARITÉ

CharitéCentrum für Human- und Gesundheitswissenschaften

Charité | Campus Charité Mitte | 10117 Berlin

Institut für Biometrie und klinische Epidemiologie (iBikE)

Direktor: Prof. Dr. Geraldine Rauch

Postanschrift:
Charitéplatz 1 | 10117 Berlin
Besucheranschrift:
Reinhardtstr. 58 | 10117 Berlin

Tel. +49 (0)30 450 562171
geraldine.rauch@charite.de
https://biometrie.charite.de/

Name, Vorname: Weidenfeld, Sarah

PromotionsbetreuerIn: Univ.-Prof. Dr. Wolfgang Kübler

Promotionsinstitution / Klinik: CC02 Institut für Physiologie

Bescheinigung

Hiermit bescheinige ich, dass Frau Sarah Weidenfeld innerhalb der Service Unit Biometrie des Instituts für Biometrie und klinische Epidemiologie (iBikE) bei mir eine statistische Beratung zu einem Promotionsvorhaben wahrgenommen hat. Folgende Beratungstermine wurden wahrgenommen:

- Termin: 06.03.2020

Folgende wesentliche Ratschläge hinsichtlich einer sinnvollen Auswertung und Interpretation der Daten wurden während der Beratung erteilt:

- Boxplot als graphische Darstellungsform zu empfehlen
- Entscheidungskriterien für parametrische Testauswahl besprochen
- Hinweis auf explorativen Charakter und entsprechende Einordnung in Bezug auf multiples Testen

Diese Bescheinigung garantiert nicht die richtige Umsetzung der in der Beratung gemachten Vorschläge, die korrekte Durchführung der empfohlenen statistischen Verfahren und die richtige Darstellung und Interpretation der Ergebnisse. Die Verantwortung hierfür obliegt allein dem Promovierenden. Das Institut für Biometrie und klinische Epidemiologie übernimmt hierfür keine Haftung.

Datum: 06.03.2020

Name des Beraters/ der Beraterin: Carolin Herrmann